Electric vehicle charging in the Dutch low-voltage grid

Sustainable Energy Technology master thesis

Bart Nijenhuis

August 26, 2020
CAES - Faculty of EEMCS
University of Twente
Enschede, the Netherlands

Graduation committee:
prof. dr. Johann L. Hurink
dr. ir. Marco E.T. Gerards
dr. Frans H.J.M. Coenen

UNIVERSITY
OF TWENTE.

Cover photo by Marc Heckner — https://unsplash.com/@herrheckner

Summary

The current transition from generating energy with fossil fuels towards a more clean and sustainable energy generation influences our society on many levels. Replacing fossil fuel cars by electric vehicles (EV) is an important step in this transition. EVs are a suitable alternative to fossil fuel cars, as they do not exhaust carbon-dioxide directly from the exhaust and are overall less environmentally damaging. However, banning out fossil fuels like gasoline and diesel does not mean our demand to travel decreases. All these EVs need to charge, preferably from a sustainable electricity source. However, our current electricity grid might not be suitable to handle a large uptake in the penetration rate of EVs. EVs use relatively high-powered chargers and the energy demands are large, which can induce a severe load on the grid. This thesis researches to what extent the Dutch low-voltage electricity grid can handle an increase in EV penetration rate.

The Dutch low-voltage (LV) grid consists out of an estimated 300,000 feeder cables. The outcome of a clustering method for a part of the Dutch LV grid is used to approximate a set of 26 feeders with different features, such as length, number of connections and cable type that can represent the Dutch LV grid. These feeders are implemented in an LV grid model in DEMKit, a tool for simulating smart grids, developed at the University of Twente. The Artificial Load Profile Generator, which works together with DEMKit, allows us to create realistic household load models. These household load models are combined with the grid models of the feeders and this allows us to simulate different types of situations.

The input for the Artificial Load Profile Generator is based on a database with statistics from the Dutch central office for statistics, or 'Centraal Bureau voor de Statistiek'. This database provides detailed demographic information about every neighborhood in the Netherlands. This coupling makes it straightforward to combine certain demographic settings to specific LV feeders. These demographic settings determine the type of houses in such a neighborhood and the household composition, which then determine the household load profile for that specific house. For each of the 26 feeders, the maximum number of simultaneously charging EVs is determined as a physical limit. Charging more EVs than specified results in violating the feeder limits by either overloading the current capacity of a feeder or creating a critical voltage drop.

We propose a model to estimate the probability that an EV is charging in a certain timeslot on a certain day, using plug-in time distributions of real EV charging sessions. Five different charging regimes are introduced and combined into a single model with two EV charging power levels. Based on this, the model calculates the probability that a certain number of EVs in a neighborhood charges simultaneously. Combining this with the limits of each feeder, we can estimate the expected number of blackouts for all possible EV penetration rates for all individual feeders. This is translated to a situation for the whole of the Netherlands. Currently, the LV grid in the Netherlands experiences 52 daily power interruptions, or blackouts, on average per day. The results show that at an EV penetration rate of 30%, the expected number of daily blackouts in the Netherlands increases by 20%. However, after surpassing this value and further increasing the EV penetration rate, the expected number of blackouts rapidly increases.

Dankwoord

Deze thesis is het resultaat van mijn master Sustainable Energy Technology. De eerste maand van dit project heb ik kunnen werken vanuit de 'Energy Shed' op de Universiteit van Twente. Vanwege de COVID-19 pandemie die onze planeet momenteel in zijn greep houdt, heb ik het grootste gedeelte van deze thesis geschreven op mijn 'thuiswerkplek' aan 'De Mina'. Online video meetings bleken een geschikt alternatief te zijn voor samenwerken op de UT, maar ik hoop dat we ergens in de nabije toekomst toch weer 'gewoon' samen kunnen werken.

Ik wil graag Marco en Johann bedanken voor de kansen die ze mij hebben gegeven. Hun begeleiding was erg leerzaam en heeft me geholpen om dit project te maken tot wat het nu is. Ik wil Gerwin bedanken voor zijn hulp met DEMKit en voor het altijd beschikbaar zijn voor vragen en advies. I would like to thank the members of the Energy Group, you all made me feel very welcome!

Het volgen van het vak Distributed Energy Management for Smart Grids in combinatie met mijn achtergrond vanuit de bachelor Automotive Technology heeft ervoor gezorgd dat we zijn uitgekomen bij het in mijn ogen zeer interessante onderwerp van dit project. Ondanks de theoretische aard van dit werk biedt het aanknopingspunten om praktische oplossingen te ontwikkelen voor de toepassing van de energietransitie. Mede door dit project heb ik ontdekt dat ik daar persoonlijk veel plezier en voldoening uit haal.

Een speciaal woord van dank aan mijn vrienden uit Brabant en alle mooie tijden die we gehad hebben en nog steeds beleven sinds we elkaar in 2013 ontmoetten tijdens onze bachelor studie aan de Universiteit van Eindhoven. De afstand Enschede-Eindhoven is nog nooit zo klein geweest dankzij de dagelijkse discussies op de 'Soepsquad' WhatsApp-chat, de online-bakkies en de online-pubquizjes van de afgelopen maanden. Bedankt mannen, tot snel! Ook wil ik mijn huisgenoten bedanken voor de afgelopen tijd. Door samen thuis te werken bleef het gezellig. Onze gezamenlijke woonkamer met balkon is altijd een mooie plek voor een fijne pauze.

Zonder de onvoorwaardelijke steun van mijn ouders en zus zou ik nooit gekomen zijn tot waar ik nu ben. Zij hebben mij geleerd om hard te werken, mijn hart achterna te gaan en in mijzelf en in anderen te geloven. Fijn dat jullie altijd achter mij staan! Als laatste wil ik Lotte bedanken, met je positieve kijk op dingen weet je me altijd op te vrolijken, ik vind het fijn dat je er bent.

Contents

Chapter 1

Introduction

1.1 Motivation

In the current energy transition from fossil fuel energy towards more clean and sustainable energy generation with e.g. solar and wind energy, a lot of interest is also going out to the transport and mobility sector. Since EVs make it possible to drive on sustainable generated energy without (directly) emitting carbon dioxide and other greenhouse gasses, they are currently seen by the Dutch government as an important piece of the energy transition. The Dutch government has propagated their ambitions on transport and mobility in the 2017 Coalition Agreement "Confidence in the Future" [1]. For passenger cars, three main goals are set:

- "By 2020, 10% of all new passenger cars sold will have an electric powertrain and plug. This goal is realized: the total share of battery electric vehicles in the sales numbers of 2019 is 13.7%.
- "By 2025, 50% of all new passenger cars sold will have an electric powertrain and a plug, and at least 30% of these vehicles (15% of the total) will be fully electric."
- "By 2030, 100% of all new passenger cars sold will be zero-emission"

To reach these goals, the Dutch government is using fiscal advantages for zero-emission cars, with success: the total number of electric vehicles (EVs) in the Netherlands is increasing. Up to the end of 2016, this increase is mainly contributed to by the sales numbers of Plug-in Hybrid Electric Vehicles (PHEV) but due to government policy reducing the fiscal advantage of PHEV these sales diminished. The fiscal advantage for PHEV owners was reduced since these cars are not considered to be zero-emission cars. The two categories considered zero-emission cars are Battery Electric Vehicles (BEV) and Fuel Cell Electric Vehicles (FCEV). FCEVs are still of small importance in the total mix of EV in the Netherlands, but the BEV share is steadily growing, according to numbers published by the *Rijksdienst voor Ondernemend Nederland* (RVO) [2].

This increase of the BEV share can have severe implications for the Dutch electricity grid infrastructure. Considering that the capacity of a Tesla Model S battery pack of 95 kWh is enough to drive up to 610 kilometers [3], but also to power a typical four person household (considering an annual electricity consumption of 3500 kWh) for up to ten days, implicates that the amount of energy needed to drive is large. All passenger cars in the Netherlands together drove 105 billion kilometers on Dutch soil in 2018 [4]. Calculating this for BEVs with an average consumption of 17.5 kWh per 100 kilometer results in about 18.4 TWh of extra electrical energy demand, while the current total annual household electricity consumption in the Netherlands is around 22.7 TWh [5]. Summarizing: if all passenger vehicle kilometers would be driven electric due to such BEVs (in a futuristic scenario), this causes an increase in electricity consumption close to the magnitude of all current household electricity consumption together. This does not even include further electrification of our society with heat pumps and induction cooking. Combining this amount of energy and expected peak demands of charging power with additional electric heating and cooking demand can result in massive power peak demands on the grid.

This research aims at analyzing the potential impact of this emerging electrification on the existing grid structures. The main scope of this thesis is to research the impact of a potential increase in BEV on the local LV grid by calculating the expected number of black-outs at certain EV penetration rates. To allow for a general method, a model is proposed that combines demographic information of neighborhoods and corresponding energy load profiles with available LV grid infrastructure. Once this method is applied to study the general case for EV charging in the Netherlands, two typical scenarios for sub-urban and rural areas are presented wherein we combine typical LV grid layouts for these areas with expected future loads. Furthermore, a scenario simulation is presented using a grid model based on an existing location.

1.2 Framework

Currently, a lot of research on EV driving, charging and infrastructure is carried out in the Netherlands. For example, [6] presents research results on public charging infrastructure mainly focusing on the four largest cities of the Netherlands. While this publication covers a lot of interesting research on different aspects like user groups and their behavior, policy making, the smart use of data and (smart) charging infrastructure for the past five years, it does not cover the actual impact on existing electricity grid structures in much detail.

The paper by Van der Burgt *et al.* [7] uses the *NEMO Tool Suite* to simulate the grid impact of EV charging. Unfortunately, the tool never got out of the development phase and was canceled later on, according to email correspondence with one of the authors. Interesting is that it targets specifically on LV grids and penetration rates of EVs in those LV grids and actively takes into account PV, more or less a similar direction that this research is aiming at.

The authors of [8] propose methods to quantify acceptable EV penetration in an existing neighborhood. This paper describes a case study in Malaysia. It presents models of an existing neighborhood and studies uncontrolled EV charging (using both unbalanced and uniform distribution of EV chargers over the three phases) as well as controlled EV charging of Nissan LEAFs with a 24 kWh battery and compares the situation for older built and newly built networks. Dubay and Santoso [9] present a thorough literature review of the impact of EV charging in residential areas and proposes methods to evaluate the impact on distribution grid voltage quality. They also propose a number of solutions in the form of smart charging algorithms to mitigate the impact of EV charging.

A field study in Lochem, the Netherlands [10] is a proper example of the problem statement of this thesis. This project studied a '2025' scenario in which 20 EVs, representing a penetration rate of 25%, were charged simultaneously in the same LV grid. Aided by local volunteers, the local grid is pushed to its limits by simultaneously using electrical ovens and other home appliances. With 'success': a huge imbalance between the phases was seen and after about 30 minutes after the start of this stress test, a fuse melted causing a service interruption.

The research in this thesis tries to extend the aforementioned publications with a broader view on the situation in the Netherlands by looking at the impact of increasing EV penetration rates on the nationwide

LV grid. It combines existing grids with possible EV penetration rates and demographic information to define possible chances and risks regarding the adoption of EVs in the Netherlands on local level.

1.3 Research questions

The main goal of this research is to explore the effects of a significant increase of EVs in the Dutch electricity grid on a local level. The hypothesis is that the existing Dutch electricity grid in its current form, without any control mechanisms, has a certain maximum penetration rate of EVs. This gives rise to the first research question:

"What penetration rate of electric vehicles may cause problems for the Dutch electricity grid in its current form, if no preventive measures are taken? "

The answers to this question depends on many different factors. This research aims to develop a method to model, analyze and quantify these factors. This leads to the following sub-questions:

"I. How to systematically model the current Dutch LV grid infrastructure, making it possible to identify different frequently occurring grid structures and avoiding the need for a case-by-case approach?"

"II. How to characterize the future loads in Dutch LV grids with regard to the integration of EV charging?

"III. How to model the expected future loads with corresponding LV grid structures to identify potential problematic combinations of loads and grid structures?"

If preventive measures in any form are taken, the possible maximum penetration rate of EVs increases, since the usable capacity of the local grid is extended. This rises the second main research question:

"What are possible solutions for scenarios with problematically high EV penetration rates in local grids and how do these solutions increase the allowed penetration rate?"

1.4 Approach

The first step towards answering the research questions is a background study on the playing field of this problem. This means that all important factors, such as the structure of the current Dutch LV electricity grid and the Dutch EV market (available EV models, capacity and charging techniques) are identified and described. This gives a basis to further classify and quantify the inputs for e.g. simulations using the DEMKit smart grid modeling software, further explained in Chapter 3.

The next step is combining all information on LV grids with information on actual existing neighborhoods. To keep flexibility in simulating different scenarios, the proposed solution considers a split between a (technical) grid model and a (demographic) user model to generate energy load profiles :

- 1. Grid model: the physical LV feeder lines, cable type, number of branches and connections: this defines the technical properties of the feeder and tells something about the maximum capacity of such a system.

- 2. Load model: uses demographic information on the type of neighborhood and its residents, e.g. rich/poor, young/old, large/small families and houses to generate energy load profiles. Furthermore, this might indicate the expected penetration rate of EV and other technologies like PV and heatpumps.

Those two models combined are the main input for the simulations. The Dutch LV grid is represented by 26 so-called 'generic feeders' that we consider representative for the entire Dutch LV grid. For every generic feeder, we determine the maximum number of simultaneously charging EVs. Charging more than this maximum number of EVs simultaneously causes a local blackout on that specific feeder. We develop a model that uses an existing EV plug-in time distribution, different energy demands and charging power levels as inputs to calculate the probability that such a blackout situation occurs. With the combination the grid model and load models, we calculate the expected number of additional blackouts in the Dutch LV grid due to EV charging at different EV penetration rates when allowing uncontrolled EV charging.

1.5 Thesis organization

This thesis is structured as follows. Chapter 2 presents all relevant technical information the Dutch LV grid and EVs. Chapter 3 introduces the proposed models, methods and input data. Chapter 4 presents the general findings regarding the EV penetration rate for the Dutch LV grid by using the proposed model and methods and explains how we arrive at the final results. To connect the general findings to real life situations and to show the working of the proposed methods in more detail, Chapter 5 presents three scenarios. Chapter 6 presents the final conclusions and recommendations.

Chapter 2

Background

2.1 Introduction

This chapter introduces relevant background information for this research. It starts with a description of the Dutch electricity grid in Section 2.2: a general overview of the grid as a whole and a more detailed description of the low-voltage grids in the distribution networks. The section also introduces the main power and voltage limit regulations for the LV grid. These limits are used later on in the thesis to define the maximum capacity of the individual feeders. Section 2.3 introduces the basic features that describe the current status of EV adoption, available charging techniques and expected future EV penetration rates. It introduces data and research that can describe the EV energy demand, as well as an introduction on Smart Charging (SC) and currently as well as soon-to-be available EV models and their properties.

2.2 The Dutch electricity grid

In the Dutch electricity grid, electricity is transported using AC current on 4 main operating voltage levels [11]. Every level has a specific function:

- **Interconnection net** or *Very high voltage grid* 220 and 380 kV, used to transport electricity over larger distances throughout the Netherlands and across the border to other parts of continental Europe.
- **Transport net** or *High voltage grid* 50, 110 and 150 kV for transmission at regional level.
- **Regional distribution net** or *Intermediate voltage grid* 3 - 30 kV for supply to large users and for distribution.
- **Local distribution net** or *Low voltage grid* 230 and 400 V for connection of small enterprise and households.

A general overview is given in Figure 2.1, which shows the traditional grid layout. We see a main generating station, connected with transmission lines (yellow) to substations in the regional and local distribution nets (purple). Traditionally, this layout has always been used in the same manner: a centralized generating station producing energy which is transported over the network in increasingly narrow 'capillaries', all in the same direction with a more or less predictable load. However, with the technological advancements over the last decades and the increasing electrification of our society with EV, PV, heatpumps and induction cooking, the traditional way of network planning is not sufficient anymore. One the one hand, while extra loads like EVs, heatpumps and induction cooking are still reasonably predictable, they impose a much higher load on the grid than it was originally designed for. On the other hand, we see emerging technologies like PV causing houses to become energy producers instead of just consumers. This is also a feature for which our traditional grid was not designed. This does not mean it is totally unfit for the tasks, but it means we have to make clever use of existing infrastructure to prevent spending a lot of money on replacing the current infrastructure.

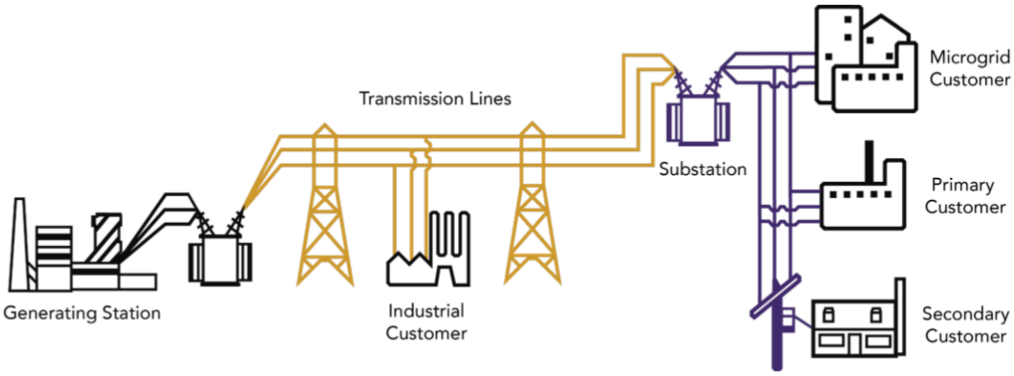

Figure 2.1: Graphical representation of the electricity grid, sorted by function [12].

2.2.1 Low voltage network

The low-voltage (LV) network in the Netherlands consists mostly out of underground cables and operates with 3-phase 230/400 V at 50 Hz. The LV network is mostly radial designed, which means it can be described as a tree-like structure, schematically shown in Figure 2.2. Every LV substation is connected to a MV network and can host multiple so-called feeders, described by the green lines in the schematic. A feeder is defined as the 1 main cable connecting a set of households directly to the LV side of a transformer. These LV feeders can vary widely in topology: while most feeders in urban areas are relatively short with a large number of connections, rural feeders are characterized by being longer and hosting less connections, which obviously is the result of the placement of buildings in the respective areas. Not only their length and number of connections vary, but also the choice of cable material is a very important feature of such LV feeders and varies widely dependent on the local situation. LV cables in the Netherlands are typically located underground at a depth of around 60 cm, consisting of 4-wires: 3 for the phases and 1 neutral. Nowadays, at the installation of new LV cables, the full length of the main cable consists out of one standardized diameter (for purchasing and installation advantage reasons) and the cables are made out of aluminum. This is contrary to before, where feeders were built out of different types of cable mixed together, using thinner (and cheaper) cables near the end of a feeder, similar to a human vein system. In addition to that, when extending the local LV grid, different types of cables are used next to the ones that are already present or it might be possible that a connection cable suddenly becomes a main cable. This is also indicated in Figure 2.2 by using different line thickness for the feeder cable parts. Since the economic lifetime of a LV grid is expected to be over 40 years, one can imagine that these 'traditional' setups and feeders are still common. More information on the modeling of LV networks is given in Section 3.2.

2.2.2 Voltage and power limitations

The low voltage parts of the Dutch grid are managed and maintained by the local grid operators. These local grids have to comply to specific power quality standards, covered by law in the Dutch *Netcode* [13]. These baseline quality standards are considered the minimum requirements for a functioning low voltage

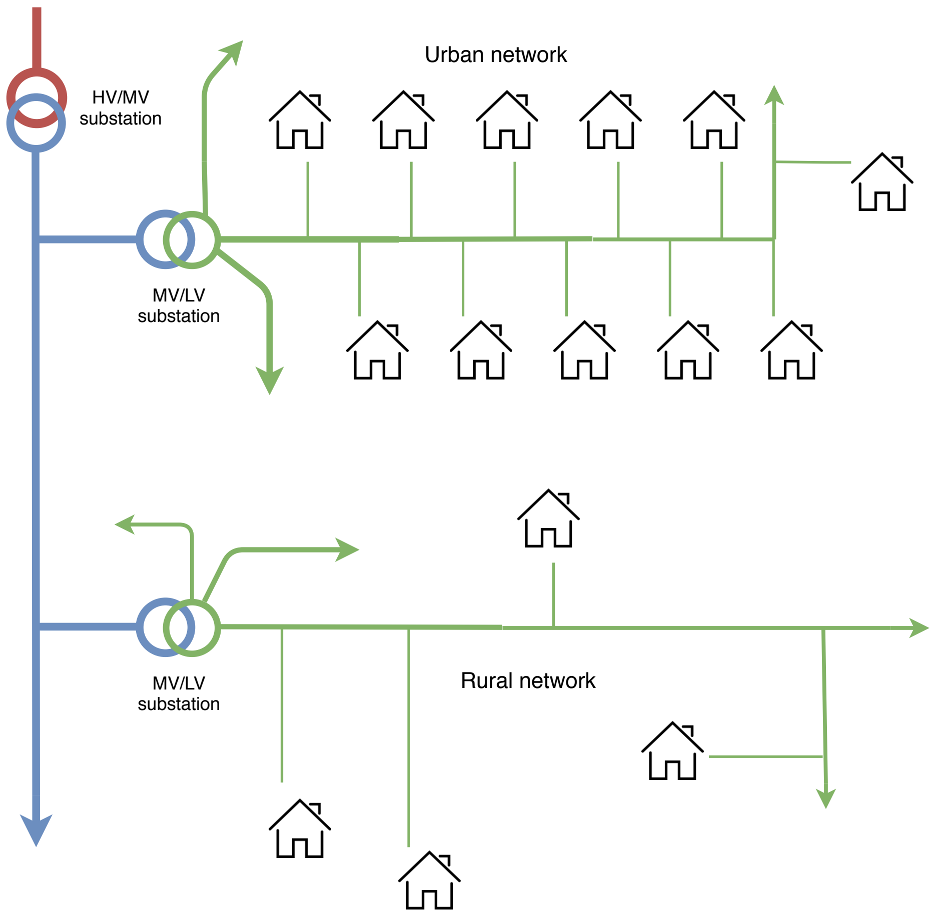

Figure 2.2: Tree-like LV grid with multiple feeder lines out of one MV/LV substation, most common situation in the Netherlands.

grid. The European version of this regulation is the NEN50160. The two most important specifications are considered to be the voltage requirement and the maximum power requirement. The voltage everywhere on the LV grid should be $+/-$ 10% of the nominal voltage of 230 V, so minimal 207 and maximal 253 V. Operating the LV grid outside of these bounds results in problems with equipment on the network and might decrease the lifetime of connected appliances, so this should be avoided. With the introduction of high power demanding equipment like EV chargers and distributed generation with PV, staying within these voltage boundaries has become increasingly difficult, as demonstrated in Figure 2.3.

Furthermore, every LV feeder in the network is protected by a main fuse located at the transformer to provide protection against short-circuit. The rating of this fuse is dependent on local factors like cable type, number of connections and type of loads. Overloading this fuse for a longer time, e.g. in the case of peak demand due to EV charging, causes the fuse to burn, creating a local black-out.

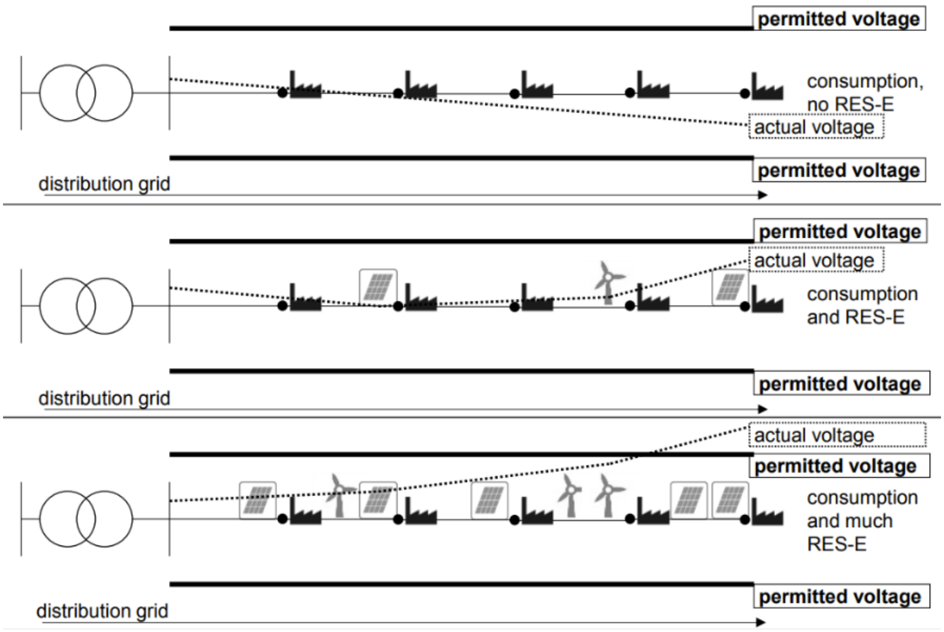

Figure 2.3: Demonstrating LV grid voltage problems in situations with increasing consumption and increasing distributed generation [14].

2.3 Electric vehicles

A 2017 study with 286 respondents [15] suggests that the typical Dutch EV driver is a well-educated middle aged man with a high-paying job. But it also suggests that, in a few years time, this may not be valid anymore. Due to an anticipated lower total cost of ownership (TCO) and an increase in the different (also smaller) EV models, EVs become accessible for a much broader public and even outperform gasoline cars in terms of TCO in some cases already [16]. To model the demand for EV charging in the Netherlands, we need background information on a number of topics, starting with the total number of EVs in the Dutch fleet, which is further described in Section 2.3.1. All these EVs in the total fleet travel certain distances, introduced in Section 2.3.2. Section 2.3.3 introduces background information on different possibilities of charging. Section 2.3.4 introduces Smart Charging and section 2.3.5 introduces currently and some future available EV models.

2.3.1 Electric vehicle fleet size

A well-known method to describe the adoption of new technology is to use the 'S-curve'. For EVs, this S-curve is described in [17] and shown in Figure 2.4. The Netherlands is already approaching the 'early majority' phase and thus the adoption of EVs is likely to grow quicker during the coming decades. Note that in different neighborhoods, the EV penetration rate might vary because of demographic circumstances, but that the remainder of this section focuses on the Dutch EV market as a whole.

While the S-curve is more of a general estimation, we also have access to more extensive research. A TNO report [18] of August 2018 makes an estimation of the EV market penetration in 2030. Information on factors such as TCO, customer purchase decisions, EV market demand, different car segmentation and the Dutch tax situation regarding private and company cars was all taken into account, combined and analyzed. The conclusion sounds that 'the uptake of EV until 2030 is beset with uncertainties.' The main bottleneck indicated here is the market for A and B segment cars (the small to reasonably sized cars such as the Opel

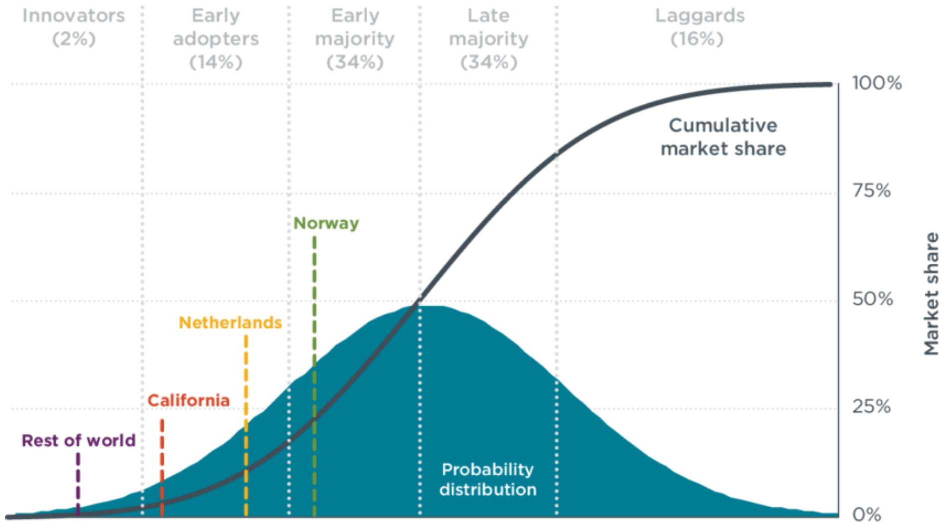

Figure 2.4: EV adoption S-curve showing the Netherlands as one of the early adopters [17].

Corsa, Volkswagen Polo and comparable), which make up almost 50% of the Dutch total passenger vehicle fleet. For these market segments EV might be less interesting, because of the relatively higher purchase price and relatively higher TCO due to the lower average annual mileages. Other factors influencing this total fleet size is the market-mismatch between second-hand cars coming out of the lease-arrangements after four or five years (which traditionally mainly have been medium to larger sized diesel cars) and the domestic demand for small petrol cars. This mismatch is possibly continued with the current generation of relatively large EVs (such as the Tesla Model S and Model 3 that are leased right now), which are likely to be too expensive for the domestic second-hand small car demand and are exported from the Netherlands in the coming years. The next generation of somewhat smaller EVs, such as the Volkswagen ID.3, Volkswagen e-Up!, Renault Zoe and Hyundai models with catalog prices of around €30,000-35,000, may be the first BEVs very suitable for the Dutch second hand market. A theoretical 'optimistic' scenario presented in the report is that in 2030, EV sales may amount to 65% of the Dutch passenger car market. This corresponds with a maximum total fleet size of 2.8 million vehicles in 2030, with the largest segment for compact family cars (C-segment). The 'less optimistic' scenario depicted in the report estimates a 45% market share of BEVs. The ElaadNL foundation suggests three possible scenarios [19] for 2030 with the number of EVs estimated at 1, 1.6 or 2.3 million vehicles which would then represent an average nationwide penetration rate of respectively 12, 19.2 and 27.6%.

The goal of the Dutch government for 2030 is set at 100% market share for zero-emission vehicles. The actual fleet size that belongs to that goal is not known, since the fleet size depends on the sales numbers and market share of the years prior to 2030. Furthermore, the government goal is defined as zero-emission vehicles (not exclusively BEVs), so this scenario is not considered in this analysis. For this thesis, we include the TNO and ElaadNL reports, which results in the following possible EV fleet size scenarios for 2030:

- TNO report optimistic scenario: 65% market share and a total fleet size of in total 2.8 million BEVs, representing a penetration rate of 33.6%;
- The ElaadNL scenarios describing BEV fleet sizes of 1, 1.6 and 2.3 million, representing penetration rates of respectively 12, 19.2 and 27.6%.

Note that 'market share' refers to the share of EVs as percentage of all newly sold car that year and that 'fleet size' represents the actual number of EVs in the total Dutch fleet up to and including that year. Penetration rate describes the percentage of EVs in the total fleet of passenger cars.

2.3.2 Traveled kilometers per day and energy demand

The average Dutch passenger car travels 38 kilometer daily, according to CBS [20]. However, the research project "Onderzoek Verplaatsingen in Nederland"(OViN) [4] shows that distances per destination vary widely: about 24 km per day for commuting, 22 km for visiting friends and family, 18 km for sports and around 7 km for a shopping trip. Another interesting finding of this research is that only 10% of passenger car drivers drive more than 125 km per day. All these driven kilometers directly say something about the required electrical energy, but also on the expected peak loads: only a few cars in the neighborhood with a large energy demand might be less of an issue compared to a lot of cars with a small energy demand but all charging at the same time instance. Also local variations might play a role: inhabitants of rural areas might be likely to cover more distance with their cars compared to inhabitants of urban areas. As for the general case, we can use data as in Figure 2.5 which shows a distribution of energy demand per charging event for private, workplace and public charging. We observe that in about half of the private charging events, more than 20 kWh is demanded. This also directly implies that not every EV is charged every day, since 20 kWh of charging represents 100 to 150 km of driving (depending on the EV model and driving style), while from CBS data we know that only 10% of the passenger cars drive more than 125 km daily. This means a major part of the charging sessions represent the driving distance of multiple days. Furthermore, the energy demand for private charging sessions is significantly higher compared to public and workplace charging sessions.

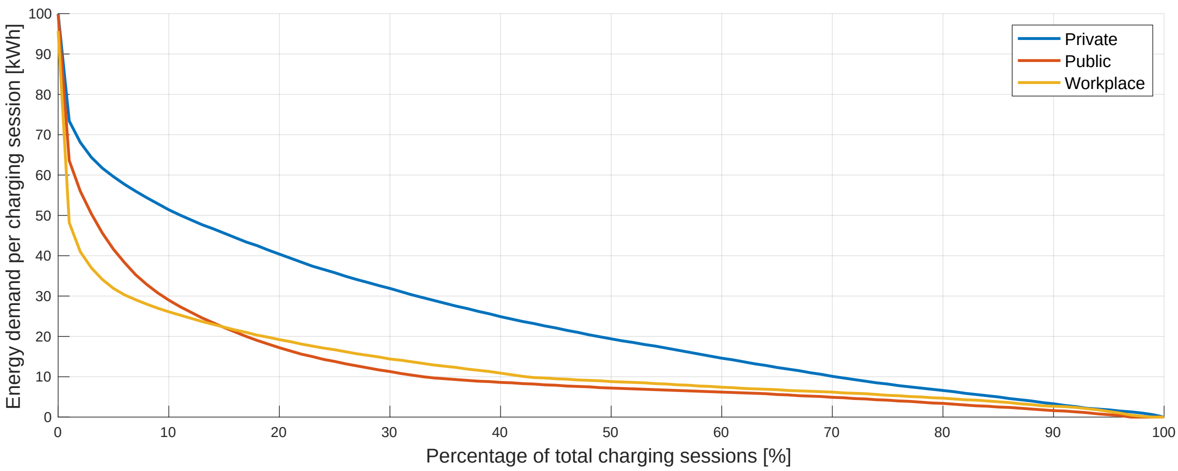

Figure 2.5: For each typical charging location (private, public and workplace), ElaadNL has generated normalized profiles based on large volumes of real charging events [21]. This figure shows the distribution of energy demand per charging session at each location type.

2.3.3 AC charging

When considering EV charging, we distinguish two main categories: AC and DC charging. AC charging is mainly used for home charging and public charging poles in LV grids. DC charging is mostly seen among highways, outside the residential LV grid. DC charging is sometimes referred to as 'fast-charging', because it can charge with powers of up to e.g. 150 kW, such as the Tesla Supercharger. These power levels are too high and therefore unrealistic for existing LV grids and this is also the reason this thesis focuses on AC charging only.

Nowadays, all common AC chargers can deliver between 2.3 kW (which can be delivered by a standard single-phase wall plug to the vehicle) up to 22 kW with a more sophisticated three-phase charger. See Table 2.1 for an overview of the different available type of AC chargers. Next to the home environment, these AC chargers are of the same type that may be installed at work locations. Furthermore, public AC charging poles rely on the same configurations.

Charging point	Max. power
single-phase 10 A wall plug	2.3 kW
single-phase 16 A charger	3.7 kW
single-phase 32 A charger	7.4 kW
three-phase 16 A charger	11 kW
three-phase 32 A charger	22 kW

Table 2.1: Possible AC charging options.

Next to the specification of the AC charger, the specification of the EV is decisive on the maximum charging speed. A Tesla Model 3 is limited to 11 kW charging power, whereas the Model S and X contain a 16.5 kW on-board charger. Smaller cars like the Skoda CITIGOe-iV contain an on-board charger with a maximum power of 7.2 kW. These restrictions only hold for AC charging, DC fast charging is independent of this since it bypasses the on-board charger. From public charging point data we know that the main charging power levels currently used are 11 kW and 3.7 kW, and that the 11 kW share is increasing over the past few years, shown in Figure 2.6. Charging at levels over 11 kW is not common. For the remainder of this thesis, we focus on the two main power levels of BEV charging: single-phase 16 A (3.7 kW) and three-phase 16 A (11 kW).

Charging at home

"An estimated one-third of the Dutch households have access to a private parking space", according to the department of the RVO that studies electrical mobility in the Netherlands, when asked. We assume that all detached and duplex houses have the luxury of a privately owned driveway and thus have the possibility of charging their EV on their own property with their own charger, either single-phase or three-phase. A part of the terraced and corner houses also have this possibility. The other part of terraced and corner houses do not have a privately owned driveway. They either park down the street and charge at a semi-public charging pole or end up in a situation like in Figure 2.7, where an EV owner powers his vehicle via a charging cable that runs over the ground in the public space. Up until today, it is up to local government how to deal with these private charging cables in public space. Some municipalities allow it, but in some municipalities it is forbidden, like in the town of Wijchen, where a law allowing these situations got rejected [22]. Residents of apartment buildings may have access to a private parking garage where they can install a private EV charger or may use a public charging point near their house.

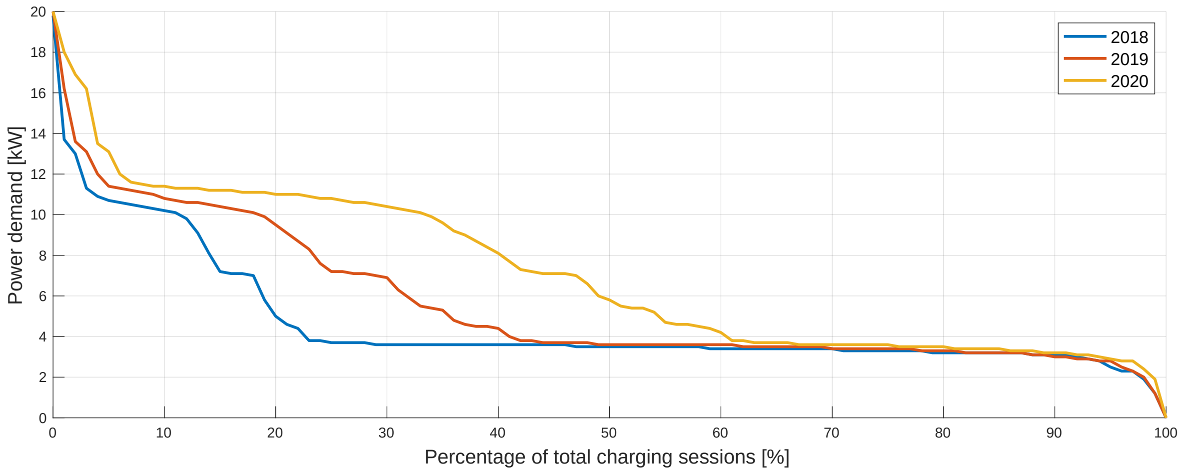

Figure 2.6: Charging data from public charging points show a trend toward higher power demand per EV [21]. Note that the power distribution for the year 2020 is based on the charging data from the first two months of the year.

Figure 2.7: Situation in the town of Wijchen, where an EV owner powers his EV via a charging cable that runs from out of his house, through the public space, into his EV that is parked on a public parking spot [22].

2.3.4 Smart Charging

Smart Charging (SC) is an umbrella term for all kind of techniques that allow controlled charging of EVs with the aim to minimize the likelihood of electricity grid overload or failure, but also to ensure that EVs are charged properly and on the right time according to mobility demands. The ElaadNL foundation aims to introduce the SC charging concept into Dutch society and recently published their 'Smart Charging Guide' [19] describing the latest progress and adoption of SC in the Netherlands. There are various ways of implementing SC, but they all share the same common goal: to reduce peak load by controlling the power level of EV chargers to prevent overloading of the local LV grid without reducing the experienced comfort level of EV drivers. In this thesis, we mainly look at uncontrolled EV charging to determine the limit (in terms of EV penetration rate) of the current LV grid. SC might help to extend this limit significantly.

Adoption of smart charging

The idea of smart charging can be widely adopted, *if* the user has the possibility to 'overrule' the smart charging system. People do not expect to use this function often, but want to have the possibility, according to a Dutch EV driver study [15]. A recent UK study [23] interviewing 60 users and prospective users of EVs shows that two-thirds prefer user-managed charging (UMC) over supplier-managed charging (SMC) because of better personal control. This studies imply that, when properly implemented and a 'overrule' button is available (either at a penalty or not), EV users are open for smart charging options.

2.3.5 Available BEV models and features

Up to and including 2016, the Dutch EV market was mainly dominated by PHEV. This ended when the government cut tax advantages for this category of EV because users were barely using the charging plug of the vehicle, so the environmental advantage was minimal. This is shown in Table 2.2: the number of registered PHEV is stable, while total BEV registrations increase steadily. The total share of FCEV is still very small, which has multiple reasons, one of them being the fact that the Netherlands only has 3 publicly accessible hydrogen refueling locations in Rhoon (near Rotterdam), Helmond and Arnhem [2]. Furthermore, hydrogen as energy energy carrier (using currently available production and storage methods) is less efficient compared to a battery as energy carrier.

	31-12-2016	**31-12-2017**	**31-12-2018**	***30-11-2019***	**31-12-2019**	**30-06-2020**
BEV	13,105	21,115	44,489	84,372	107,536	122,195
FCEV	30	41	50	177	215	265
PHEV	98,903	98,217	97,702	96,010	95,885	99,642
Total	122,083	119,373	142,736	180,559	203,636	222,102

Table 2.2: Number of electric passenger cars registered in the Netherlands [2].

The total number of passenger cars in the Netherlands is currently approximately 8.5 million, thus the current penetration rate of BEVs and PHEVs together is approximately 2.6%. The BEV and PHEV market share in June 2020 is 11.3% and 4.5% respectively. An interesting finding in Table 2.2 is the peak in BEV sales in December 2019, just before the government tax advantages were sobered down for 2020: the 'bijtelling' arrangement went from 4% to 8%, meaning that it becomes more expensive to drive cars in that arrangement. More than half of these sales in December 2019 are Tesla Model 3's, the most popular BEV in the Netherlands at that moment. For the Model 3, the new tax rules resulted in a net cost increase of about €1000. [24] This indicates that tax incentives still play a major role in the adoption of EV. A further breakdown of these BEV registrations show the following top 10 most popular models in the Netherlands up to and including June 2020 as shown in Table 2.3.

This overview is relevant since it shows the models that are available in the future composition of the Dutch BEV fleet. The most important specifications like availability, usable battery capacity, AC charger capacity, expected range and catalog price for a number of popular models are depicted in Table 2.4.

Position	Make/model	Number	Since last month (MtM)	Since the same month previous year (YtY)
1	*Tesla Model 3*	32,597	+722	+26,534
2	*Tesla Model S*	12,849	-28	+205
3	*Nissan LEAF*	9,678	+100	+2,794
4	*Volkswagen e-Golf*	8,988	+332	+3,739
5	*Hyundai Kona*	7,695	+357	+4,781
6	*BMW i3*	6,735	+75	+2,190
7	*Renault Zoe*	6,654	+149	+2,109
8	*Kia Niro*	6,130	+548	+4,296
9	*Tesla Model X*	5,203	+19	+507
10	*Jaguar I-Pace*	4,338	-1	+711

Table 2.3: Top 10 BEV models registered in the Netherlands up to and including June 2020 [2].

Model	Available	Usable capacity [kWh]	AC charger kW]	Range [km]	Price NL
Tesla Model 3 LRDM	now	72,5	11	460	€ 59.998
Tesla Model 3 SR	expected	40	11	265	€ 43.500
Tesla Model 3 SR+	now	47,5	11	315	€ 49.998
Tesla Model 3 LR P	now	72,5	11	445	€ 65.598
Tesla Model S LR	now	95	16,5	525	€ 88.818
Tesla Model S P	now	95	16,5	510	€ 105.718
Tesla Model X L	now	95	16,5	460	€ 94.618
Tesla Model X P	now	95	16,5	445	€ 110.818
Tesla Model Y LRDM	from 2021	75	11	425	€ 65.018
Tesla Model Y LR P	from 2021	75	11	410	€ 71.018
Nissan Leaf	now	36	3,6	220	€ 36.990
Nissan Leaf e+	now	56	6,6	330	€ 45.850
Volkswagen e-Golf	now	32	7,2	190	€ 34.295
Volkswagen ID.3 SR	late 2020*	45	7,2	275	€ 30.000
Volkswagen ID.3 MR	late 2020*	58	11	345	€ 40.000
Volkswagen ID.3 LR	late 2020*	77	11	450	€ 47.500
Volkswagen e-Up!	now	32,2	7,2	200	€ 23.475
BMW i3	now	37,9	11	235	€ 42.411
BMW iX3	late 2020*	74	11	350	€ 70.000
Hyundai Kona E 39	now	39,2	11	250	€ 36.795
Hyundai Kona E 64	now	64	11	400	€ 41.595
Renault Zoe ZE50	now	52	22	320	€ 33.590
Jaguar I-Pace	now	84,7	7,4	370	€ 81.800
Hyunday IONIQ	now	38,3	7,2	260	€ 36.995
Audi e-tron 50 quattro	now	64,7	11	285	€ 71.900

Table 2.4: Most relevant specifications for currently and soon to be available BEVs [25].

Chapter 3

Modeling

3.1 Introduction

To simulate future scenarios of EV penetration rates in the Netherlands, the software package DEMKit [26] is used, together with the Artificial Load Profile Generator (ALPG) [27]. The Decentralized Energy Management toolKit (DEMKit) is a software tool developed at the University of Twente for research on smart grid technologies. DEMKit offers a framework to simulate complete neighborhoods equipped with commonly available technologies like photovoltaic (PV) installations, heatpumps, battery systems, electric vehicle charging and other devices e.g. washing machines and dishwashers. As input for these simulations, reliable household consumption profiles and usage patterns are necessary, which are generated by the ALPG.

To ensure flexibility when simulating different scenarios, we choose to subdivide the model in different entities. These entities then can be altered separately without modifying the entire model. We start with a model of the physical LV grid, described in Section 3.2. The LV grid model carries information on the physical LV feeders, such as cable type, cable length, topology and number of connections. Next is the so-called 'Household load model', described in Section 3.3. This model takes demographic information as input and translates this by using the ALPG to household load profiles. This allows us to quickly adapt the model to all kinds of circumstances and neighborhoods. Section 3.4 describes the implementation of EVs and the corresponding modeling inputs. Section 3.5 describes the implementation of PV. Section 3.6 describes how we define a blackout on an LV feeder.

Defining EVs and PV installations as a separate device load next to the uncontrollable household loads instead of including them in the uncontrollable household loads makes it possible to increase or decrease the penetration rate of these technologies independently. The different loads are placed on a grid topology to simulate and analyze the outcomes of such combinations. A schematic for these four entities is given in Figure 3.1.

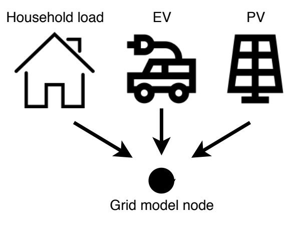

Figure 3.1: The four entities of the presented model.

3.2 Grid model

As described in Section 2.2, the Dutch LV distribution net consists mostly out of radially designed nets. This section describes the way that the LV grid is modeled for this thesis. The relevant DEMKit features used in this thesis are introduced here, starting with the general construction of an LV grid model for a neighborhood, consisting of nodes representing the households and connections between the nodes representing the cables. Furthermore, nodes representing transformers or cable junctions may be added. This allows the user to build virtually every possible radial network configuration by adding different nodes and branches. The main advantage of this structure is that it allows us to determine what happens anywhere in the simulation of a local LV grid. DEMKit furthermore contains options for load flow modeling, which makes it convenient to analyze voltage levels at every node and detect possible exceeding of boundaries.

3.2.1 Nodes and connections

The LV grid model in DEMKit has a tree-like structure with the transformer as the root node (see Figure 3.2). For the other nodes and the connections between the nodes the following holds:

- All nodes are identified by a unique number;
- the nodes itself do not have any physical attributes with respect to the grid model;
- all leaf nodes represent houses that can host loads in the form of appliances;

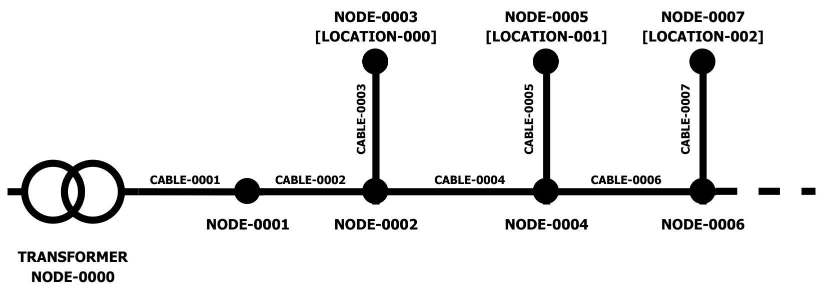

Figure 3.2: DEMkit basic grid structure.

Each leaf node represents a position that can host a load in the form of a household load profile (with an optional EV or PV installation), see Figure 3.3. These household load profiles vary with different household configurations and are further explained in Section 3.3. When in this thesis is stated that we place EVs or PV installations in 'the end of the feeder', we mean that we place these loads on the available positions on the feeder starting from the last position on the feeder (as seen from the transformer) working towards the transformer. Similarly, when we state that we place loads 'from the beginning' of the feeder, we place the loads on the feeder by starting at the first position (as seen from the transformer) towards the end. E.g. if we place two EVs 'from the beginning' of the feeder or 'on the first positions', we place the EVs on *NODE-0003* and *NODE-0005* in Figure 3.3, i.e. the first available positions for such loads.

3.2.2 Cables

The cables are specified as a conductor by a basic *pi-model* [11] without the capacitance effect, resulting in a series impedance Z in ohms (Ω) per kilometer for each conductor:

$$Z = R + jX \tag{3.1}$$

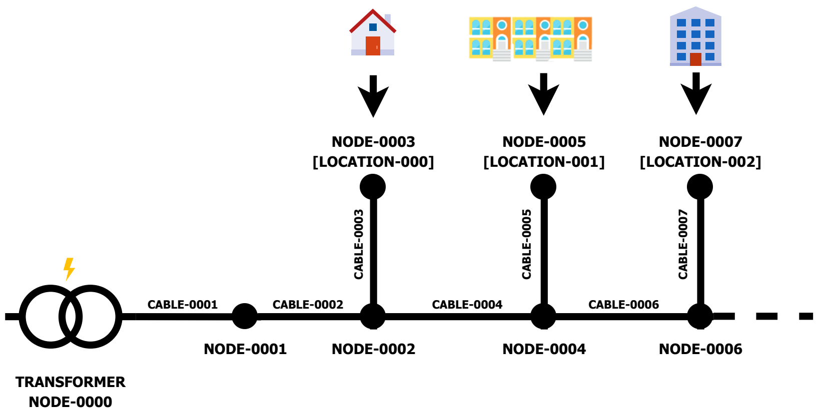

Figure 3.3: DEMkit grid model with loads.

where R describes the resistance of the conductor in ohms (Ω) per kilometer cable and X describes the reactance of the conductor in ohms (Ω) per kilometer cable. Furthermore, every cable type has a nominal current capacity in [A] which should not be exceeded for longer periods of time. Table 3.1 shows the parameters used for the different types of cables. The type of cable is described with a number for its cross section in mm^2 and a notation for the material, either Al for aluminum or Cu for copper. Note that the actual resistance and reactance also depend on surrounding temperature, moisture content of the ground in which the cables are located and the physical condition of the cables. However, to reduce the number of parameters in the model, this approach with standardized values [11] is considered sufficient. The length of the cables is dependent on the specific grid structure topology.

Type	R [Ω/km]	X [Ω/km]	Capacity [A]
50 Al	0.64	0.088	115
70 Al	0.44	0.085	130
95 Al	0.32	0.082	175
150 Al	0.21	0.079	230
35 Cu	0.53	0.074	100
50 Cu	0.39	0.072	125
70 Cu	0.27	0.070	155
95 Cu	0.19	0.069	190
150 Cu	0.13	0.063	255

Table 3.1: Cable properties used in the model [11].

3.2.3 Low voltage network topologies

Every LV feeder in the Netherlands may be more or less unique in terms of its properties such as cable type, cable length and the number of connections to the cable. However, many of these feeders are also very similar to each other and it is useful to exploit this feature. A 2015 CIRED paper on clustering of LV networks [28] describes a method to cluster a large number of feeders with different properties and create a smaller set of 'generic' feeders that can accurately describe the original set. Figure 3.4 shows the distributions of feeder length, customers per feeder and cable types of the original dataset. From 88,000 feeders in the network of a Dutch DSO, the researchers were able to construct a generic feeder set of only 94 classes using a fuzzy k-means clustering approach. With the 26 most common clusters, we are able to reconstruct 71.3% of the total LV network of this specific DSO. The PhD thesis [29] that also contains this work describes the full list. Note here that the original source data is already somewhat outdated, so it is not possible to draw conclusions on the state of the LV grid of the specific DSO. However, this research is considered relevant and detailed enough to give an estimation on the main feeder configurations used in the Dutch LV grid. Note that, in practice, feeders might consist of segments with different cable types and thicknesses, as was mentioned in Section 2.2.1, but that this is too detailed to use in the proposed modeling method, so all main feeder cables are modeled as a single main cable type. Also, all clusters are considered to be a single piece of main cable with all houses attached to it, i.e. without any branches. The length in between the connections is specified as the average length, thus dividing the total feeder length by the number of connections. For the remainder of this thesis, all these generic feeders are described using these features and referred to as a Cluster with a corresponding number.

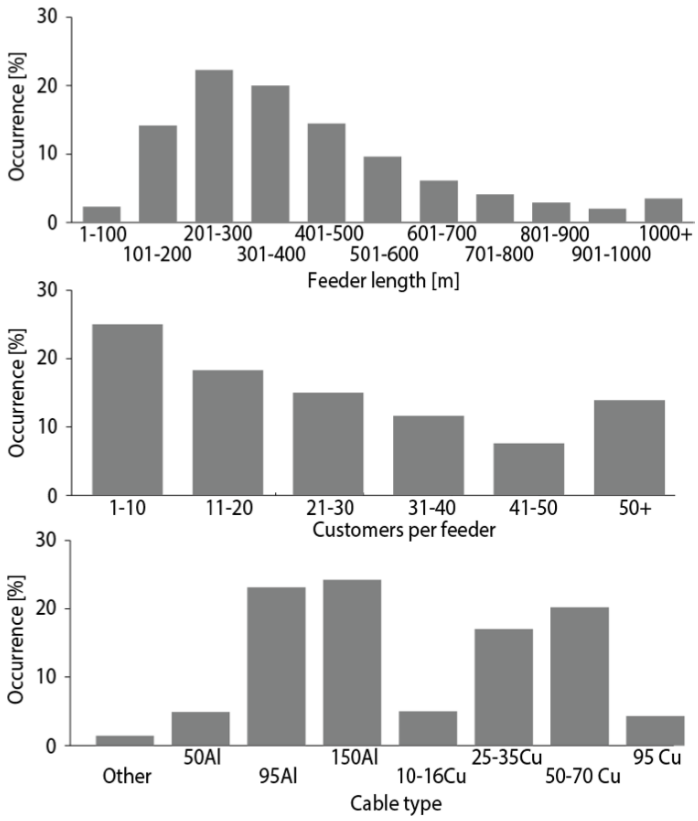

Figure 3.4: Distribution of the feeder length, customers per feeder and cable types in the LV grid of a Dutch DSO [28].

3.2.4 Residential connections

The residential consumer can choose the different connections at Liander (the largest network operator in the Netherlands) given in Table 3.3. These connections are also available at other locations and network operators in the Netherlands (with only minor differences), so these connections listed in Table 3.3 are considered to be the standard. Heavier connections are possible in the LV grid in the form of 3x50 A, 3x63 A and 3x80 A, however these are aimed at small shops and businesses and thus are not considered here. Both in real life and in the model, loads can either be connected to one of the three phases in a single-phase connection or are connected using a three phase connection to divide the loads over the three phases. For PV installations above 3.7 kW and/or EV chargers above that limit, a three-phase connection

Cluster	Length [m]	Main cable type	Total household connections [#]	Occurence [%]
01	150	150 Al	17	6.4
02	270	70 Cu	24	4.5
03	266	95 Al	39	4.5
04	218	50 Cu	19	4.4
05	362	150 Al	32	4.1
06	290	50 Al	26	3.4
07	386	95 Al	49	3.4
08	633	150 Al	70	3.3

Table 3.2: First eight most common feeder clusters [28].

is advised by DSOs, so in our model, houses with these installation sizes receive a three-phase connection, all other houses receive a single-phase connection.

In case of single-phase connections to a MV/LV transformer, the preferred situation for the DSO would be that the houses on a feeder would all be divided uniformly over the different phases, since this reduces load-balancing problems. In practice, this is not always the case and the exact distribution is not known. In this thesis, the distribution of single-phase connections over the different phases is done uniformly unless mentioned otherwise.

Modeling assumption 1. *Households with PV installations and/or EV chargers rated 3.7 kW or above, a three-phase connection is required.*

Modeling assumption 2. *All single-phase connections are divided uniformly over the households unless mentioned otherwise.*

Configuration	Power	Number of connections in NL	Features
Single-phase 40 A	9,2 kW	*"Still very common in a lot of houses"*	*"Standard appliances + small number of PV panels*
Three-phase 25 A	17 kW	*"One in three houses"*	*"For additional PV, heat pump and EV charging"*
Three-phase 40 A	27 kW	No information	*"Additional power for e.g. sauna/jacuzzi"*

Table 3.3: Most common type of residential connections in the Netherlands according to Liander [30].

3.3 Household load model

This section describes the implementation of the household load model. Section 3.3.1 introduces the functionality of the tool that is used to simulate household power profiles. Section 3.3.2 describes the coupling between the available demographic data and the inputs for the ALPG.

3.3.1 Energy load of a house

The energy load of a house depends on the type of house and its residents. A household can consist out of adults, either jobless, working (part- or full-time) or retired, students and children. A set of these persons together form a household. The annual consumption of these households follows a Gaussian distribution with the mean and variation listed in Table 3.4. The Artificial Load Profile Generator (ALPG) then takes care of creating a realistic power profile while incorporating the average annual consumption, extensively described in [27]. The ALPG incorporates a realistic household load based on all commonly available household equipment i.e. fridges, washing machines, televisions, computers, lighting etc. and simulates flexibility and user behavior by incorporating different types of persons within households. It creates pseudo-random schedules with varying leave and arrival times, also accounting for random family outings e.g. shopping trips. The ALPG outputs all necessary data of day-to-day household activity that is representative for an actual household power consumption curve. Furthermore it allows for operation of control mechanisms by communicating about possible flexibility in the form of outputting start-times and end-times of all equipment.

Household type	Annual consumption	Persons (Adults)
Single worker	2010 ± 400 kWh	1 (1)
Dual worker	3360 ± 700 kWh	2 (2)
Family dual worker	5260 ± 1800 kWh	3 - 6 (2)
Family single worker	5260 ± 1800 kWh	3 - 6 (2)
Family single parent	4400 ± 1800 kWh	2 - 5 (1)
Dual retired	3360 ± 700 kWh	2 (2)
Single retired	2010 ± 400 kWh	1 (1)

Table 3.4: Predefined household configurations [27].

To show the impact of different household configurations, simulations of a neighborhood consisting of 39 households of the same type were done. In these simulations no PV and EV was included. Note that this is a rather extreme case, since it is unlikely that every household on a feeder is of the same type, but this example is used to indicate the significant differences between the different household configurations. Figure 3.5 shows the summed meter output of each of the household sets. Severe peak load differences are possible as seen in Figure 3.6 e.g. of 35 kW between the *Family dual parent* and *Single retired* set. This stresses the importance of the different base load scenarios since this peak load difference can in theory make room on a feeder for e.g. three 11-kW EV chargers (or e.g. ten 3.7-kW chargers!).

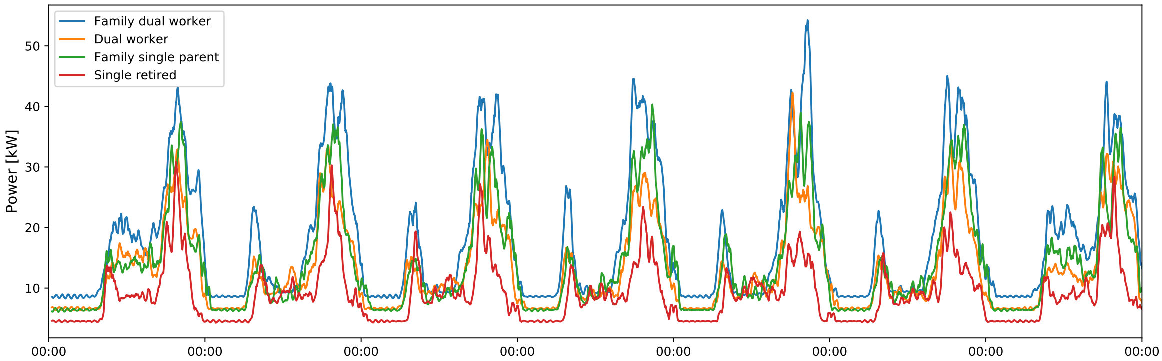

Figure 3.5: One week of simulations on sets of 39 of the same household types: 30-minute average. These simulations are done without any EV or PV installation.

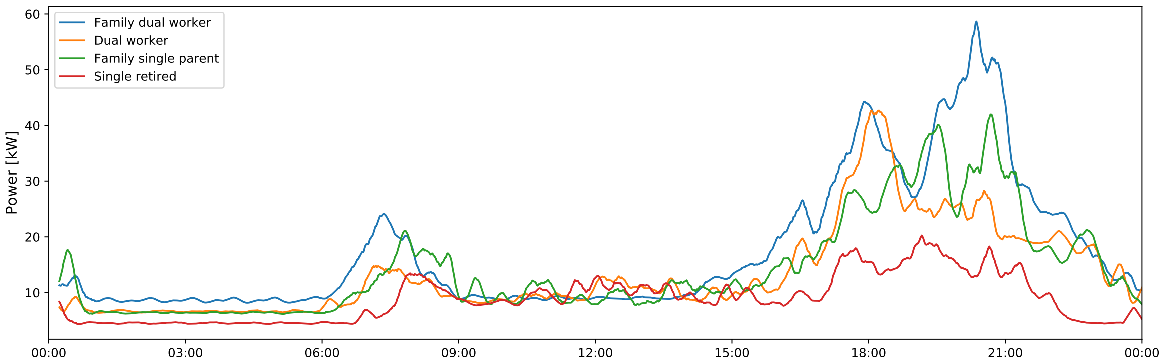

Figure 3.6: One day simulation on sets of 39 of the same household types: 15-minute average. These simulations are done without any EV or PV installation.

3.3.2 Demographic inputs

The Dutch Central Office for Statistics ('Centraal Bureau voor de Statistiek' (CBS)) publishes the annual report 'Kerncijfers wijken en buurten' ('Key figures for neighborhoods') [31]. This data set contains information on the main demographic statistics of every individual neighborhood in the Netherlands and is used as the basis for the demographic classification in this thesis. It distinguishes between five main types of houses and three main types of households. The most recent complete data set originates from 2017 and is used in this thesis. This section describes the considerations and assumptions needed to classify the type of houses and households.

Type of houses

The following five housing types are distinguished by CBS:

- Detached house or 'vrijstaand huis';
- Duplex house or 'twee-onder-één-kap-woning';
- Terraced house or 'tussenwoning';
- Corner house or 'hoekwoning';
- Apartment houses.

Next to this classification, CBS registers the average market value of the houses and the percentage of single-family and multiple-family houses in all individual neighborhoods in the Netherlands. A single-family house is defined as a house that forms one physical building, so basically every detached, duplex, terraced and corner house. Multiple-family houses are defined as houses that form a building together with other houses, so these classify as apartments. The data set contains information on age classes and also distinguishes between single- and multiple person households, households with and without children and lists an average household size. Another advantage of the CBS data set is that it contains data on income and details about vehicle possession. These features can be used as base to make assumptions about the adoption of EV in different locations.

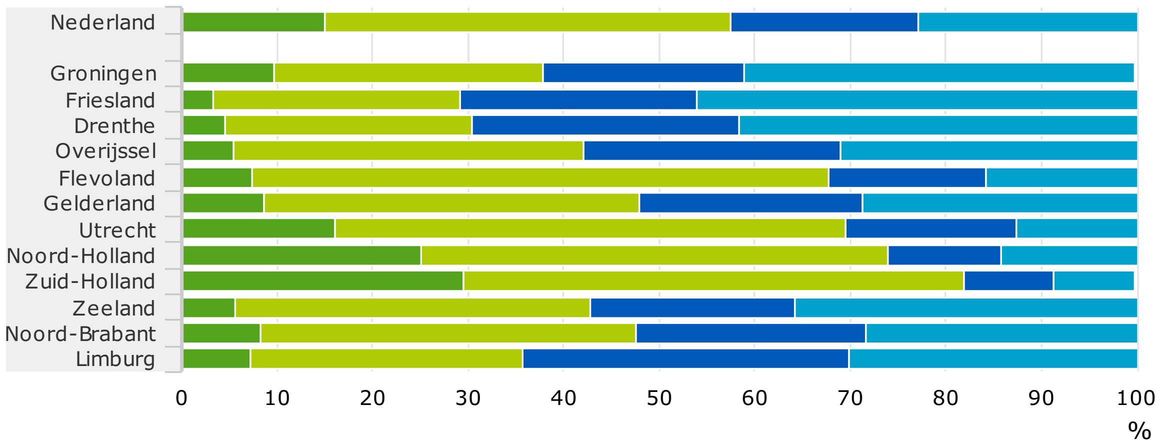

Figure 3.7: Type of houses of per province and for the whole of the Netherlands [32]. Dark green represents apartment houses, light green are terraced and corner houses, dark blue represents duplex houses and light blue represents the detached houses.

Figure 3.7 shows the type of houses per province and for the whole of the Netherlands. The large majority of 42.5% of the Dutch people live in a terraced or corner house, 23% live in a detached house, 19.6% live in a duplex house and the remaining 14.9% of the people live in an apartment.

Type of households

On January 1, 2017, the Netherlands counted 7.8 million households. CBS classifies these households in three main groups: single-person households, multiple-person households with children and multiple-person households without children, according to the following definitions:

Definition 1. *A single-person household is a household consisting out of one adult person.*

Definition 2. *A multiple-person household with children consist out of un-married pairs with children, married pairs with children and 1-parent households.*

Definition 3. *A multiple-person household without children consist out of un-married pairs without children, married pairs without children and all other households.*

The ratio between for the whole of the Netherlands between those three classifications is 38% for 1-person households, 33% for multiple-person households with children and 29% for multiple-person households without children. To couple this demographic data of the CBS to the ALPG models of Section 3.3, additional general CBS classifications are used:

- Of the multiple-person households with children, 22% is a single-parent household, classifying 7% of the total households as *FamilySingleParent*.
- About 80% of the couples in the Netherlands are two-earners (called dual workers in the model), which is used to distinguish between *FamilyDualWorker* and *FamilySingleWorker*.
- About 27% of the total households in the Netherlands receive AOW (general retirement fund), meaning at least one of the persons in the household has retired. Of these retired households, 40% (about 11% total) is classified as *SingleRetired* and 60% (about 16% total) is classified as *DualRetired*.
- We assume that adults that have not yet retired and are living in a single-person household or as a couple without children all either work or study, so the remaining households are classified as *SingleWorker* or *DualWorker*. We do not consider a separate household model for jobless people: we assume their energy usage comparable to households with working people. In theory, jobless people might even consume more energy since they might be in the house more often, but this group is assumed to be too small to have a large impact on the final results, thus we choose to not unnecessarily complicate the model.

Adopting these classifications makes it possible to introduce the 'classification factors' of Table 3.5 to quickly adapt the model inputs per location: we choose a neighborhood out of the 'Kerncijfers wijken en buurten', we read out the household ratios and then apply the classification factors. The result is a load model that represents the demographic distribution in that particular neighborhood. For the whole of the Netherlands, the result is shown in Figure 3.8.

CBS 'Kerncijfers Wijken en Buurten'	Classification factor	ALPG model
Single-person	0.29	*SingleRetired*
	0.71	*SingleWorker*
Multiple-person with children	0.21	*FamilySingleParent*
	0.64	*FamilyDualWorker*
	0.15	*FamilySingleWorker*
Multiple-person without children	0.55	*DualRetired*
	0.45	*DualWorker*

Table 3.5: Household type classification factors.

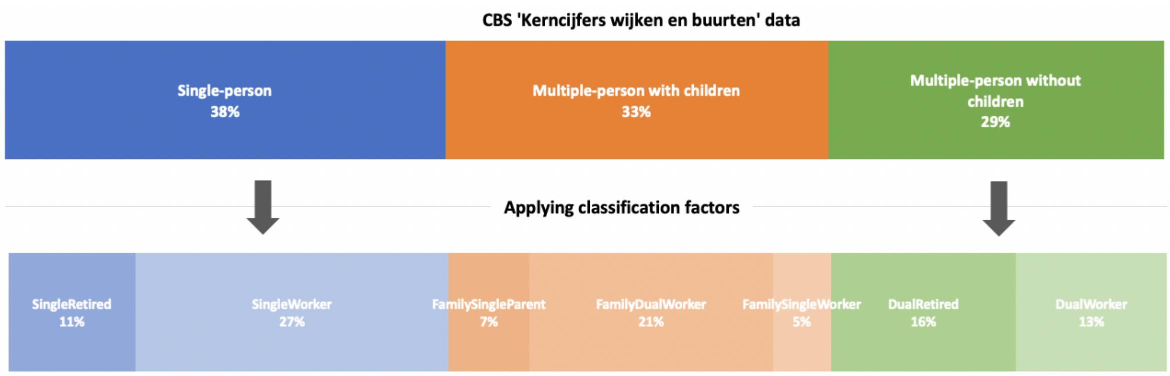

Figure 3.8: The demographic household distribution for the Netherlands.

3.4 Electric vehicle model

This section describes all methods and inputs used for the modeling of EVs in this thesis. Section 3.4.1 introduces the main parameters and connection to the rest of the model structure. Section 3.4.2 describes a definition on 'charging behavior' to get an indication on how, when and where people charge their EVs. Section 3.4.3 introduces the used method and data to model the EV charging probability based on plug-in time data and charging time duration data of a UK-based project that involves Nissan LEAFs. Section 3.4.5 introduces a dataset provided by *ElaadNL* that can also serve as a plug-in time distribution for the proposed model.

3.4.1 Main parameters

An EV can be assigned to an individual household. As mentioned in Section 2.3.3, the EV charging options are restricted to either a three-phase (3x16A) 11 kW charger or a single-phase (1x16A) 3.7 kW charger. The outputs of the ALPG for the EV model are the departure time in the morning, plug-in time in the evening and the required charge in Wh. This is sufficient information for DEMKit to simulate EV usage: when no control mechanism is applied, charging always starts at the earliest possible time at the maximum available charging power and the EV always charges to full when connected.

3.4.2 Charging behavior

Charging behavior is defined as the way that people use the available charging infrastructure and is related to the charging power, battery capacity and the number of kilometers driven (or energy needed): the Dutch driver study [15] mentioned earlier confirms that the charging frequency is negatively correlated to battery size. Tesla Model S owners with large battery packs charge significantly less often than Nissan LEAF (with only a 24 kWh battery pack) drivers do: 62% of the Model S drivers state that they charge no more than three times per week, while 80% of the LEAF drivers state they charge four to six times a week.

Statistical analysis of EV charging behavior

Statistical analysis of 221 Nissan LEAF users spread across the United Kingdom [33] gives insight into charging behavior, using data from the My Electric Avenue (MEA) [34] project. Probability density functions (PDFs) of the number of connections per days, start charging time, initial SOC and final SOC per connection for both weekdays and weekends have been created that are very useful in simulating and verifying actual EV charging cycles. Approximately 70% of the EVs connects once a day, typically when the SOC is between 25 and 75% and approximately 65% of the EVs finish their first daily charging session with a full battery. Downside of this research is that it only concluded Nissan LEAF models with a limited battery capacity of 24 kWh, which is rather small compared to e.g. the popular Tesla models with capacities of 40 to 95 kWh. Another research project using real-world EV charging session data from a charging-at-home field trial in Flanders with about 8.5k charging sessions (iMove) and a large-scale EV public charging pole deployment in The Netherlands (ElaadNL) with 90k charging sessions [35] found three distinct charging behaviors:

- *Charge near home*: arrival mostly late in the afternoon and evening, departures mostly in the morning with long sojourn times averaging over 15 hours, sometimes multiple days.
- *Charge near work*: arrivals early in the morning, departures in the late afternoon with sojourn averaging around nine hours. Probably people that park and charge their car at work or at commute points e.g. near train stations.

- *Park to charge*: short sojourn times averaging a little over three hours lasting not much longer than the time that was required to charge the battery. The research paper hypothesizes that these people park specifically with the aim to charge their EV battery.

Since the iMove project considers only home chargers, the *park near work* behavior is not seen in that data. For the ElaadNL dataset used in [35], considering only public charging poles, the researchers hypothesize that people in the *charge near home* cluster are people that live nearby the public charging pole and park their car overnight. An interesting finding is the ratio of *charge near home* (59.1%) and *park to charge* (40.9%) for the iMove charge-at-home trial, implying that only three out of five charging sessions is overnight, with the remaining sessions scattered over the day.

3.4.3 Modeling EV charging probability

Charging an EV is defined as an EV charging session, consisting out of two parameters that influence the outcome of such a session to the system: the start time of the charging session and the duration of the charging session, which is directly related to the required energy and the charging power. To demonstrate the model, we consider a street with a certain number of EVs, somewhere in the Netherlands. To determine the probability that an EV somewhere in the street is charging, we assume a charging session as an independent event that has a probability distribution. With the two main parameters, plug-in time $\mathrm{p_{plugin}}$ and charging duration $\mathrm{p_{duration}}$, it is possible to define the probability that an EV in the system is charging in a given discretized time interval. For evaluating $\mathrm{p_{plugin}}$ and $\mathrm{p_{duration}}$, data from the UK-based project My Electric Avenue (MEA) [34] is used. Figure 3.9 shows the hourly probability distribution of EV start charging times, $\mathrm{p_{plugin}}$, from the MEA project.

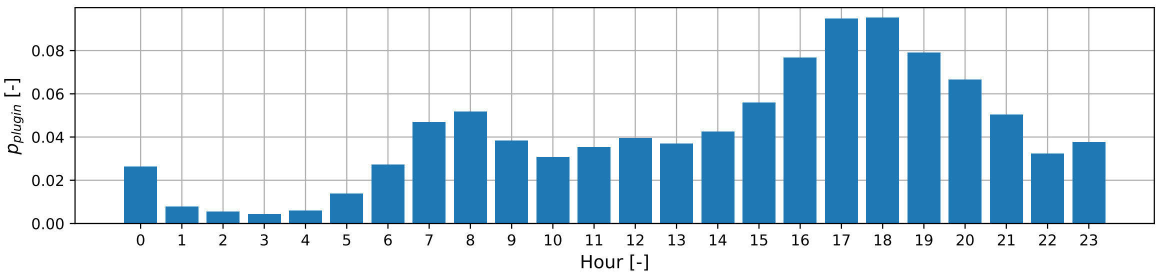

Figure 3.9: Hourly probability distribution of the EV start charging times $\mathrm{p_{plugin}}$ for weekdays. Start charging in hour 8 is defined as plugging in between 08:00 and 08:59.

Next to this start charging time, the time the EV actually spends charging is necessary to define the status of the EV. For each charging session in the data set, the length is known. If we bin these charging sessions into 1-hour bins, we know how many EVs stop charging every hour and what the probability is that an EV is still charging after a certain number of hours since the start of the charging session. At hour 1, the probability an EV is charging is 1, since it just arrived to the system. At hour 2, some EVs have already finished charging and are leaving the system and the probability that it is still charging is 0.776. The distribution for this is called $\mathrm{p_{duration}}$ and is shown in Table 3.6.

1st hour	2nd hour	3rd hour	4th hour	5th hour	6th hour
1.000	*0.776*	*0.624*	*0.474*	*0.324*	*0.195*

Table 3.6: Probability $\mathrm{p_{duration}}$ showing the probability that an EV is still charging after n hours.

Combining p_{plugin} and p_{duration} by multiplying them results in Table 3.7. This value is called $p_{\text{EVcharging}}$ and describes the probability that an EV is charging at that specific moment.

$$p_{\text{EVcharging}} = p_{\text{plugin}} \cdot p_{\text{duration}} \tag{3.2}$$

Consider the following example: for every EV in the system it holds that at e.g. 16:00, the probability is 0.077 that it is charging, which is directly related to the probability distribution of the start charging times in Figure 3.9. For the next time intervals, this start charging probability p_{plugin} is multiplied by the probability it is still charging in the next time interval, p_{duration}. Using this approach, we can calculate the probability that an EV is in the charging state is the highest in the 19:00-20:00 time slot.

EV arrival time \ Time of day	*15:00*	*16:00*	*17:00*	*18:00*	*19:00*	*20:00*
15:00	**0.056**	0.043	0.027	0.013	0.004	0.001
16:00	0	**0.077**	0.060	0.037	0.018	0.006
17:00	0	0	**0.095**	0.073	0.046	0.022
18:00	0	0	0	**0.095**	0.074	0.046
19:00	0	0	0	0	**0.079**	0.061
20:00	0	0	0	0	0	**0.067**
Probability an EV is charging:	**0.056**	**0.0120**	**0.181**	**0.219**	**0.220**	**0.202**

Table 3.7: Part of the hourly probability distribution for charging of an EV.

Note that by using this approach and modeling charging sessions as independent events, we cannot account for dependent events, such as days when the national team plays a football match. Because the normal schedule of a significant share of the people changes and synchronizes, the proposed probability distributions for plug-in times might not be valid anymore.

3.4.4 Charging time duration as input

Instead of using data of charging events for the charging time duration, we modify the charging duration probability p_{duration} to create a generalized method with inputs for charging power and energy demand. We still use the MEA data of the previous section to define the plug-in time distribution p_{plugin}, but we modify p_{duration} by making it a model input. we also choose a higher resolution (15-minute intervals vs. 60-minute intervals). A 15-minute interval is chosen since we consider this small enough to detect a blackout: overloading a feeder fuse for a short time is often not immediately problematic due to their dynamic rating, but overloading a fuse for longer than 15 minutes can result in a burning fuse. Using the same concept as for the hourly discretized situation, the MEA data on start times of EV charging is binned into 15-minute intervals, resulting in a 15-minute interval plug-in time probability distribution p_{plugin} shown in Figure 3.10.

Now, p_{duration} is not based on the MEA project data anymore, but on a model input t_{charge}, the vehicle charging time, which is based on the number of driven kilometers, per-km energy consumption and charging power. So the plug-in time distribution is borrowed from the MEA project, but the actual charging *duration* depends on chosen inputs. The EV charging time is defined as:

$$t_{\text{charge}} = \frac{s_{\text{driven}} \eta_{\text{EV}}}{P_{\text{charging}}} = \frac{E_{\text{charged}}}{P_{\text{charging}}} \tag{3.3}$$

where s_{driven} is the range in kilometers that is going to be charged into the EV, η_{EV} the energy-efficiency of the EV and P_{charging} defines the charging power. η_{EV} is set at a specific value, so t_{charge} is directly related to the required energy, E_{charged}, and the charging power. For the remainder of this thesis, the traveled

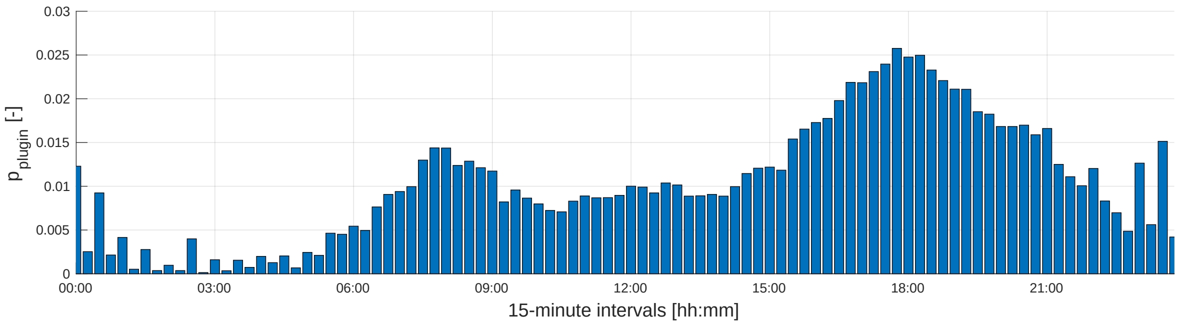

Figure 3.10: Distribution of the EV start charging times p_{plugin} for weekdays. Start charging in interval 18:00 is defined as plugging in between 18:00 and 18:15.

distance, s_{driven} is chosen as a discretized value. Future work may extend the model by introducing e.g. a Gaussian distribution shown in Figure 3.11 for the traveled distance such that the traveled distance varies among the different EVs. The resulting charging time duration probability $p_{duration}$ for this is shown in Figure 3.12.

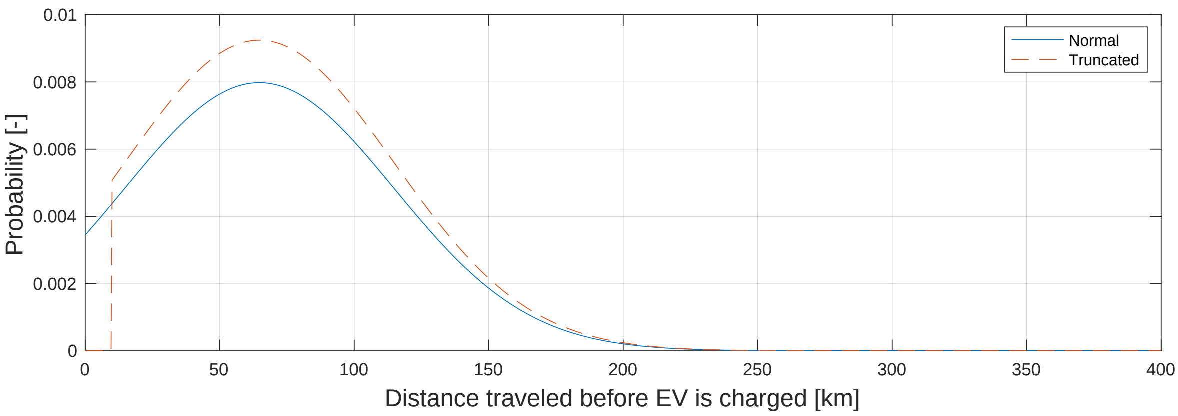

Figure 3.11: Truncated normal distribution of the number of kilometers driven before an EV is charged.

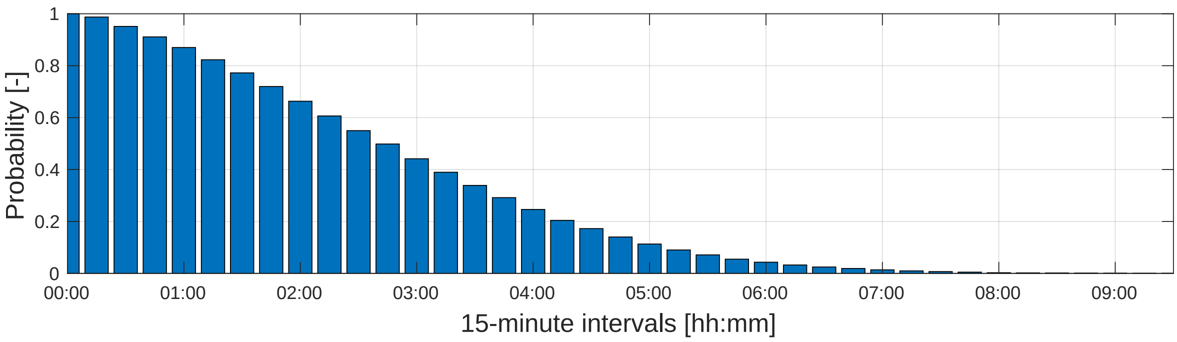

Figure 3.12: Distribution of charging time duration probability $p_{duration}$ for n 15-minute intervals by using the truncated normal distribution as input and a charging power of 3.7 kW.

Again, by multiplying the plug-in time distribution p_{plugin} with the charging time duration $p_{duration}$ we calculate the EV charging probability $p_{EVcharging}$. For the sketched situation, $p_{EVcharging}$ for every 15-minute interval is shown in Figure 3.13. With this information, we can predict the probability that an EV is in the state of charging for any 15 minute timeslot of a day. The graph shows us that during the night from 03:00

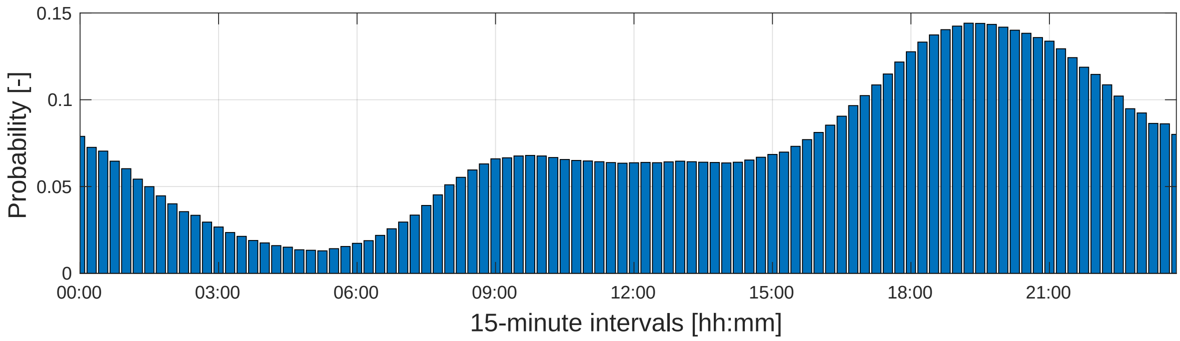

Figure 3.13: Result of the plug-in time distribution multiplied by the charging time duration probability distribution: the probability that any single EV is charging at a specific 15-minute time interval, known as $\mathrm{p}_{\mathrm{EVcharging}}$.

to 06:00 the probability that an EV is charging is relatively low compared to the evening peaks between 18:00 and 21:00. People plug in their EVs more often in the evening, which results in a higher EV charging probability.

3.4.5 ElaadNL dataset

Next to the MEA dataset, a dataset from *ElaadNL* is introduced in this section. This dataset contains ready-made plug-in time distributions for EVs for private and public charging sessions based on large volumes of real charging events. The plug-in time distribution for weekdays is given in Figure 3.14.

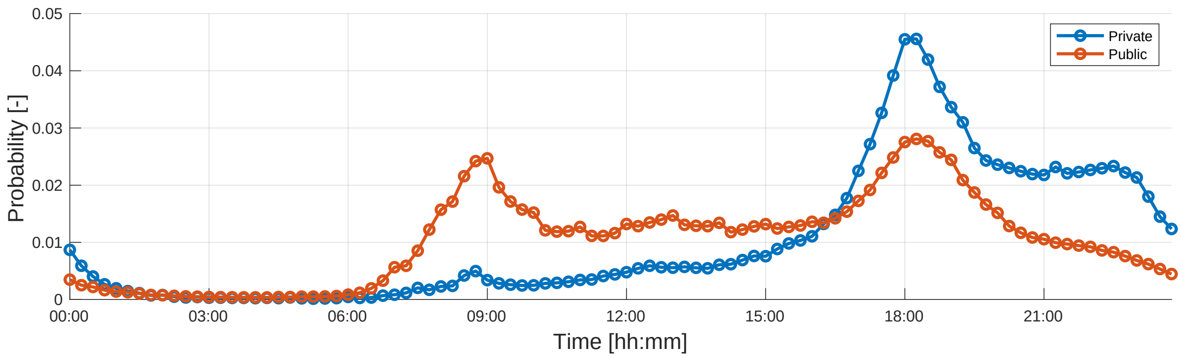

Figure 3.14: ElaadNL dataset on distribution of EV plug-in times on weekdays.

Since public AC chargers are mostly situated in the LV grid, we choose to combine the private and public distributions to create one plug-in time distribution as model input for the remainder of this thesis. From the ElaadNL dataset we also know that the distribution of private and public charging sessions among weekdays is more or less evenly distributed, shown in Figure 3.15. The ElaadNL has a number of advantages over the MEA dataset, since it combines multiple data sources and has more variety in EV models compared to only 221 Nissan LEAF models of the MEA dataset. Furthermore, the ElaadNL dataset is already processed, compared to the MEA data which might contain irregularities. The influence on the proposed model for both the MEA and ElaadNL datasets is compared in Section 4.4.

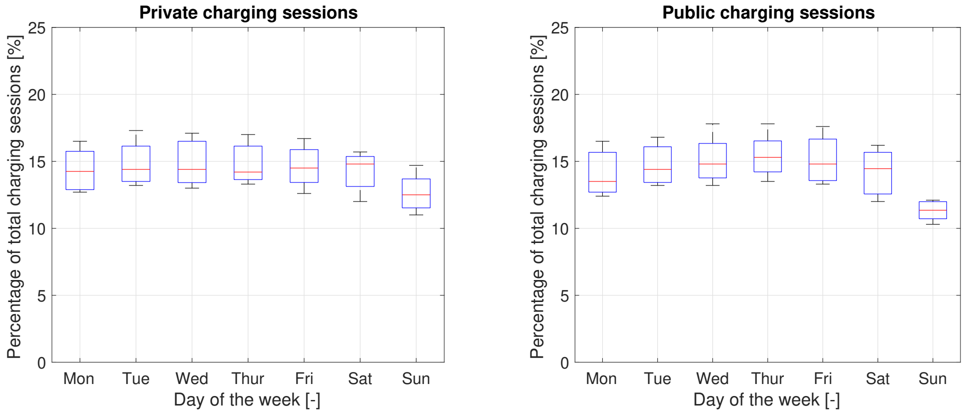

Figure 3.15: Distribution of charging sessions over the days of the week per location type [21]. Note that for both private and public charging, all weekday sessions (Monday to Friday) are distributed almost uniformly over the different weekdays.

3.5 PV production model

The generated PV power is modeled by real-world irradiance data over a full year. The chosen size for the PV installation is based on the current Dutch support scheme based on yearly netmetering. As such, the size is chosen such that the yearly PV production gets close to the expected yearly power consumption specifies by the base load (see last subsection). Furthermore, it is possible to assign a PV setup to each house individually and the rooftop orientation is randomly chosen using a Gaussian distribution, as described in [27]. The PV model takes hourly irradiance data as input and sends a (linear interpolated) minute power profile as output. Note that the irradiance data is directly related to the geographical location, so a set of hourly-irradiance data of the desired location can be used as input. Since the solar irradiance in the Netherlands is quite constant, i.e. people in the southern provinces do not benefit significantly more from their PV installation compared to people in the northern provinces, we chose to use a solar irradiance profile of the region Twente, already included in DEMkit. Note that this production model based on the Dutch netmetering scheme does not include situations in which houseowners install additional PV to compensate for their EV or heat pump consumption.

3.6 LV feeder blackout

An LV feeder blackout is defined as either a capacity overload, i.e. when the maximum power in the feeder is reached, or voltage levels in the feeder drop below the allowed limit. Since reliable data on fuse values in the current LV grid is unavailable because these are determined locally by the applicable situation, the maximum power in the feeder is defined as the maximum nominal current in the feeder cable.

Modeling assumption 3 (LV feeder blackout)**.** *An LV feeder blackout is defined as overloading the LV feeder, either by overloading the feeder cable current carrying capacity or voltage levels either exceeding 253 V or dropping below 207 V.*

3.6.1 Blackouts due to EV charging

If we have a set of n EVs, the probability that K EVs in that set charge in a specific time interval is represented by the probability mass function of a binomial distribution:

$$P(K = k) = \binom{n}{k} p^k (1-p)^{n-k} \tag{3.4}$$

where p is defined as the probability that a single EV charges on a certain time interval (as described in Section 3.4.3). However, we are not interested in the situation of precisely k EVs charging, but in the situation of a possible blackout, where *at least* k EVs charge simultaneously. For this we take the sum:

$$\begin{aligned} \mathrm{p_{blackout}} &= P(K \geq k) \\ &= \sum_{k}^{n} P(K = k) \end{aligned} \tag{3.5}$$

for $K \in \{k \rightarrow n\}$. Note that $\mathrm{p_{blackout}}$ represents the blackout probability for one physical feeder at a certain time interval. To find the total number of local blackouts for the whole of the Netherlands, we multiply $\mathrm{p_{blackout}}$ by the total number of feeders of that specific type. To demonstrate this, we show the results for Cluster 03 in Figure 3.16. Cluster 03 features a 266 meter cable of the 95 Al type with 39 household connections and represents 4.5% of the total network of approximately 300,000 LV feeders. We assume the maximum number of simultaneously charging EVs to be 9. Thus, a blackout occurs at $k = 10$, n varies with the penetration rate. E.g. if $n = 20$, the EV penetration rate is $\frac{20}{39} = 51\%$ and we sum all situations for $K \in \{10 \rightarrow 20\}$, resulting in $\mathrm{p_{blackout}}$ for that specific penetration rate. For the next step, EV penetration rate $\frac{21}{39} = 54\%$, we take $K \in \{10 \rightarrow 21\}$, and so on. In the case of this example, $\mathrm{p} = 0.13$ between 19:15 and 19:30. This means that we assume that all individual EVs in the set have the same charging probability of 0.13 during that time interval. We use Equation 3.5 to calculate the probability that ten or more out of the total set of n households are charging an EV at that time interval. At around 85% EV penetration rate, the probability of a blackout for a single feeder, $\mathrm{p_{blackout}} =$ 0.005 between 19:15 and 19:30. This means that this part of the grid, representing 4.5% of the total feeders, encounters $0.045 \times 300,000 \times 0.005 \approx$ 68 blackouts daily *on that specific time interval* where $\mathrm{p} = 0.13$.

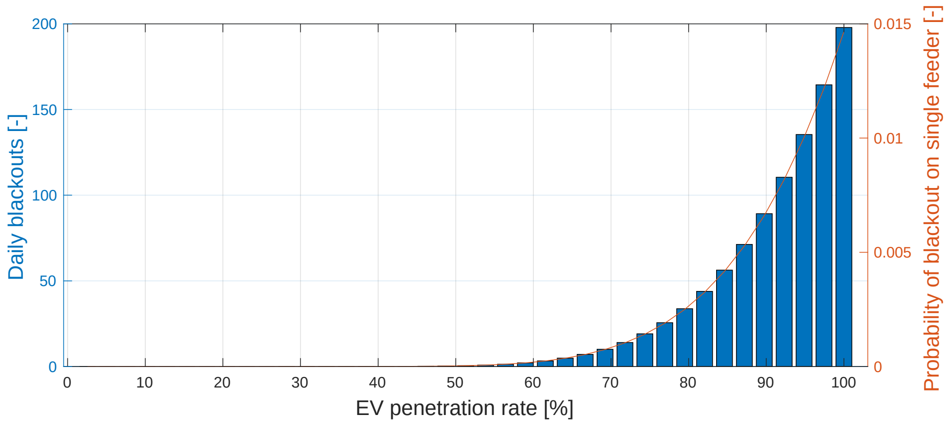

Figure 3.16: Number of blackouts occurring on all Cluster 03 type feeders with $\mathrm{p_{EVcharging}} = 0.13$ and corresponding blackout probability for a single feeder at all possible EV penetration rates.

3.6.2 Maximum PV capacity

Instead of creating blackouts and voltage problems by drawing too much power from the grid when e.g. charging EVs, it is also possible to create voltage problems and even blackouts by injecting too much power into the grid, as was described in Section 2.2.2. Since PV inverters shut down or curtail themselves when the grid voltage rises too high, it is unlikely that these inverters cause severe grid problems. However, this is highly inconvenient for the owner of such a PV installation, since it means a lower than expected yield. In practice, the PV installations with the largest distance to the transformer shut down or curtail first, since the voltage rises the highest in that location. To determine the maximum PV capacity, we choose the day with the highest solar peak irradiance and increase the number of installations on the feeder until either the current or voltage limits are violated. The capacity of the individual PV installations is determined by the Dutch support scheme based on yearly netmetering, as was explained in Section 3.5.

3.7 Summary

This chapter introduced the technical details of the proposed model. By making a direct coupling of demographic data of all areas in the Netherlands with the ALPG, we can quickly adapt the model for different demographic situations. However, assumptions and generalizations were needed to guarantee the flexibility that was aimed for. The separation between the grid model, a basic household load model and an EV and PV model allows for variations in the penetration rates of these technologies and an ease of adaption of LV grid properties.

To assure the usability of the LV grid models for this thesis, several simplifications and assumptions where needed. This was a deliberate choice, since too much details would create too many different situations which would require more research and simulation time. Introducing the clustering approach makes it possible to describe the Dutch LV grid as a whole with only a small set of clusters, without the need for a case-by-case approach for every part of the LV grid.

To model EV charging sessions, two datasets are used, with the ElaadNL dataset as preferred dataset because of its features and the fact that it is already pre-processed. The EV charging sessions itself are modeled as independent events with a plug-in time probability and a charging time duration probability. By estimating the probability that a single EV in the system charges at a certain time interval, we calculate the probability that more than a given number of EVs in a set charges simultaneously. Such a situation is defined as a blackout caused by EV charging and thus identifies the limit in terms of simultaneously charging EVs of all specified clusters. Each of the specified clusters represents a part of the LV grid and the occurrence rate of each of these clusters in the Dutch LV grid is known. We use this to make an estimation of the maximum EV penetration rate for the Netherlands in the next chapter.

Chapter 4

General results

4.1 Introduction

This chapter describes the general results and findings that have been acquired by using the described methods. The goal of this chapter is to derive the maximum penetration rate of EVs in the current LV grid and identify from which penetration rate problems in the current infrastructure start to appear. Here, we show a more general approach on the Dutch LV grid as a whole, in contrast to Chapter 5, which focuses on scenarios with specific example cases.

The chapter starts with an estimation of the maximum number of EV chargers that in theory can simultaneously operate on a single feeder, in Section 4.2. To do this, we use the top 26 generic feeder clusters, which together represent over 70% of the Dutch LV grid (this was explained in Section 3.2.3 of the previous chapter). Also, the effect of location of the EV charger within a feeder (with respect to the transformer) is discussed in this section. When the maximum capacity of the LV networks in the grid is determined, we continue with estimating from which EV penetration rates possible feeder blackouts start to appear and what the consequences of these feeder blackouts are for the Dutch LV grid as a whole.

We do this by looking at the different factors that influence the EV charging probability. The EV charging probability is defined in the previous chapter as the product of a plug-in time distribution and a charging time duration, thus dependent on energy demand and charging power. Section 4.3 shows the effect of increasing charging duration on the value of probability that an EV charges at a certain moment in time. Section 4.4 shows the effects of different plug-in time distributions. In Section 4.5 we shortly investigate what the effect of the EV charging probability on the probability of a blackout on a single feeder is.

In Section 4.6 we extend the used model in such a way that we can take into account that not all EVs charge every day. We propose a method to describe different charging session frequencies and show the impact of this on the probability of a blackout on an LV feeder. All the results of the proposed methods on the clusters of Section 4.2 are then combined to create a general result for the Dutch LV grid as a whole. We do this in Section 4.7, where we show the final outcomes of the analysis by counting the estimated daily blackouts by uncontrolled EV charging for the Dutch LV grid and comparing these values to the current situation. This allows us to draw a conclusion regarding the maximum EV penetration rate in the Netherlands using the described assumptions and proposed description of the Dutch LV grid.

4.2 Maximum number of EVs on feeder

The two main properties that determine the maximum capacity of a feeder are the current level at the transformer (should not exceed the cable capacity) and the voltage level in the feeder (should not exceed +- 10% of 230 V) as was described in Section 2.2.1. We do not consider any PV installation in these simulations, so we calculate the current in the first segment of the cable, since that is where we assume the highest current. The voltage is calculated at the last segment of the cable. To determine he maximum feeder capacity in terms of number of EV chargers, every cluster is simulated and simultaneously charging EVs are added one-by-one to mimic increasing EV penetration rates for both 3.7 and 11 kW chargers. The maximum capacity of a feeder is defined by either a violation of the cable current limit or a critical voltage drop over the cable. To demonstrate how this works, Figure 4.1 shows part of the simulation result for Cluster 08. Observe that, although the feeder cable could carry more current, the voltage at the end of the feeder drops below 207 V starting from six simultaneously charging 11 kW chargers. This is thus the maximum feeder capacity in this case.

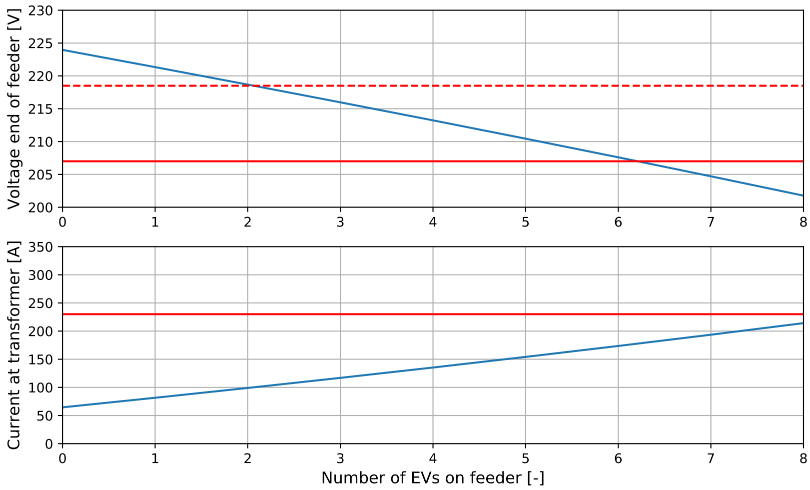

Figure 4.1: Simulation of Cluster 08 with 11 kW chargers located at the last positions of the feeder. The bold red lines represent the voltage and current limits, the dashed red line represents the -5% voltage drop level.

4.2.1 Effect of location on feeder

The physical location of the loads on the feeder might influence the results, e.g. when placing all loads on the end of the feeder, a voltage level violation might occur before a current level violation. To address this, all simulations are done twice, once by locating the EV charger loads starting from the end to the begin of the feeder (on the last positions viewed form the transformer) and once from the begin to the end of the feeder (on the first positions viewed from the transformer). Examples from Cluster 04 with 11 kW chargers are shown in Figure 4.2 and Figure 4.3. Note that the difference of the voltage curve is quite substantial and that the difference in current in both situations due to the placement strategy of the EV chargers are only minor. For the final result on this specific cluster, this has no implications, as the black-out situation still occurs when charging seven EVs simultaneously since the current limit is violated earlier than the voltage limit in both cases.

4.2.2 Individual cluster simulation results

The results for all simulated clusters are summarized in Table 4.1. All simulations are carried out with a transformer voltage level of 230 V. The maximal number of simultaneous charging EVs within each cluster is defined as sketched in the previous sections. Hereby, a violation of the feeder power capacity is indicated with a (P), while a feeder voltage violation is indicated by a (V). Note that for 11 kW charging, taking into account the occurrence rates of the clusters, about 71% of the capacity problems is power related (overloading the LV cable with too much current), the other 29% is related to voltage drops. For 3.7 kW charging, this ratio shifts to 83% and 27% for power and voltage problems respectively. Note that in the presented results, the loads are always spread over the phases as uniformly as possible.

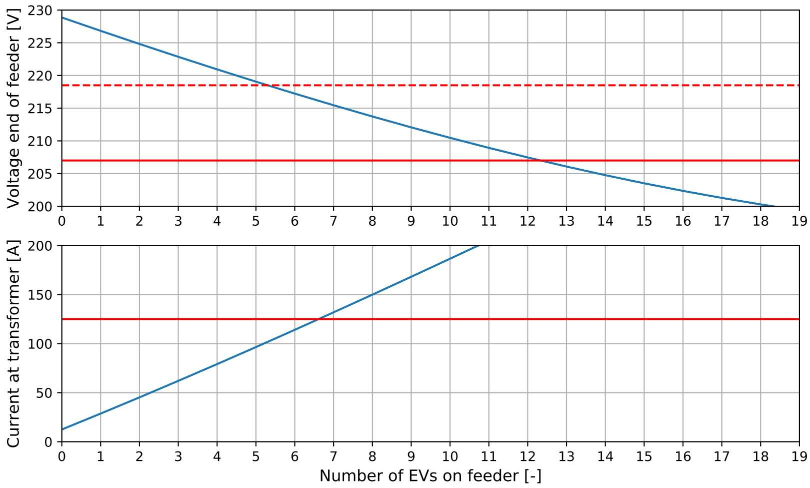

Figure 4.2: Simulation of Cluster 04 with 11 kW chargers located at the last positions of the feeder. The bold red lines represent the voltage and current limits, the dashed red line represents the -5% voltage drop level. With seven simultaneously charging home chargers with 11 kW power rating, a blackout occurs, thus the maximum is set at six.

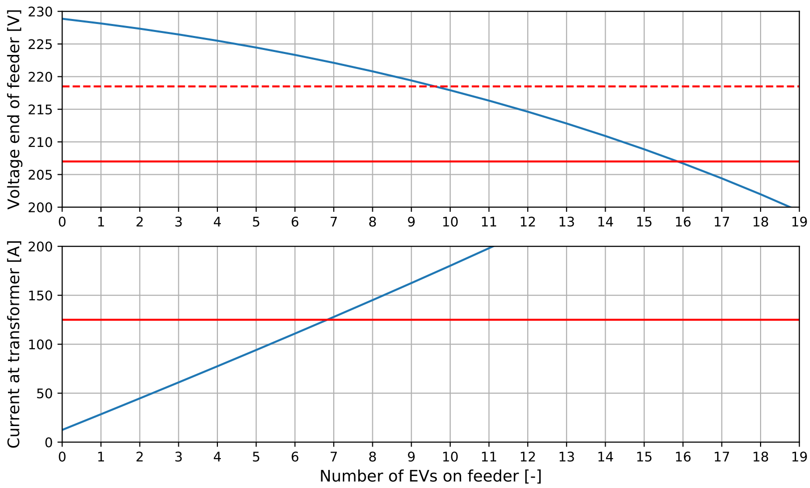

Figure 4.3: Simulation of Cluster 04 with 11 kW chargers located at the first positions of the feeder. The bold red lines represent the voltage and current limits, the dashed red line represents the -5% voltage drop level. With seven simultaneously charging home chargers with 11 kW power rating, a blackout occurs, thus the maximum is set at six.

Cluster	Total HH [-]	Cable type	max. simultaneous 11 kW charger [-]	max. simultaneous 3.7 kW charger [-]	Occurence [%]
01	17	*150 Al - 150 m*	13 (76%) - (P)	17 (100%) - (-)	6.4
02	24	*70 Cu - 270 m*	8 (33%) - (P)	24 (100%) - (-)	4.5
03	39	*95 Al - 266 m*	8 (21%) - (P)	25 (64%) - (P)	4.5
04	19	*50 Cu - 218 m*	6 (32%) - (P)	19 (100%) - (-)	4.4
05	32	*150 Al - 362 m*	11 (34%) - (P)	32 (100%) - (-)	4.1
06	26	*50 Al - 290 m*	5 (19%) - (V)	16 (62%) - (P)	3.4
07	49	*95 Al - 386 m*	8 (16%) - (V)	22 (45%) - (P)	3.4
08	70	*150 Al - 633 m*	6 (9%) - (V)	20 (29%) - (V)	3.3
09	27	*50 Cu - 320 m*	5 (19%) - (P)	15 (56%) - (P)	3.2
10	35	*95 Al - 439 m*	8 (23%) - (V)	24 (69%) - (P)	2.9
11	33	*95 Al - 371 m*	8 (24%) - (P)	24 (73%) - (P)	2.9
12	13	*35 Cu - 277 m*	5 (38%) - (P)	13 (100%) - (-)	2.8
13	62	*150 Al - 499 m*	10 (16%) - (V)	29 (47%) - (P)	2.6
14	38	*95 Al - 227 m*	8 (21%) - (P)	24 (63%) - (P)	2.5
15	51	*95 Al - 567 m*	5 (10%) - (V)	17 (33%) - (V)	2.2
16	26	*150 Al - 354 m*	11 (42%) - (P)	26 (100%) - (-)	2.1
17	67	*70 Cu - 233 m*	6 (9%) - (P)	17 (25%) - (P)	2.1
18	11	*35 Cu - 187 m*	5 (45%) - (P)	11 (100%) - (-)	1.8
19	13	*35 Cu - 190 m*	5 (38%)- (P)	13 (100%) - (-)	1.8
20	33	*70 Cu - 595 m*	7 (21%) - (V)	20 (61%) - (P)	1.7
21	46	*150 Al - 498 m*	10 (22%) - (P)	30 (65%) - (P)	1.6
22	12	*35 Cu - 146 m*	5 (42%) - (P)	12 (100%) - (-)	1.6
23	26	*35 Cu - 392 m*	4 (15%) - (P)	12 (46%) - (P)	1.5
24	58	*95 Cu - 1011 m*	5 (9%) - (V)	16 (28%) - (V)	1.5
25	30	*50 Cu - 246 m*	5 (17%) - (P)	15 (50%) - (P)	1.3
26	25	*150 Al - 453 m*	11 (44%) - (P)	25 (100%) (-)	1.2

Table 4.1: Maximum feeder capacity in terms of simultaneously charging EVs and corresponding EV penetration rate on that feeder (percentage between brackets). The table also indicates if either the feeder power capacity (P) is reached or a critical voltage drop (V) appears. Total HH denotes the number of households on the feeder, while Occurence represents the percentage of feeders in the Dutch LV grid that are resembled by that cluster.

4.3 Effect of charging time on EV charging probability

To determine the effect of the charging time t_{charge} on the EV charging probability $p_{EVcharging}$, the required energy per charging session $E_{charged}$ is based on a set of values corresponding to travel distances of 50 to 300 km with 50 km intervals. This means that, whenever an EV charges, it charges the exact amount of energy to cover the specified travel distance at the specified charging power. Figure 4.4 and Figure 4.5 show the results for $P_{charging} = 3.7$ kW and $P_{charging} = 11$ kW respectively using the plug-in time distribution of the MEA dataset.

With Figure 4.4 and Figure 4.5 we describe the probability that an EV is charging in a certain timeslot when it charges a specified energy demand (7.5, 15, 22.5, 30, 37.5 or 45 kWh) using a specified charging power (either 3.7 kW or 11 kW) for a single EV. When the amount of energy that is charged in a session increases, the charging time increases and thus the probability that an EV is charging in a certain time interval, the EV charging probability $p_{EVcharging}$ increases. This also works the other way around: increasing the charging power leads to a lower EV charging probability for the same energy demands, since the time needed for charging decreases an thus the probability that an EV is in the state of charging decreases. This is why the EV charging probability $p_{EVcharging}$ for 11 kW charging is generally much lower. In coming sections, we use $p_{EVcharging}$ to describe the expected behavior of a set of EVs, e.g. in a street, and thus to calculate the probability of charging more than a given number of EVs simultaneously on a certain timeslot.

Note, that the charging time t_{charge} for 100 km (15 kWh) at $P_{charging} = 3.7$ kW is similar to t_{charge} for 300 km (45 kWh) at $P_{charging} = 11$ kW (both 4 hours) and thus both cases show a similar EV charging probability. After all, the time the EV spends charging is the same in both cases, thus the probability that they are in the charging state is the same. We observe that an increasing t_{charge} also results in a shift in peak moment time. This also holds for charging power, where for 11 kW charging the maximum $p_{EVcharging}$ is visible around 19:00, while for 3.7 kW charging the peak moment shifts to around 22:00 (in the case of charging 30 kWh). This is again explained by the corresponding increase in charging time, which by definition results in an EV that is in the state of charging for a longer time period after its plug-in moment.

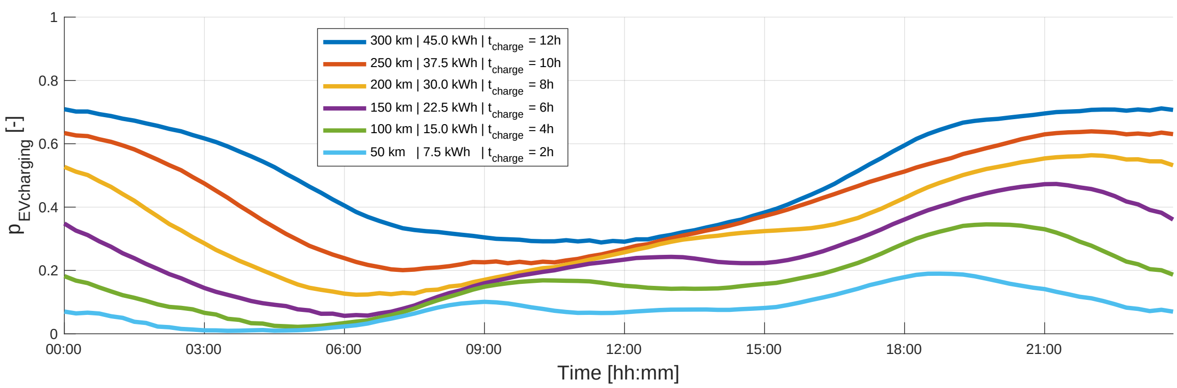

Figure 4.4: Effect of increasing charging time t_{charge} on EV charging probability ($p_{EVcharging}$), results shown for 3.7 kW charging with the MEA plug-in time data. Every line represents the probability that an EV is charging in a certain 15-minute timeslot, in the case of charging the according energy demand on a certain day.

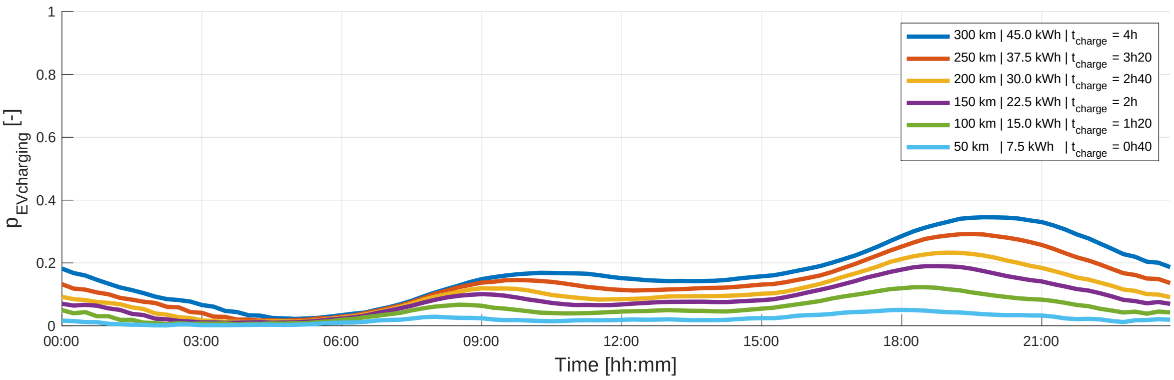

Figure 4.5: Effect of increasing charging time t_{charge} on EV charging probability ($p_{EVcharging}$), results shown for 11 kW charging with the MEA plug-in time data. Every line represents the probability that an EV is charging in a certain 15-minute timeslot, in the case of charging the according energy demand on a certain day.

Figure 4.6 shows the maximum value of the EV charging probability distribution, but for energy demands of 5 to 25 kWh for both charging power levels of 3.7 and 11 kW. Notice the steady increase of $p_{EVcharging}$: the more energy demand is needed by every individual EV every day, the higher the maximum probability an EV is charging.

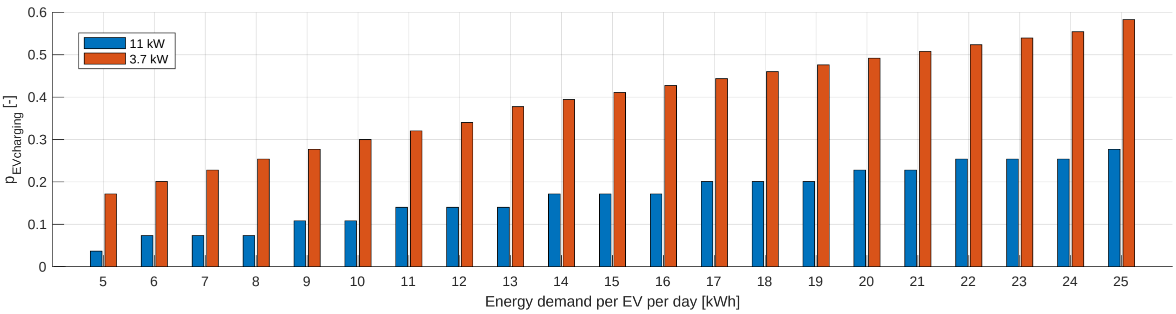

Figure 4.6: Energy demand per EV per day and corresponding maximum $p_{EVcharging}$ value.

4.4 Effect of plug in time on EV charging probability

Next to the MEA dataset that was introduced in Section 3.4.2 and used as example when modeling the EV charging probability, the Dutch foundation *ElaadNL* also provides a regularly updated open dataset, introduced in Section 3.4.5. The dataset contains EV arrival plug-times in private, public and work environments. To check the effect of this plug in time probability distribution resulting from this dataset, we compare both datasets by creating a similar plot for the ElaadNL data as we did for the MEA data in the previous section.

Comparing the Figures 4.7 and 4.8 with the Figures 4.4 and 4.5, we observe for both distributions a similar behavior in terms of peak moment, but a main difference in the maximum EV charging probability value: 0.411 (3.7 kW ElaadNL) and 0.172 (11 kW ElaadNL) compared to 0.345 (3.7 kW MEA) and 0.123 (11 kW MEA) for e.g. 15 kWh-charging. The advantages of the ElaadNL data already discussed in Section 3.4.5, such as combining multiple data sources (instead of using only Nissan LEAF models for the MEA dataset) makes the ElaadNL data our preferred data set for the remainder of this thesis.

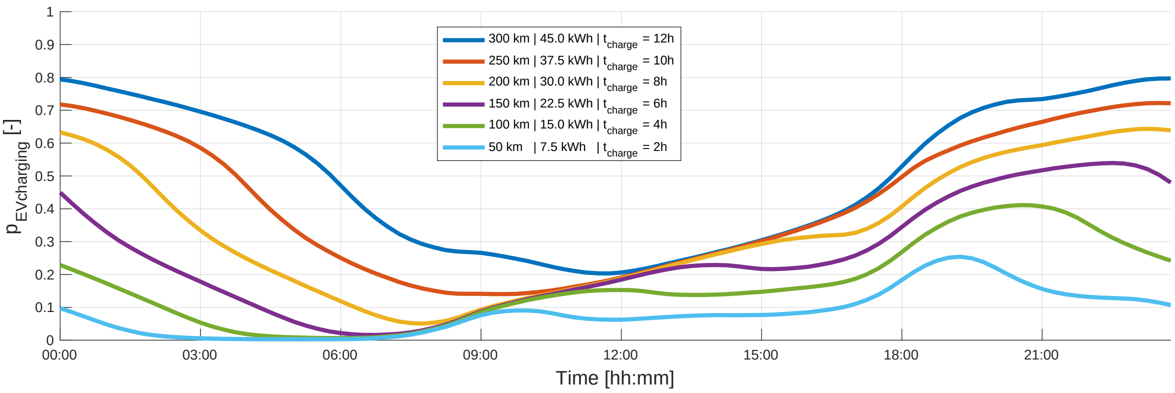

Figure 4.7: EV charging probability for five different energy demands, results shown for 3.7 kW charging with the plug-in time distribution based on the ElaadNL data for private and public charging sessions combined.

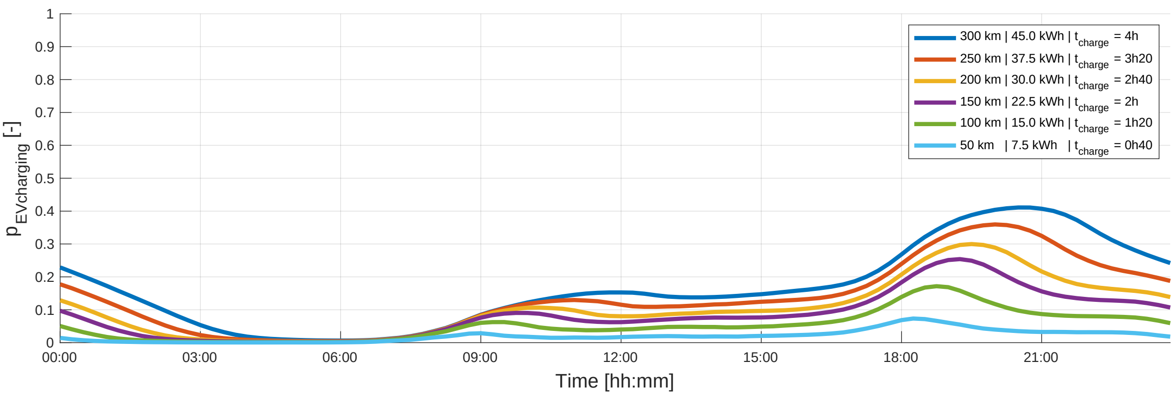

Figure 4.8: EV charging probability for five different energy demands, results shown for 11 kW charging with the plug-in time distribution based on the ElaadNL data for private and public charging sessions combined.

We observe an evening peak for both charging power levels. However, the 3.7 kW charging power level of Figure 4.7 shows also an increased EV charging probability during the night. This is due to the fact that EVs that charge with the lower 3.7 kW power level require more time to charge the given energy demand compared to charging with 11 kW. This increases $p_{\mathrm{EVcharging}}$: the probability that an EV is in state of charging. Overall, the EV charging probability for 11 kW charging is much lower due to this effect of reduced charging time.

4.5 Effect of EV charging probability on blackout probability

To show the effect of the EV charging probability ($p_{\mathrm{EVcharging}}$) on the feeder blackout probability (p_{blackout}), p_{blackout} is calculated for $p_{\mathrm{EVcharging}}$ values ranging from 0.05 to 0.30 with increments of 0.05. As example, the result of Cluster 03 shown in Figure 4.9. The orange line of the right y-axis represents p_{blackout} for a single feeder and the blue bars (left y-axis) represent the total number of daily blackouts in the LV grid, as defined in Section 3.6.1. In Figure 4.10, these calculations are summarized in one graph.

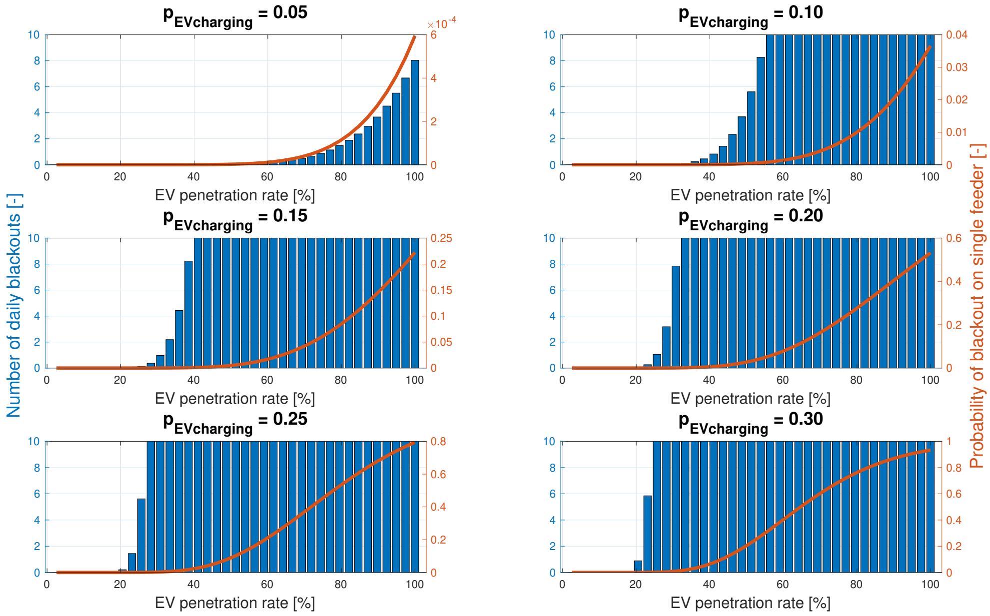

Figure 4.9: Effect of increasing $p_{\mathrm{EVcharging}}$ on total daily blackouts, results shown for Cluster 03, representing 4.5% of the Dutch LV network, using 11 kW EV chargers.

These graphs show that an increasing EV charging probability leads to an increase in blackouts. In other words: when people charge more EVs simultaneously, the risk of LV feeder blackouts increases. The example for Cluster 03 in Figure 4.10 shows this. Cluster 03 represents 4.5% of the Dutch LV grid (with an estimated 300,000 feeders total). If the maximum EV blackout probability value (which depends on energy demand, charging frequency and charging time) for a certain timeslot is determined at 0.15, this leads to roughly two blackouts per day in 4.5% of the Dutch LV grid when the EV penetration rate reaches about 33%, indicated by the yellow line in Figure 4.10. However, this method of calculating the blackout probability contains a number of simplifications. Firstly, we assume here that all EVs charge everyday with the same energy demand, which we consider highly unlikely. Secondly, to calculate the blackout probability on a certain day, we only consider the timeslot with the highest EV charging probability. This is unfair, since blackouts might also occur in other timeslots. If we want to know the probability of a blackout on a certain day, we also need to take the other timeslots into account. Thirdly, we assume here that all EVs charge with the same power level, either 3.7 or 11 kW, which we also consider to be unlikely. In the next section, we address these simplifications and introduce methods to avoid these simplifications.

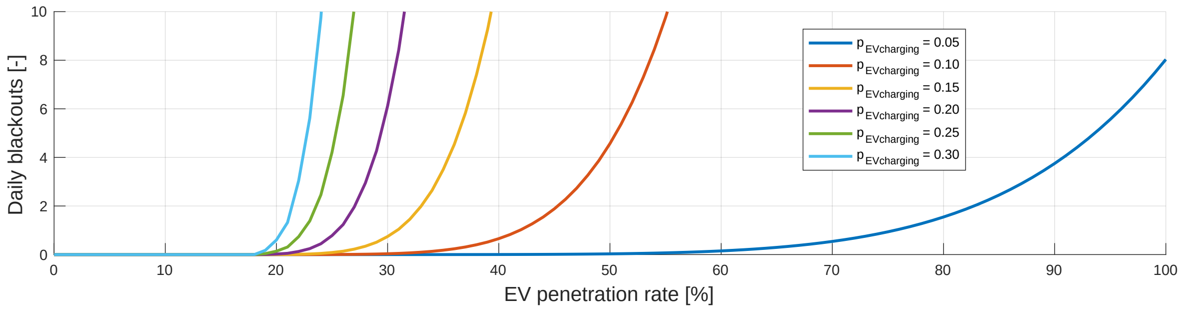

Figure 4.10: Effect of EV penetration rate and $p_{\mathrm{EVcharging}}$ on daily blackouts, results shown for Cluster 03, representing 4.5% of the Dutch LV network, using 11 kW EV chargers. This graph summarizes Figure 4.9.

4.6 Effect of charging frequency

This section introduces a method to analyze the effect of the trade-off between charging more frequently, but shorter and charging less frequently, but longer. From the previous sections it is evident that a longer charging time t_{charge} increases the probability that an EV charges for each time interval on a certain day. After all, increasing the duration of the time an EV needs to charge (regardless if that is caused by lowering charging power or increasing energy demand) ensures that the EV charges for a longer period of time and thus has a higher probability to be in the charging state. This also implies that the probability that any given EV charges simultaneously with other EVs increases, which is something we want to avoid since it increases the probability on a blackout. This means that a smaller t_{charge} seems to be beneficial. One way to reduce t_{charge} is to charge more frequently in a certain time span, since this reduces the energy demand per charging session and thus the time per session that an EV charges. However, more charging sessions might on the other hand also increase the peak loads on the grid again, and thus increase the probability of a blackout. The previous section estimated the daily blackouts for a scenario in which all EVs charge everyday and with the same amount of energy. In practice, this distribution is unlikely. People use different EV models with different battery sizes and exhibit different charging behavior. This means that the charging frequency, i.e. the number of charging sessions in a certain period, may vary among different EV owners. Some EV owners may charge their EV only 2-3 times per week, other EV owners plug in their EV e.g. every day.

To analyze the impact of these varying number of EV charging sessions on the load of an LV feeder, we determine four things: (1) if an EV is charging on any given day, (2) the energy demand for that session, (3) the time the charging sessions starts (the plug-in time) and (4) the duration of the charging sessions (which depends on the charging power and energy demand)(4). The chosen approach to model these aspects is based on a number of assumptions. First, we assume that every EV drives 38 kilometer per day (this is in line with CBS statistics [20]). We use this average only to demonstrate the model. In future work, this part can be extended by using e.g. a distribution with an average and a standard deviation for driven kilometers. We choose an average energy efficiency of 0.175 kWh per kilometer. The required energy is assumed to be charged with an AC charger in the LV grid, either a home charger or a (semi-) public charging pole in the LV grid, near the house of the EV owner, thus connected on the same LV feeder as the house. Secondly, we assume that any given EV charges according to one of five predefined charging options: charging the energy equivalent of 38 km every day, charging the energy equivalent of $2 \times 38 = 76$ km every other day, charging the energy equivalent of $3 \times 38 = 114$ km every third day, and so on up to charging the energy equivalent of $5 \times 38 = 190$ kilometer every fifth day. We call these options 'charging regimes'. Once we assign an EV to any given charging regime, the probability that it charges at a specific quarter over the day is given according to the distributions seen in Figure 4.11 and Figure 4.12. This probability distribution applies for the day the EV is scheduled to charge. For the other days, where it does not charge, the EV has no charging distribution. These probability distributions combine the plug-in time probability with the charging duration of the discretized energy demands, as was introduced in Section 3.4.3. The next section, Section 4.6.1, applies this method to a uniform distribution of the charging regimes to determine the number of EVs that is charging on a certain day and the corresponding probability of a blackout on every individual timeslot (quarter of the day). Section 4.6.2 shows how to accumulate these probabilities to calculate the probability of a blackout on a certain day. Section 4.6.3 introduces an alternative distribution of charging regimes and compares this to the other available distributions of charging regimes. Finally, Section 4.6.4 combines both 3.7 and 11 kW power levels into one model.

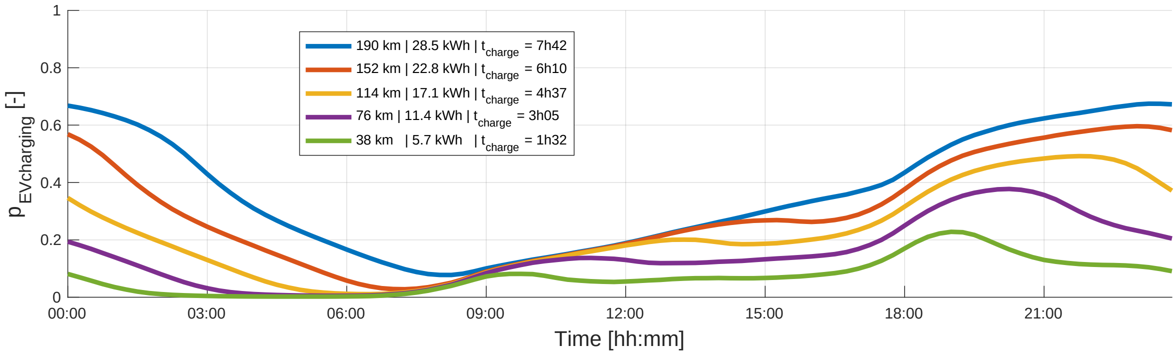

Figure 4.11: EV charging probability $\mathrm{p_{EVcharging}}$ using 3.7 kW charging for five different energy demands.

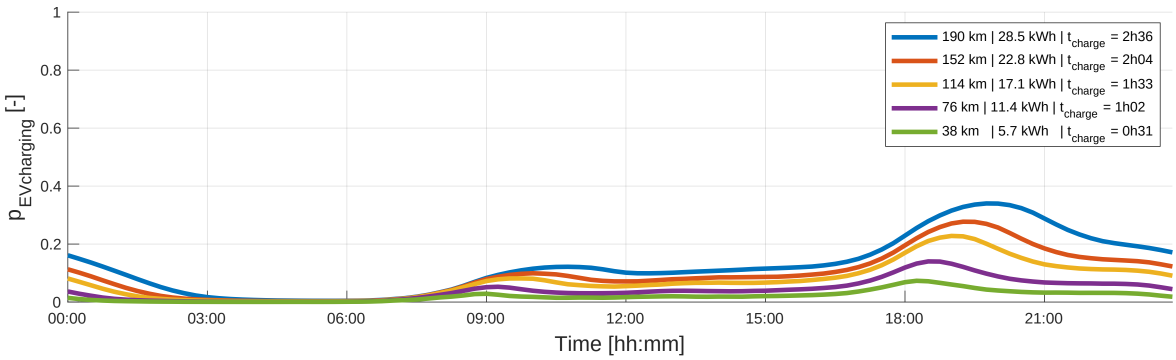

Figure 4.12: EV charging probability $\mathrm{p_{EVcharging}}$ using 11 kW charging for five different energy demands.

4.6.1 Modeling different charging regimes

As mentioned earlier, we consider five discretized charging charging regimes: we charge every day the energy equivalent of 38 kilometer, every two days the energy equivalent of $2 \times 38 = 76$ kilometer up to charging the energy equivalent of 190 kilometer every five days. We charge each of the given EVs according to one charging regime only. This implies that not every EV charges every day. For the EVs charging according to regime 1, the probability that the EV charges on a certain day is 1, since they charge every day. For the EVs that charge according to regime 2, the possibility that the EV charges on a certain day is 0.5, since this EV only charges once in two days. For charging regime 3, 4 and 5 the same structure holds. We denote this probability by α_{x}, with x the charging regime number. We assume further that the five charging regimes are distributed uniformly over the EV owners, e.g. 20% of the EV owners show the behavior of charging regime 1, 20% of the EV owners show behavior of charging regime 2 etc. We call this probability β_{x}, where x again denotes the charging regime number. Note that, for a given charging regime, the energy demand has to be specified. E.g. when charging once every three days, the EV charges the energy equivalent of $3 \times 38 = 114$ kilometers. Note that the α_{x} values for every regime are fixed, but that β_{x} depends on the scenarios, i.e. if in certain scenarios 80% of the EV owners charge every day, β_1 should be set to 0.8. With these values, we can calculate the expected number of EVs that charge on a specific day. For a given charging regime x, the number of EVs that charge, k_x, is defined as:

$$k_x = N \times \beta_x \times \alpha_x \tag{4.1}$$

where N represents the total number of EVs in the set. Since we can not charge e.g. 25 and 'one-fifth' EV on a day, we round k_x to whole numbers. To find the expected total number n of EVs that charge on a specific day, we take the sum over all charging regimes:

$$n = \sum_{x=1}^{5} k_x \tag{4.2}$$

To demonstrate this, we consider a street, somewhere in the Netherlands, with 60 households connected to one feeder. Of the 60 households, 40 possess an EV (N=40), representing an EV penetration rate of 67%. We use Equation 4.1 to calculate k_x: $40 \times 0.2 \times \frac{1}{1} = 8$ EVs charge according to regime 1, $40 \times 0.2 \times \frac{1}{2} = 4$ EVs charge according to regime 2 and so on. The results for all charging regimes are displayed in Table 4.2. Accumulating all values for k_x according to Equation 4.2 results in the expected number n of EVs charging on a certain day is 19. Note that, using this equal distribution for β_x, only $\frac{19}{40}$ = 47.5% of the EVs charge on a certain day, the other 21 EVs do not charge that day.

Charging regime x	α_x	β_x	k_x
1	$\frac{1}{1}$	0.2	8
2	$\frac{1}{2}$	0.2	4
3	$\frac{1}{3}$	0.2	3
4	$\frac{1}{4}$	0.2	3
5	$\frac{1}{5}$	0.2	1

Table 4.2: Example values for the five charging regimes. α_x indicates the probability that an EV charges on a certain day. β_x indicates the share of the total EVs in the set that show that particular behavior. Using $N = 40$ results in the values k_x, the number of EVs that charges that day according to regime k_x.

For a given charging regime, we can determine the EV charging probability at a certain time interval $\mathrm{p}_{\mathrm{EVcharging}}$, based on the results in Section 4.4 (shown for 3.7 kW charging in Figure 4.11). Note that for every charging regime, the corresponding $\mathrm{p}_{\mathrm{EVcharging}}$ is denoted by p_x with x the charging regime number. By using the EV charging probability, we combine the plug-in time with the duration of the charging session. This explains that, for charging regimes with a higher energy demand, the EV charging probability $\mathrm{p}_{\mathrm{EVcharging}}$ is higher, since EVs charge longer. If we consider the charging sessions as independent events with a probability of 'success' (i.e. when charging happens) given by the EV charging probability for the different charging regimes p_x, we get a binomial distribution for the probability that exactly $\bar{n}$ out of the set of n EVs charge in a timeslot t:

$$p_{\bar{n}}^{n}(t) = \binom{n}{\bar{n}} \big(p_x(t)\big)^{(\bar{n})} \big(1 - p_x(t)\big)^{(n-\bar{n})} \tag{4.3}$$

Note that p_x varies for every EV. Every charging regime has its own given p_x distribution, with k_x EVs following that given distribution. In this example, only $k_1 = 8$ EVs follow the distribution for p_1, $k_2 = 4$ EVs for p_2 and so on. This is different from a binomial distribution with identically distributed p_x, where all $\bar{n}$ EVs would follow the same p_x. This requires us to multiply the power terms with a factor $\frac{k_x}{n}$, i.e. only the fraction of n (the total EVs) that charge according to the specified charging regime. This ensures that only k_x EVs follow a certain distribution p_x.

$$\begin{aligned} p_{\bar{n}}^{n}(t) = &\binom{n}{\bar{n}}\Big(p_1(t)\Big)^{(\bar{n}\times\frac{k_1}{n})}\Big(1-p_1(t)\Big)^{\left((n-\bar{n})\times\frac{k_1}{n}\right)} \\ &\times\Big(p_2(t)\Big)^{(\bar{n}\times\frac{k_2}{n})}\Big(1-p_2(t)\Big)^{\left((n-\bar{n})\times\frac{k_2}{n}\right)} \\ &\times\Big(p_3(t)\Big)^{(\bar{n}\times\frac{k_3}{n})}\Big(1-p_3(t)\Big)^{\left((n-\bar{n})\times\frac{k_3}{n}\right)} \\ &\times\Big(p_4(t)\Big)^{(\bar{n}\times\frac{k_4}{n})}\Big(1-p_4(t)\Big)^{\left((n-\bar{n})\times\frac{k_4}{n}\right)} \\ &\times\Big(p_5(t)\Big)^{(\bar{n}\times\frac{k_5}{n})}\Big(1-p_5(t)\Big)^{\left((n-\bar{n})\times\frac{k_5}{n}\right)}, \end{aligned} \tag{4.4}$$

where $p_{\bar{n}}^{n}$ is the probability that $\bar{n}$ of the total n EVs charge on a certain time interval and k_x is the number of EVs that charge according to EV charging probability distribution p_x with $x \in \{1, 2, 3, 4, 5\}$. Note that we use time dependent probabilities p_x. This allows us to estimate the time slot with the largest probability of a blackout. To demonstrate this, we continue with the introduced example: a street in the Netherlands, with 60 households connected to one feeder. We assume that on this particular feeder, we can allow only a maximum of 12 simultaneously operating 3.7 kW EV chargers. Furthermore we assume that out of the 60 households, 40 possess an EV. This represents an EV penetration rate of 67%. We use the charging regimes with corresponding β_x values of Table 4.2. Using Equation 4.2, we have already calculated that the expected number of EVs charging on a day is 19. Notice that this is the direct consequence of the equal distribution of charging regimes among the EVs. As this grid capacity is 12 EVs, we are interested in the probability of the situation that 13 or more EVs charge simultaneously, since this represents a blackout situation. Figure 4.13 shows all probabilities of a certain number of EVs charging, represented by the colored bars. The legend of the plot indicates how many EVs charge simultaneously, e.g. *'EVs charging = 13'* indicates the probability that exactly 13 EVs charge simultaneously, *'EVs charging = 14'* for exactly 14 simultaneously charging EVs and so on. Note that each dashed line represents the individual case according to the legend. Also note that the probability for the higher numbers, e.g. *'EVs charging = 17'* are not visible in the plot, since that probability is very low, almost negligible and thus not visible on this scale. The solid bold line is the sum of all these probabilities, i.e. the total probability that 9 or more EVs charge in the same timeslot. That means that the solid bold line represents the total probability of a blackout, with a maximum probability of 1.2×10^{-3} in the timeslot of 19:15 - 19:30. In practice this means that, in this scenario, the situation with more than 12 simultaneously charging EVs is estimated to occur once every 833 days *in that time slot*.

We can make the same calculation for a penetration rate of 100%. This implies $N = 60$, from that follows that $n = 27$ EVs are expected to charge on a particular day and the maximum blackout probability becomes 0.033, see the blue line in Figure 4.14. This results in a potential blackout due to EV charging once every 30 days *in this specific timeslot*. The probability of a blackout *during that entire day* is higher, since blackouts do occur not only at the timeslot with the highest probability, but also on other timeslots. The probability of a blackout in these other timeslots is admittedly lower, but to find the total blackout probability on a certain day we need to accumulate all the probabilities of a blackout for every timeslot. This is shown in the next section.

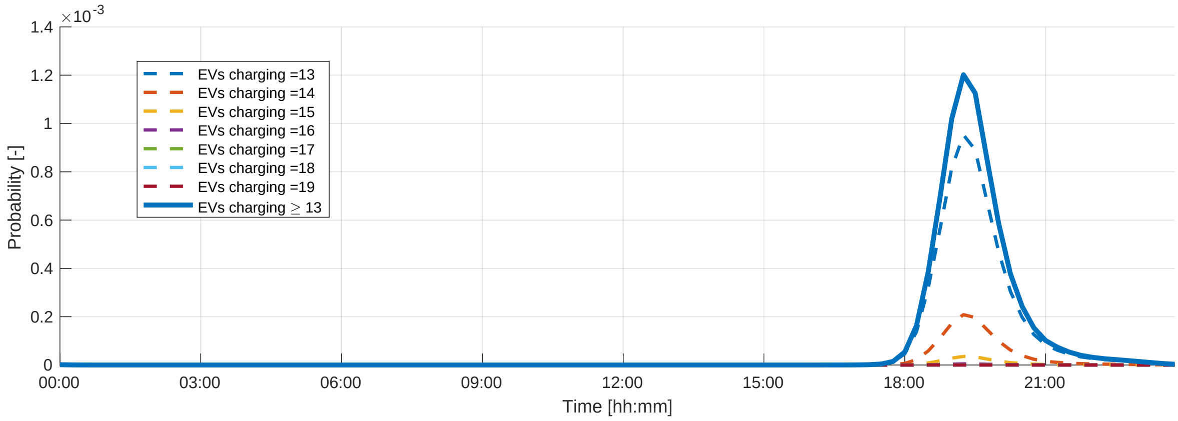

Figure 4.13: Blackout probability for 13 up to 19 charging EVs on a certain day. The dashed lines represent the individual situations, e.g. *'EVs charging = 13'* indicates the probability that exactly 13 EVs are charging simultaneously. The solid bold line represents the sum of all the individual dashed lines and thus represents the total probability of a blackout.

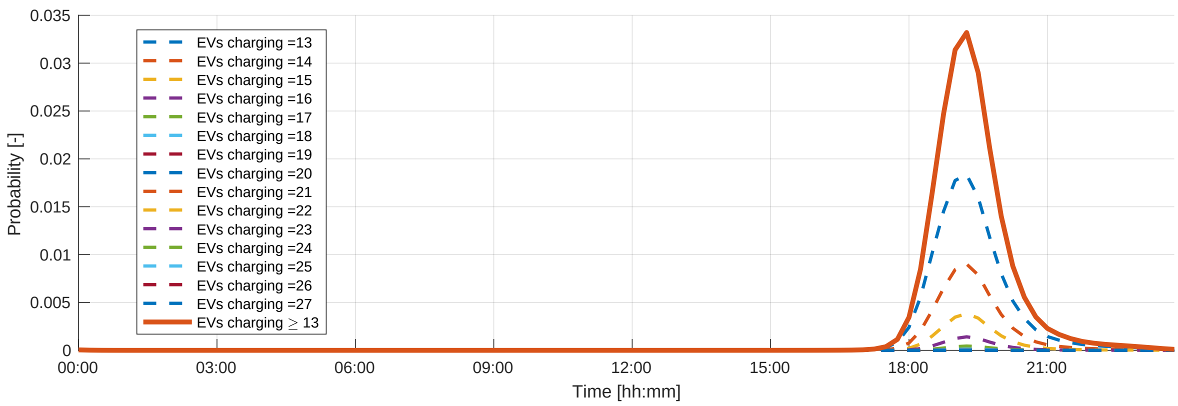

Figure 4.14: Blackout probability for 13 up to 27 charging EVs on a certain day. The dashed lines represent the individual situations, e.g. *'EVs charging = 13'* indicates the probability that exactly 13 EVs are charging simultaneously. The solid bold line represents the sum of all the individual dashed lines and thus represents the total probability of a blackout.

4.6.2 Blackout probability for a full day

To accumulate probabilities, we have to consider all possible outcomes. We have 96 possible timeslots for a blackout. In any timeslot, a blackout can or can not occur and we know the probability of this by the solid bold in Figure 4.13. However, for a blackout to appear in a time period t we also need to know that there has not been a blackout in the previous time periods $1 \rightarrow t-1$. Otherwise the system would not have 'reached' time period t. To demonstrate this, we give in Table 4.3 the blackout probability values for five timeslots as p_{xx} with xx as the timeslot number, e.g. timeslot 72 for 18:00-18:15. Note that p_{xx} describes the probability of a blackout at that certain timeslot, while $(1-p_{xx})$ describes the probability that a blackout does not occur at that time slot.

18:00-18:15	*18:15-18:30*	*18:30-18:45*	*18:45-19:00*	*19:00-19:15*
p_{72}	-	-	-	-
$(1-p_{72})$	p_{73}	-	-	-
$(1-p_{72})$	$(1-p_{73})$	p_{74}	-	-
$(1-p_{72})$	$(1-p_{73})$	$(1-p_{74})$	p_{75}	-
$(1-p_{72})$	$(1-p_{73})$	$(1-p_{74})$	$(1-p_{75})$	p_{76}

Table 4.3: Example table to demonstrate cumulative blackout probability.

Every row describes a possible outcome. In every timeslot a blackout can or can not happen and we assume that a blackout can only happen once per possible outcome. By taking the product of all values in a row, the probability of that single outcome is calculated. To calculate the probability for a whole day, we sum all 96 possible outcomes to calculate the probability that in any of these 96 timeslots a blackout occurs. For the case of Figure 4.13, this results in a blackout probability of 0.0073 (once every 137 days). The case of Figure 4.14 results in a blackout probability of 0.192 (once every five days).

This indicates that EV penetration rates of 67% and 100% result in serious problems for the local grid in the sketched situation. To show the relation between the blackout probability and EV penetration rate, we plot these in Figure 4.15. To make this plot, we calculate $p_{\bar{n}}^{n}$ (Equation 4.4) for every number of EVs from 0 to 60, so from 0 to 100% penetration rate and for each of these cases we calculate the blackout probability for the entire day. Next to this, the same figure also shows the plots of expected days before a blackout occurs and the corresponding expected number of blackouts per year. Note that the lines are not perfectly smooth and that the variation is not the same among the different EV penetration rates. This is due to the necessary rounding of the k_x values since it is practically impossible to charge e.g. 0.8 EVs. Furthermore, to execute the calculations, the binomial coefficient $\bar{n}$ needs to be a positive integer by definition.

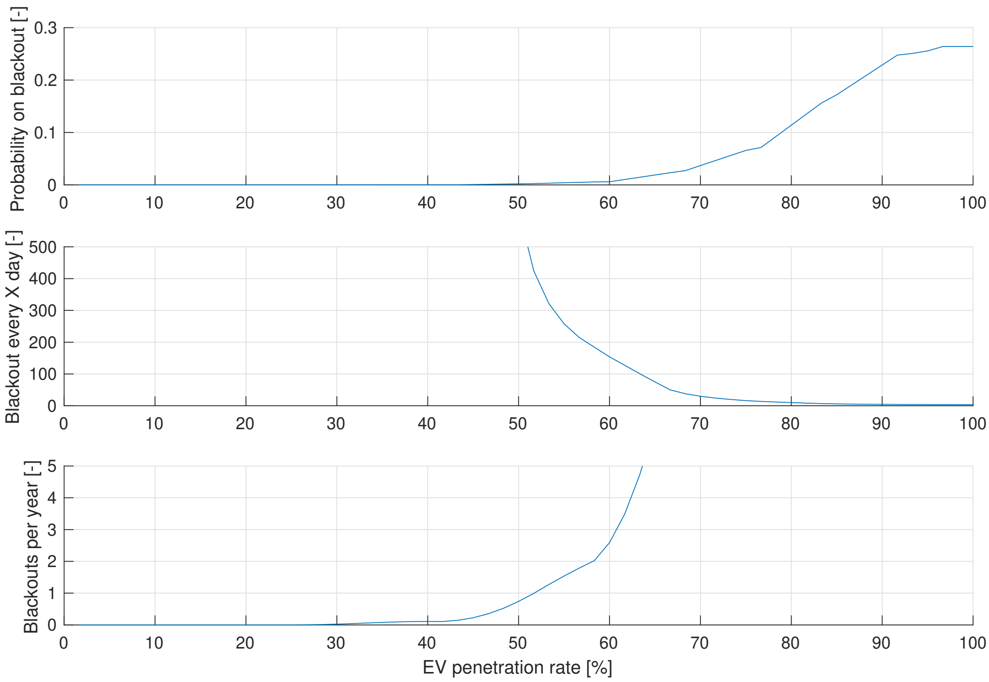

Figure 4.15: Blackout probability, number of days for an estimated blackout and expected blackouts per year for the sketched scenario using 3.7 kW charging only.

4.6.3 Altering the charging regime distribution

In the previously introduced example, we assumed β_x, the share of EVs that follow one of the five charging regimes, equal for every charging regime. From statistical analysis of EV charging sessions, introduced in Section 3.4.2, we know that charging frequency varies and is negatively correlated to battery size: EVs with smaller batteries charge more often: 80% of the Nissan LEAF drivers (with only a 24 kWh battery pack) state that they charge 4 to 6 times per week, while 62% of the Tesla Model S (with a 95 kWh battery pack) drivers state they charge no more than 3 times per week. Based on this information, we adapt the distribution of the charging regimes, i.e. we alter the value for β_x. We propose the distribution shown in Table 4.4, where we use $N = 40$ (67% EV penetration rate) as example. We choose α_x as 0.55, 0.15, 0.10, 0.10 and 0.10, thus 55% of the EVs following charging regime 1, 15% following charging regime 2 and so on. We call this charging regime distribution *55/15/10/10/10*. Using this example, 28 out of the total 40 EVs (70%) are charging every day.

Charging regime x	α_x	β_x	k_x
1	$\frac{1}{1}$	0.55	22
2	$\frac{1}{2}$	0.15	3
3	$\frac{1}{3}$	0.10	1
4	$\frac{1}{4}$	0.10	1
5	$\frac{1}{5}$	0.10	1

Table 4.4: Values for the *55/15/10/10/10* charging regime distribution. α_x indicates the possibility that an EV is charging on a certain day. β_x indicates the share of of the total EVs in the set that show that particular behavior. Using $N = 40$ (for 67% EV penetration rate) results in the shown values for k_x.

Figure 4.16 shows the results of the *55/15/10/10/10* distribution of EV charging regimes. Comparing this to the equal β_x distribution of the previous section in Figure 4.15, we see that the blackouts occur already at a lower penetration rate, from 35-40% onwards instead of beyond 45-50%. Furthermore, the maximum probability on a blackout is higher compared to the previous example. This result is due to the fact that more EVs charge on a certain day with this new distribution: 70% vs. only 47.5% of the equal *20/20/20/20/20* distribution.

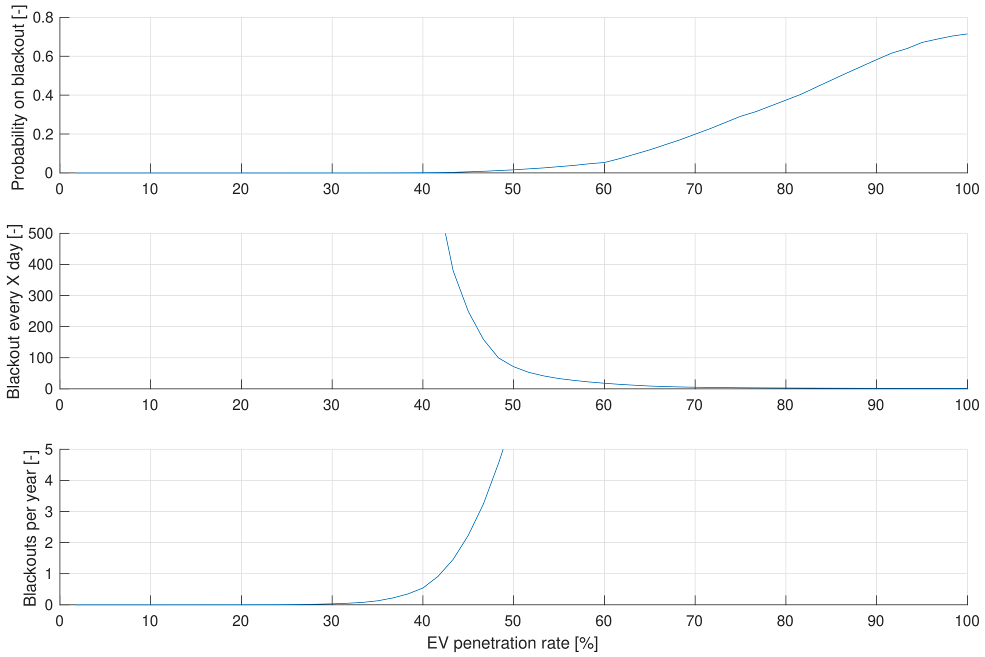

Figure 4.16: Blackout probability, number of days for an estimated blackout and expected blackouts per year for the *55/15/10/10/10* charging regime distribution using 3.7 kW charging only.

We make the same calculations for 11 kW charging, using the EV charging probability distributions for 11 kW charging shown in Figure 4.12. Since charging with 11 kW is about 3 times faster compared to 3.7 kW, the EV charging probability is much lower, since t_{charge} decreases. However, we can also host roughly 3 times less of these higher powered EV chargers at the same time because of feeder limitations. Figure 4.17 shows the results for the *55/15/10/10/10* charging regime distribution with a maximum of 4 simultaneously charging 11 kW chargers. Now, blackouts are expected already from 15-20% EV penetration rate onwards due to the lower number of possible simultaneously charging EVs: the feeder limit is reached earlier since we only need 4 simultaneously charging EVs instead of 12.

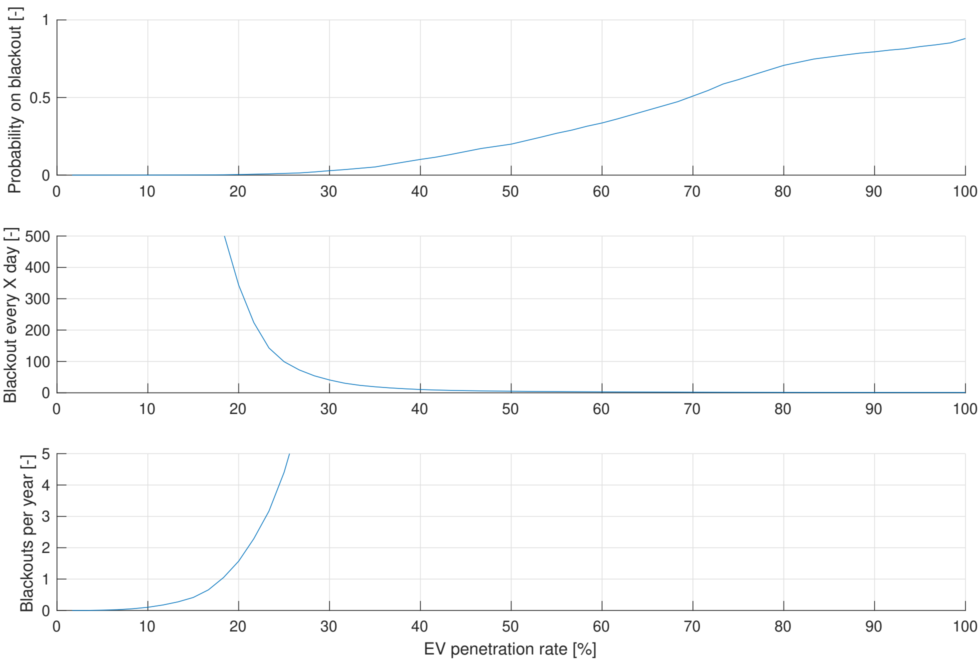

Figure 4.17: Blackout probability, number of days for an estimated blackout and expected blackouts per year for the *55/15/10/10/10* charging regime distribution using 11 kW charging only.

4.6.4 Combining power levels

We assume that it is unlikely that all EV owners and all (semi-)public charging poles in a neighborhood use the same power level (either 3.7 or 11 kW). Therefore we propose to combine these power levels with a certain ratio. This means that, if we have a number of EV chargers in a set, a share of them are 11 kW chargers and the other share consists out 3.7 kW chargers. Thus, the EVs with of 3.7 kW chargers follow one of the five charging regimes available for that 3.7 kW power level, the other EVs, in the share of 11 kW chargers, follow one of the five charging regimes available for the 11 kW power level. To model this, we extend Equation 4.4 with another 5 terms. Now, we have in total 10 terms, 5 terms for each power level and 2 terms for each charging regime. Since a share of the EVs now is charged with one of the two power levels, we multiply the power term for each 3.7 kW charging regime with the charging power factor F_P and the power term for each 11 kW charging regime with $(1 - F_P)$. This means that number of EVs k_x is multiplied by F_P or $(1 - F_P)$ to account for the share of EVs that charge either with 3.7 or 11 kW charging power. If e.g. 70% of the EVs charge with 3.7 kW, $F_P = 0.7$ and $(1 - F_P)$ becomes 0.3.

$$
\begin{aligned}
p_{\bar{n}}^{n}(t) = \binom{n}{\bar{n}} & \left(p_1^{3.7}(t)\right)^{(\bar{n}\times\frac{k_1}{n}\times F_P)}\left(1-p_1^{3.7}(t)\right)^{\left((n-\bar{n})\times\frac{k_1}{n}\times F_P\right)} \\
& \times\left(p_2^{3.7}(t)\right)^{(\bar{n}\times\frac{k_2}{n}\times F_P)}\left(1-p_2^{3.7}(t)\right)^{\left((n-\bar{n})\times\frac{k_2}{n}\times F_P\right)} \\
& \times\left(p_3^{3.7}(t)\right)^{(\bar{n}\times\frac{k_3}{n}\times F_P)}\left(1-p_3^{3.7}(t)\right)^{\left((n-\bar{n})\times\frac{k_3}{n}\times F_P\right)} \\
& \times\left(p_4^{3.7}(t)\right)^{(\bar{n}\times\frac{k_4}{n}\times F_P)}\left(1-p_4^{3.7}(t)\right)^{\left((n-\bar{n})\times\frac{k_4}{n}\times F_P\right)} \\
& \times\left(p_5^{3.7}(t)\right)^{(\bar{n}\times\frac{k_5}{n}\times F_P)}\left(1-p_5^{3.7}(t)\right)^{\left((n-\bar{n})\times\frac{k_5}{n}\times F_P\right)} \\
& \times\left(p_1^{11}(t)\right)^{(\bar{n}\times\frac{k_1}{n}\times(1-F_P))}\left(1-p_1^{11}(t)\right)^{\left((n-\bar{n})\times\frac{k_1}{n}\times(1-F_P)\right)} \\
& \times\left(p_2^{11}(t)\right)^{(\bar{n}\times\frac{k_2}{n}\times(1-F_P))}\left(1-p_2^{11}(t)\right)^{\left((n-\bar{n})\times\frac{k_2}{n}\times(1-F_P)\right)} \\
& \times\left(p_3^{11}(t)\right)^{(\bar{n}\times\frac{k_3}{n}\times(1-F_P))}\left(1-p_3^{11}(t)\right)^{\left((n-\bar{n})\times\frac{k_3}{n}\times(1-F_P)\right)} \\
& \times\left(p_4^{11}(t)\right)^{(\bar{n}\times\frac{k_4}{n}\times(1-F_P))}\left(1-p_4^{11}(t)\right)^{\left((n-\bar{n})\times\frac{k_4}{n}\times(1-F_P)\right)} \\
& \times\left(p_5^{11}(t)\right)^{(\bar{n}\times\frac{k_5}{n}\times(1-F_P))}\left(1-p_5^{11}(t)\right)^{\left((n-\bar{n})\times\frac{k_5}{n}\times(1-F_P)\right)},
\end{aligned}
\tag{4.5}
$$

where $p_{\bar{n}}^{n}$ is the probability that $\bar{n}$ of the total n EVs are charging on a certain time interval, k_x is the number of EVs that charge according to EV charging probability distribution p_x^z with $x \in \{1, 2, 3, 4, 5\}$ and z indicates the charging power level, either 3.7 or 11 kW. The data on public charging points presented in Section 2.3.3 show a trend towards higher power demand per charging session, thus we assume a 50/50 ratio between 3.7 and 11 kW here. For the cases with only one power level, the maximal allowed simultaneous charging sessions could be calculated directly. However now this is no longer possible as this number depends on the type of the EVs present at the charging stations. To simplify the situation, we assume for the maximum allowed number of simultaneous charging sessions that we have an equal number of both power levels, i.e. a 50/50 ratio. This implies that now the maximum number of simultaneously charging EVs is six: three of each power level, since $(3 \times 3.7) + (3 \times 11) = 44.1$ which closely approaches the maximum capacity of $12 \times 3.7 = 44.4$ kW. Figure 4.18 shows the result of this approach for the *55/15/10/10/10* charging regime distribution. Comparing this result to the Figure 4.16 and Figure 4.17 shows that problems with the combined power levels start at higher EV penetration rates compared to the situation that we charge with 11 kW only, but at lower EV penetration rates compared to when we charge with 3.7 kW only.

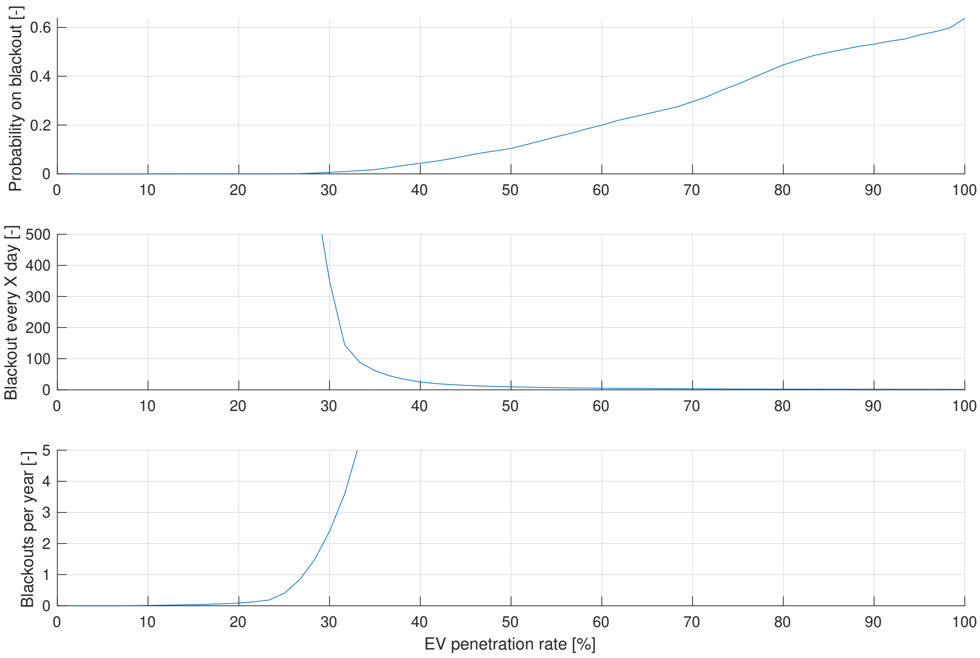

Figure 4.18: Blackout probability, number of days for an estimated blackout and expected blackouts per year for the sketched scenario using a 50/50 ratio of both charging power levels 3.7 and 11 kW.

4.7 Effects on the national LV grid

According to statistics from Netbeheer Nederland [36], the Dutch grid experienced 19.962 power interruptions on average per year between 2014-2018, which is almost 55 power interruptions per day. It is in common interest to keep this value as low as possible, so any significant increase is considered unacceptable. Note that 10 additional daily interruptions leads to an increase of nearly 20%, which we consider to be the maximum acceptable value.

To investigate the effects on the national LV grid, we propose to apply two methods. The first method we call the 'single charging regime' method, since every EV in the set is expected to show the same behavior, e.g. for $p_{\text{EVcharging}} = 0.20$ at 3.7 kW charging, the energy demand per EV per day is about 6 kWh and each EV is charged every day with exactly that amount of energy. This is based on the work of Section 4.5 and makes it straightforward to show the effect of EV energy demand and charging power on the Dutch LV grid. This method is shown in Section 4.7.1. However, in practice, such an homogeneous EV charging scenario is unrealistic and is regarded as a rather simplistic initial way of modeling the charging of EVs. Section 3.4.2 showed that not every EV is charged every day and that the number of charging sessions during a week is dependent on external factors such as battery size. The previous Section 4.6 introduced a method to account for this. The method can be a basis for estimating the expected blackout probability by taking into account two different power levels and five different charging regimes for each power level. Section 4.7.2 shows the results for this case.

4.7.1 Single charging regime method

To quantify the impact of increasing EV penetration rates on the number of daily blackouts, we determine all the single feeder daily blackouts that occur in the whole Dutch LV grid at different EV penetration rates and charging probabilities $p_{EVcharging}$. Since the occurrence rate of all simulated clusters is known (Table 4.1 in Section 4.2.2), we can extrapolate from the 26 simulated clusters (representing 71.3% of the Dutch LV grid) to 100% to estimate the number of daily blackouts in the estimated total of 300,000 LV feeders in the Netherlands. The results are presented in Figure 4.19 and 4.20 for 3.7 kW and 11 kW charging respectively. Observe that the number of daily blackouts is sensitive to the EV charging probability, $p_{EVcharging}$, and that for the 3.7 kW chargers a broader range for $p_{EVcharging}$ is required, since the charging time t_{charge} increases at lower charging powers. Note that $p_{EVcharging}$ describes the probability that an EV charges at a certain time by combining the charging start time probability and the duration of a charging session. For the 38 km per day scenario we know that $p_{EVcharging}$ is 0.228 for 3.7 kW charging and 0.073 for 11 kW charging.

From this method, we can conclude that, when applying only relatively high-power 11 kW charging, the current LV grid already may experience significant problems in terms of additional daily blackouts from EV penetration rates of 20%-25% and beyond. Applying only relatively low-power 3.7 kW charging, problems might be postponed to EV penetration rates of about 50%. In practice, there is a mix of both power levels present. Thus, the maximum EV penetration rate is expected somewhere in the range 14-50%. The main weakness of this method is that we can only consider one charging regime at a time. We have to choose a single value for $p_{EVcharging}$, which defines the charging regime and power level that all EVs in the set follow. We also have to assume that every EV has to charge every day. As this does not seem to be very realistic, we introduced a model that can incorporate different charging regimes and power levels at the same time in Section 4.6. The next section shows the results of that improved model.

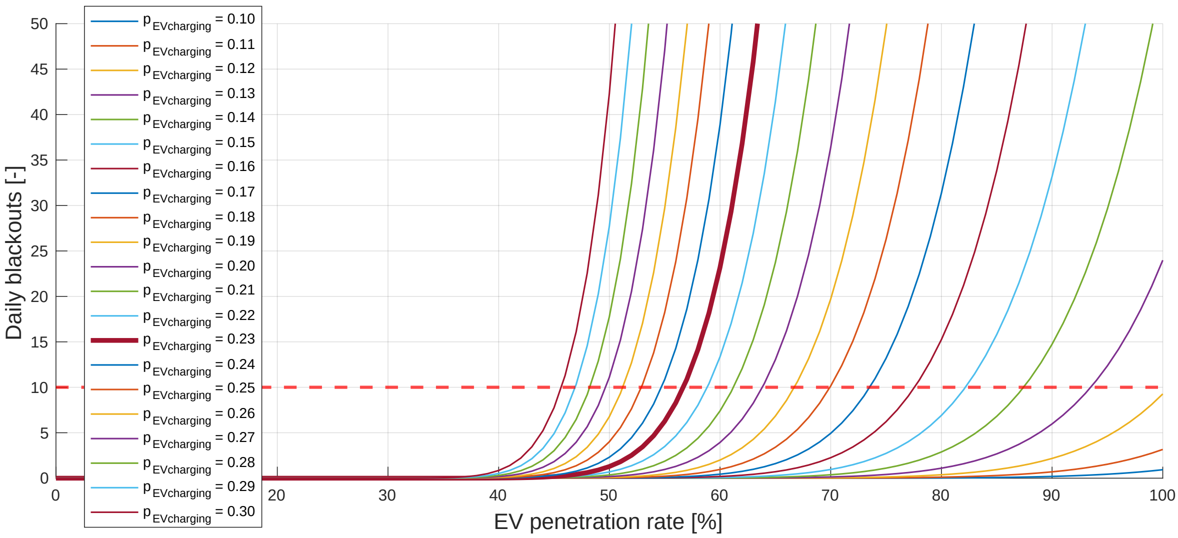

Figure 4.19: Effect of EV penetration rate and EV charging probability, $p_{EVcharging}$, on number of blackouts in the Netherlands, using 3.7 kW EV chargers. The data in this graph takes into account all estimated 300,000 feeders in the Dutch LV grid. The line in bold represents the estimated maximum EV charging probability for the '38 kilometer per day' charging scenario, while the red dashed line represents the 20% black-out increase level.

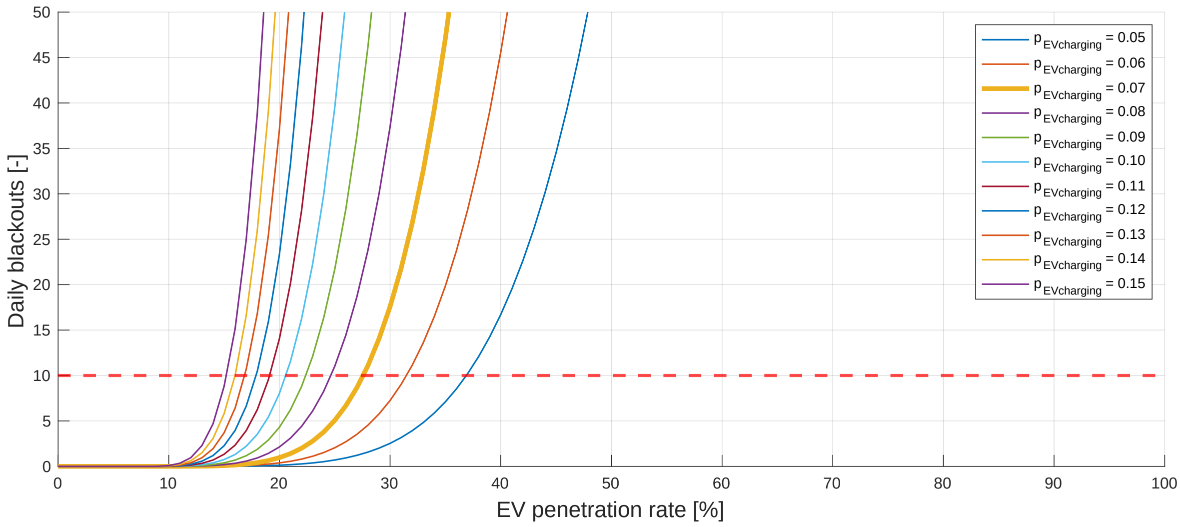

Figure 4.20: Effect of EV penetration rate and EV charging probability, $p_{\text{EVcharging}}$, on number of blackouts in the Netherlands, using 11 kW EV chargers. The data in this graph takes into account all estimated 300,000 feeders in the Dutch LV grid. The line in bold represents the estimated maximum EV charging probability for the '38 kilometer per day' charging scenario, while the red dashed line represents the 20% black-out increase level.

4.7.2 Multiple charging regimes method

Where the single charging regime method assumes that every EV charges every day and charges the same amount of energy, this multiple charging regime method considers that only a subset of the total number of available EVs on a feeder charges on a certain day and that there is a variety in the amount of energy these EVs charge. The EVs that do not charge on a certain day are putting no stress on the grid on that day but they are part of the EV penetration rate. To show the results of an increasing EV penetration rate on the expected daily blackouts in the Dutch LV grid, we use the *55/15/10/10/10* charging regime distribution proposed in Section 4.6.3, where 55% of the EVs follows regime 1, 15% regime 2 and so on. With this charging regime distribution, 70% of the available EVs on a feeder is charging on a certain day, while the other 30% is not charging. Applying this method for both 3.7 kW and 11 kW charging results respectively in the Figures 4.21 and 4.22. Note that the five clusters causing problems for 3.7 kW charging are the same clusters which cause the first problems for 11 kW charging, namely Cluster 8, 15, 17, 23 and 24. These are also the clusters with relatively the lowest possibilities for simultaneously charging EVs, according to Table 4.1 in Section 4.2. These five clusters represent about 15% of the total LV feeders in the Netherlands (corrected for the total estimated 300,000).

The main advantage of this multiple charging regime method is that we can combine different charging behavior, whereas with the single charging regime method we are restricted to a single charging regime for every EV in the model. In Figure 4.23 and 4.24, 7 charging regimes for both 3.7 and 11 kW are compared: the uniformly distributed *20/20/20/20/20* charging regime distribution, the *55/15/10/10/10* charging regime distribution and the situations in which all EVs follow 1 of the 5 separate charging regimes. Note again that 'charging regime 1' means that every EV is charging the energy equivalent of 38 km every day, 'charging regime 2' is used to indicate that an EV charges the energy equivalent of $2 \times 38 = 76$ km every days, and so on. Comparing all EVs charging according to regime 1 (charging every EV every day) with the *55/15/10/10/10* charging regime distribution, we observe that, for 3.7 kW charging, the acceptable EV penetration rate is extended by 15-20%. For 11 kW charging, the effect is weaker, but the allowable

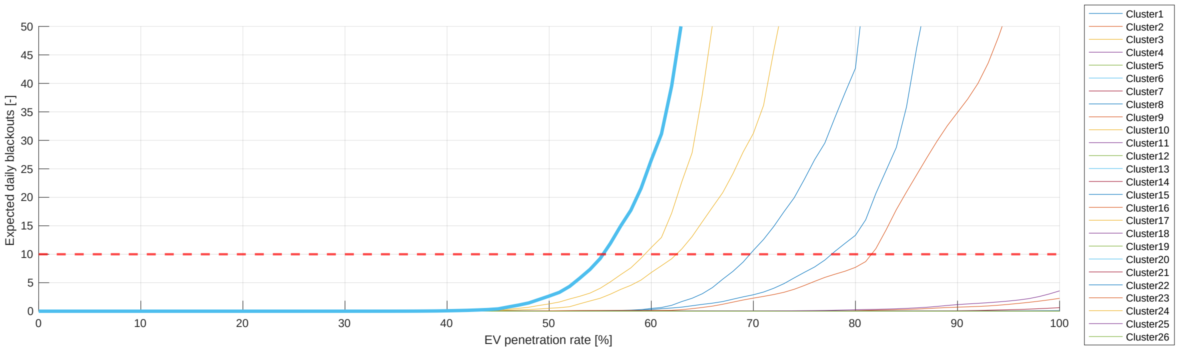

Figure 4.21: Expected daily blackouts using 3.7 kW charging and the proposed charging regime distribution. The line in bold represents the total number of daily blackouts corrected for all feeders in the Netherlands.

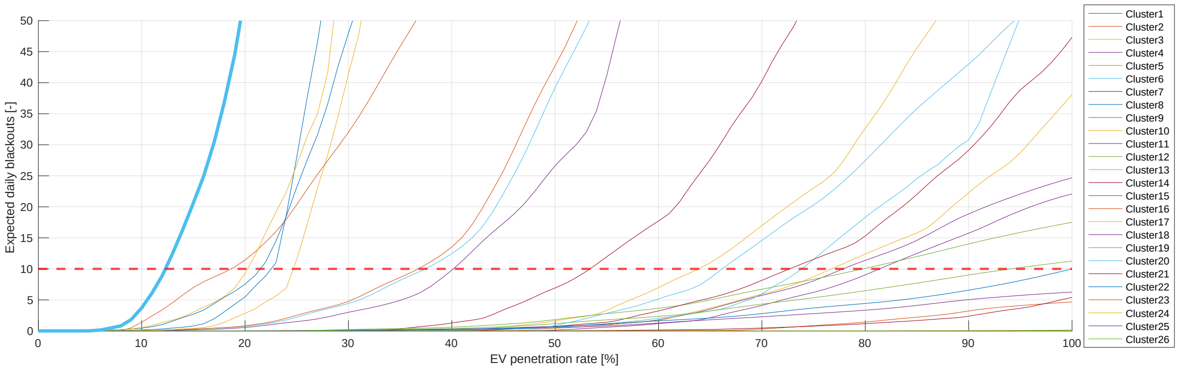

Figure 4.22: Expected daily blackouts using 11 kW charging and the proposed charging regime distribution. The line in bold represents the total number of daily blackouts corrected for all feeders in the Netherlands.

EV penetration rate can still be extended by about 5-10%. Changing the charging regime to an equal distribution among the five different regimes increases the allowable EV penetration rate even further: an extra 20-25% for 3.7 kW charging and about 5% extra for the 11 kW charging case. This result can be explained by the fact that such an uniformly distributed charging regime lowers the number of charging sessions on a certain day. Although the average length of the charging sessions on such a day increases, the final blackout probability decreases since the probability of overloading a feeder is lower.

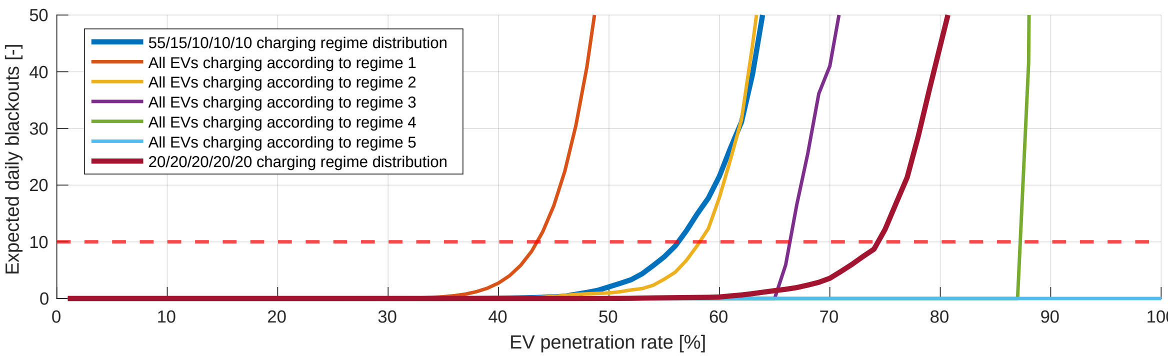

Figure 4.23: Comparison of the impact of different 3.7 kW charging regimes on expected daily blackouts in the Netherlands.

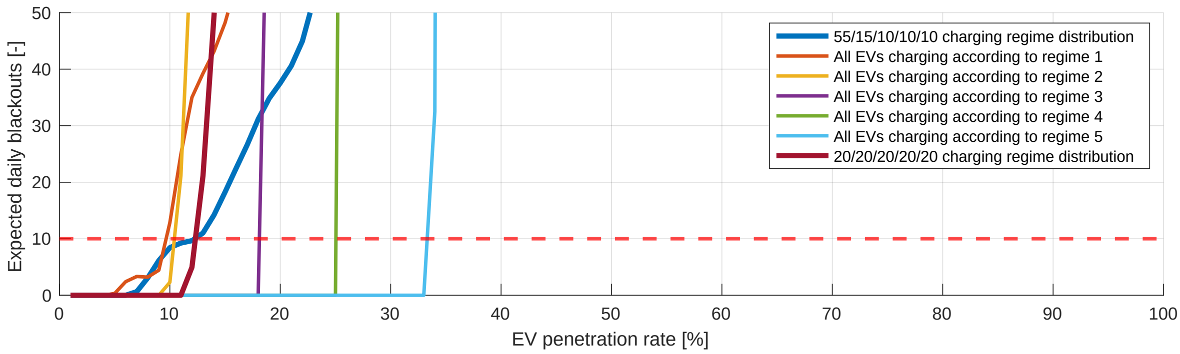

Figure 4.24: Comparison of the impact of different 11 kW charging regimes on expected daily blackouts in the Netherlands.

Notice that we would expect "All EVs charging according to regime 1" to match the bold lines in Figure 4.19 and Figure 4.20 for the corresponding power level in the single charging regime method, since they both represent the same charging regime. However, this is not the case, since the single regime charging method only takes into account the probability of a blackout on the timeslot with the highest probability, not for a full day. This is another advantage of the multiple charging regime method over the single charging regime method.

4.7.3 Combining power levels

In Section 4.6.4 we already stated that we assume it unlikely that all EV chargers charge according to the same power level and we proposed to use a 50/50 ratio of 3.7 and 11 kW chargers for this model. This means that, if we have a number of EV chargers in a set, roughly half of them are 11 kW chargers and the other half are 3.7 kW chargers. So, we end up with one single value for simultaneously charging EVs instead of one value for 11 kW charging and one value for 3.7 kW charging. To do this, we use the results from Table 4.1 from Section 4.2.2, which show the maximum simultaneously charging EVs for the two different power levels. From this, we can estimate the available peak power for each cluster and divide that peak capacity among the 2 charging power levels. We take Cluster 02 as example. Cluster 02 can in theory handle eight simultaneously charging 11 kW chargers. This is roughly a 8×11 kW $= 88$ kW load. This defines the available maximum capacity available for EV charging. To divide this 50/50 among 11 and 3.7 kW charging power levels, we end up with six possible chargers for each power level, since 6×11 kW$= 66$ kW and 6×3.7 kW$= 22.2$ kW, which is roughly 88 kW. The total number of simultaneously charging EVs on this feeder becomes 12, on the condition that roughly half of these EVs charge with 11 kW and roughly the other half charges with 3.7 kW. The result of the combinations for all 26 clusters is shown in Table 4.5. Figure 4.25 shows the EV penetration rate plotted against the expected daily blackouts for the using both 3.7 and 11 kW charging power levels in a 50/50 distribution. Comparing this to Figure 4.21 and Figure 4.22 that represent the cases for 3.7 and 11 kW charging only, we find that the 50/50 ratio falls in between both curves, as expected.

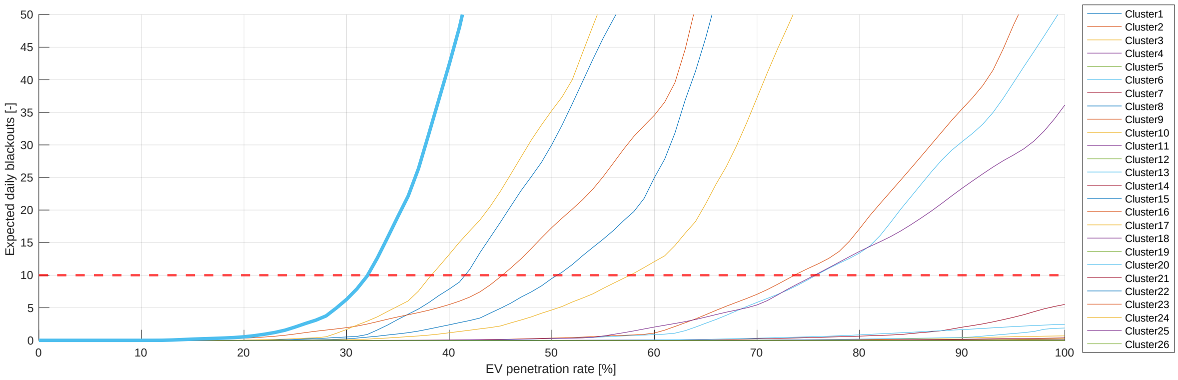

Figure 4.25: Expected daily blackouts using both 3.7 and 11 kW chargers (in a 50/50 ratio) for the proposed charging regime distribution. The line in bold represents the total number of daily blackouts corrected for all feeders in the Netherlands.

Cluster	Total HH [-]	max. simultaneous chargers [-]	Occurence [%]
01	17	17 (100%)	6.4
02	24	12 (50%)	4.5
03	39	12 (31%)	4.5
04	19	10 (53%)	4.4
05	32	16 (50%)	4.1
06	26	8 (31%)	3.4
07	49	12 (25%)	3.4
08	70	10 (19%)	3.3
09	27	8 (30%)	3.2
10	35	12 (34%)	2.9
11	33	12 (36%)	2.9
12	13	8 (62%)	2.8
13	62	14 (23%)	2.6
14	38	12 (32%)	2.5
15	51	8 (16%)	2.2
16	26	16 (62%)	2.1
17	67	10 (15%)	2.1
18	11	8 (73%)	1.8
19	13	8 (62%)	1.8
20	33	10 (31%)	1.7
21	46	14 (31%)	1.6
22	12	8 (67%)	1.6
23	26	6 (23%)	1.5
24	58	8 (14%)	1.5
25	30	8 (27%)	1.3
26	25	16 (64%)	1.2

Table 4.5: Maximum feeder capacity in terms of simultaneously charging EVs following a 50/50 ratio for 3.7 and 11 kW chargers. The corresponding EV penetration rate on that feeder is denoted by the percentage between brackets. Total HH denotes the number of households on the feeder, while Occurence represents the percentage of feeders in the Dutch LV grid that are resembled by that cluster.

4.7.4 Summary

In this section, two methods to analyse the impact of an increasing EV penetration rate on the Dutch LV grid are introduced: the so called 'single charging regime method' and the 'multiple charging regime method'. With the single charging regime method, we get a feeling for what happens when all EVs in general increase their energy demand. When the energy demand increases, the charging time increases and thus the probability that EVs charge during the same time interval, $p_{\mathrm{EVcharging}}$, increases. This increases the number of estimated daily blackouts.

The multiple charging regime method allows us to extend the first observations by also taking into account that not every EV charges every day and taking into account different charging regimes per EV. The proposed method makes it possible to compare different charging regimes and different charging powers. By showing the effect of different charging regimes, we can conclude that dividing the charging sessions evenly among weekdays is preferable in terms of reducing the load on the LV grid. However, this is not very realistic or applicable, since we although we may try to influence charging behavior, we can not force people to charge their EV only on certain days. Using the *55/15/10/10/10* charging regime distribution and the 50/50 ratio of 3.7 and 11 kW power levels, the maximum EV penetration rate for the Netherlands estimated to be around 30%. The model can be used to further study the effect of different charging regime distributions and to estimate the probabilities of simultaneously charging EVs in uncontrolled charging situations.

4.8 Summary

The methods and corresponding results of this chapter show that the current LV grid infrastructure in the Netherlands faces problems when we assume uncontrolled EV charging. We use a set of generic feeders to describe a large part of the LV grid. For each of the generic feeders we find a maximum allowable number of simultaneous EV charging sessions. In about 70% of the feeder cables, the current capacity limit is reached before a critical voltage drop appears. In the other 30%, a critical voltage drop near the end of the feeder occurs earlier than a current capacity problem. Voltage drops might be prevented by increasing the transformer voltage level, but this can induce problems on sunny days with relatively high PV power production. We assume that these generic feeders proportionally represent the whole LV grid, so we can make statements about the expected number of blackouts in the Netherlands with uncontrolled EV charging.

By describing the probability of an EV charging session, $p_{\mathrm{EVcharging}}$, we capture the influence of energy demand, charging power and plug-in time distribution in one single value. This approach allows us to draw conclusions on the EV penetration rate for the whole Dutch LV grid. From the graphs in Section 4.7.1, we know that this value heavily influences the results. This indicates that how often, when and with what power and energy demand people are charging their EV is crucial to say something about the possible EV penetration rate. However, with the available data we can make an estimation for a general scenario in which every EV drives 38 kilometers per day. The results show that, using the proposed 38 kilometer per day scenario, a 20% increase from the current level of daily blackouts is to be expected from as early as 20-25% EV penetration rate when expecting 3-phase 11 kW charging only. Decreasing power levels to 3.7 kW significantly extends this point to beyond 50%. However, in reality deal with varying power levels, so the maximum EV penetration rate for the whole of the Netherlands is considered to be somewhere in between the mentioned boundaries.

Section 4.7.2 shows the results for the proposed 'multiple charging regime' model that also incorporates the effect of EVs that charge according to different charging regimes, but still for the two charging power levels separately. Charging with only 3.7 kW, problematic EV penetration rate is found aroun 55%, while charging all EVs in residential areas with 11 kW charges, problems already rise around 10% EV penetration rate. In Section 4.7.3 these two power levels are combined into one model in which the ratio between the two power levels can be adjusted. Using this last method, the problematic nationwide EV penetration rate is 30%. An interesting finding here is that out of the 26 clusters, five given feeders are typically causing the first problems. These feeders are mainly characterized by their high number of connections, creating a higher probability of simultaneously charging EVs.

To arrive at the conclusions regarding the effects on the national LV grid, some assumptions were needed. First of all, it is still questionable if the presented generic feeders correctly represent the entire Dutch LV grid, the current method only estimates the situation by using relatively outdated feeder data and a clustering method in which details may be lost. Secondly, the feeder limits used are not chosen according to a very conservative estimate. There is a fair chance that the chosen limits for peak power capacity overhead are too high. Local situations with combinations of different cable properties might create a blackout at lower EV penetration rates than what is projected in this method. Next to these LV feeder limits, we also have to deal with transformer limits. In general, the stacked capacity of every individual feeder connected to the same transformer is significantly higher than the capacity of the transformer. This means that if e.g. five feeders are connected to one transformer and all five feeders operate at e.g. 85% of their maximum capacity, the transformer limit might be already reached, without ever reaching the limit of even one of the feeders. Thirdly, with the available data, we can make predictions on charging sessions as being independent events and thus estimate the probability on problematic situations on normal weekdays. In the case of any special event that might make the EV charging sessions dependent, e.g. a popular soccer match of the national football team for which a lot of people arrive at home early or around the same time, expected charging behavior changes. In such a case, the number of maximum simultaneously charging EVs remains the same, but the probability of problematic situations might increase. Additionally, other emerging electrification technologies like heatpumps and induction cooking might play a role in the maximum capacity of a feeder. Another important assumption we make for the final conclusion on maximum EV penetration rate is that all EV energy demand is charged with a charger in an LV residential area. Since EV owners might also be able to charge their EV e.g. at work, in shopping malls or along highways,the energy demand charged in the LV feeders in residential areas might be lower than the proposed energy equivalent of 38 kilometer per day.

Chapter 5

Scenario simulations

5.1 Introduction

This chapter presents a number of scenarios in detail to demonstrate the working of the proposed modeling methods in different situations, which enables us to analyze how local settings influence the result of the more general results on the whole Dutch LV grid of Section 4.7. Two typical scenarios for sub-urban and rural areas, with characteristics based on the work in [37], are tested by using artificial grid models combined with existing demographic settings. Next to maximum EV penetration rates, we investigate the maximum PV penetration rates in these situations and problems with voltage rise. Section 5.2 starts with the analysis of the sub-urban scenario, followed by Section 5.3 which considers a typical rural area feeder. The last case is on a verified grid model used in a field test in Lochem [10] and is presented in Section 5.4.

5.2 Sub-urban feeder scenario

The chosen sub-urban-scenario feeder is 225 meters long, utilizes a 150 Al cable and hosts 58 connected houses. These features are derived from the work in [29] and we consider this to be a typical feeder in sub-urban areas, with houses relatively close together, but a variety in housing types, i.e. mainly duplex and detached houses mixed together. As demographic input for this specific scenario, we chose the neighborhood Eilermarke in the municipality of Enschede. It is the youngest (in terms of residents) area in Enschede: it hosts mostly young families with slightly above average incomes.

5.2.1 Demographic inputs of Eilermarke

The CBS database for Eilermarke specifies 13% single-person households, 65% multiple-person households with kids and only 22% multiple-person households without children. Some other statistics about Eilermarke in 2017 are:

- 39.9% of the population is 24 years old or younger, only 5.3% is 65 years or older;
- Relatively little poverty: only 3.5% around social minimum;
- 687 houses, 70% owner-occupied, 24% rented from a housing association, other 6% privately rented. All houses are built after the year 2000, average market value €210k;
- 600 multiple-person households of which 450 (75%) have children.
- Average yearly electricity consumption of 3590 kWh, average yearly gas consumption of 1160 m^3.

- On average 1,2 cars per household.

Using the demographic input method described in Section 3.3.2, this results in the demographic household distribution in Figure 5.1. Figure 5.2 shows a Google Maps satellite image of the area, showing its typical sub-urban features and layout. Taking into account the relatively low age of the residents (mostly families), the slightly-above average income and the number of cars per household, this might become a neighborhood with a relatively large uptake of EV in the coming decades. Also, the layout of the neighborhood provides parking space, either an individual driveway or enough public parking space with options to host public AC chargers.

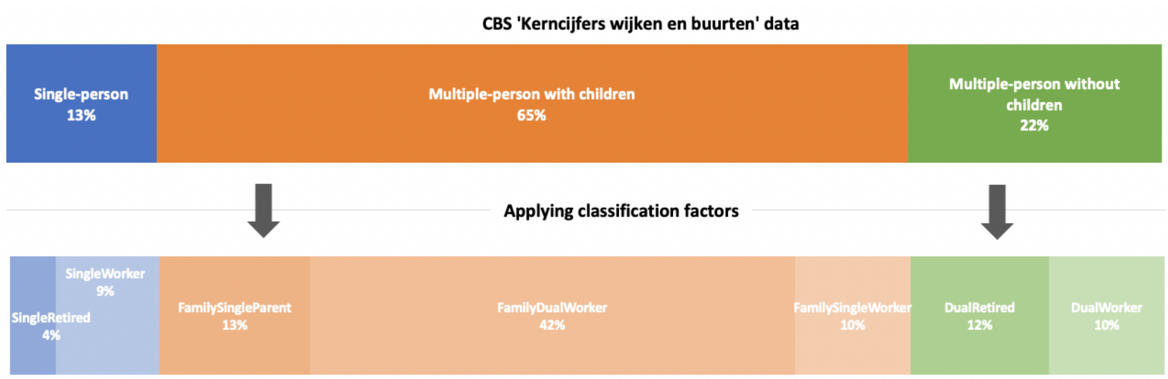

Figure 5.1: The demographic household distribution for the Eilermarke, municipality of Enschede.

5.2.2 Feeder limits

From the results of simulations, we know that on this feeder the maximum number of simultaneously operating EV chargers is 10 x 11 kW or 30 x 3.7 kW. Charging with these loads, which is about 111 kW total peak (about 37 kW per phase) causes a blackout. At these numbers, voltages are still within the acceptable limits due to the short length of the feeder, but current levels reach the maximum capacity of the 150 Al cable and an LV network blackout is very likely due to overloading. Since voltage levels stay within the allowed limits, the location of EV charging loads within the feeder is not taken into account. When we assume the EVs in this neighborhood charge according to a 50/50 mix of both charging power levels, the maximum number of simultaneously charging EVs is chosen to be 14: seven of each power level, resulting in a total power peak of around 103 kW. This is slightly under the 111 kW level, leaving some room for unforeseen loads e.g. cooking equipment.

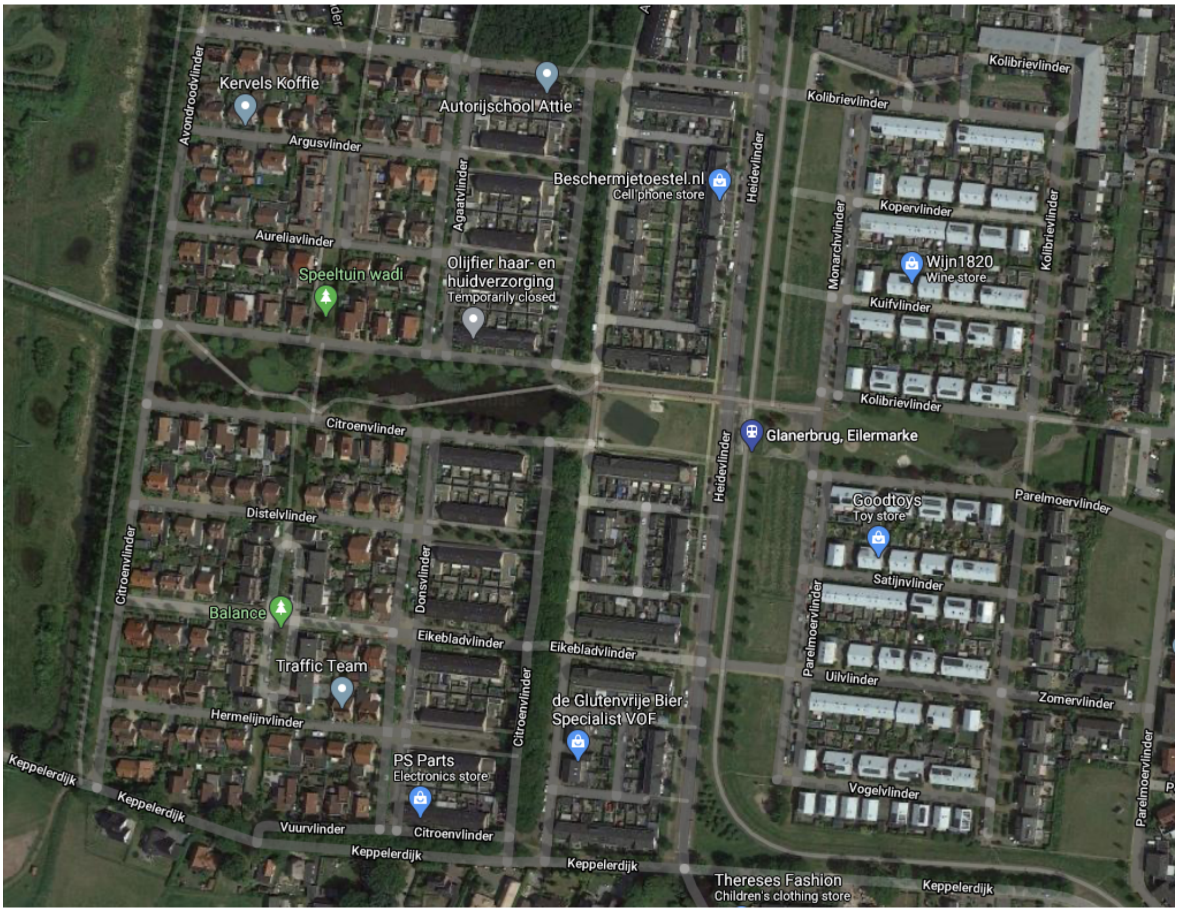

Figure 5.2: Google Maps satellite image of the Eilermarke, municipality of Enschede. This neighborhood is considered to be a typical sub-urban area, containing both detached and terraced houses and plenty of parking space.

5.2.3 EV penetration

To obtain insight in the influence of the EV penetration rate in this combination of LV grid structure and demographic composition, we consider the 38 km per day scenario from Section 4.6, imposing an energy demand of 33.25 kWh per five days that can be charged according to one of the five charging regimes. For this scenario we calculate the number of expected blackouts per year for this specific feeder depending on EV penetration rate. The achieved results are given in Figure 5.3. The expected blackouts per year are calculated using the proposed charging regime distribution *55/15/10/10/10* and a 50/50 ratio between 3.7 kW and 11 kW charging power.

Although for a single LV feeder the achieved result might not be very alarming, since even at around 80% EV penetration rate we expect at most one blackout per year. However, all Dutch LV grids contain an estimated 300,000 feeders. If e.g. only 3.33% (10,000) of the total feeders in the Netherlands are comparable to this type, the expected additional yearly blackouts will be significant, as can be seen in Figure 5.4. Note that on a national level this means we can expect an increase in blackouts of about 100 already at 50% EV penetration rate and that this increases very quickly, with an expected 100 additional blackouts at around 70% EV penetration rate, only for these group of 10,000 feeders. This is significant, since nowadays the yearly average for the Netherlands is 19,962 power interruptions per year, as we mentioned in Section 4.7.

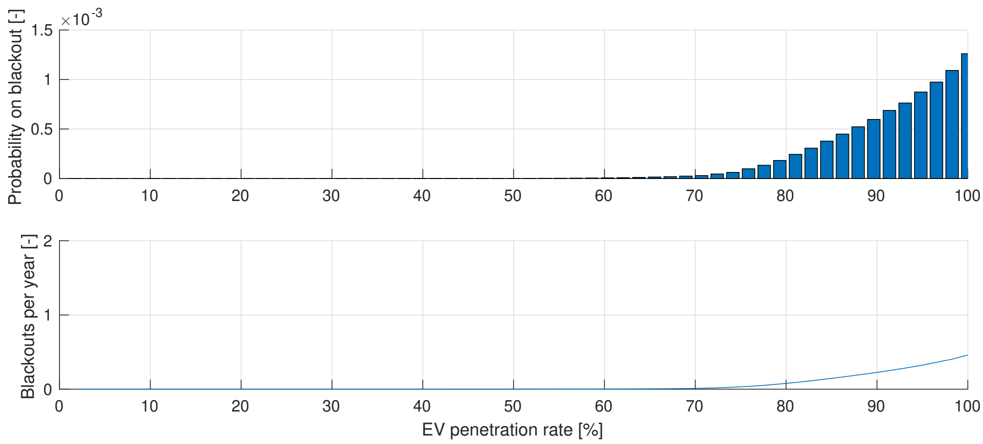

Figure 5.3: Expected blackouts per year at all possible EV penetration rates for the sub-urban scenario single feeder, using the *55/15/10/10/10* charging regime distribution and the 50/50 ratio between 3.7 and 11 kW charging power.

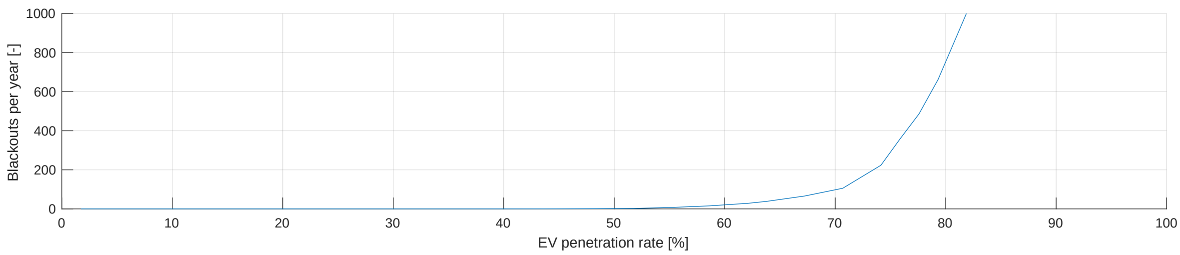

Figure 5.4: Expected number of blackouts per year for all possible EV penetration rates in all 10,000 of the sub-urban scenario single feeders together, using the *55/15/10/10/10* charging regime distribution and the 50/50 ratio between 3.7 and 11 kW charging power.

5.2.4 PV penetration

To determine the maximum PV penetration level for this type of feeder and the given demographic distribution, we determine the maximum number of PV installations on the feeder for which the simulation for the day with the highest solar irradiance peak still does not lead to problems. The properties of the PV installations are determined according to the approach from Section 3.5. Furthermore, we add installations starting from end of the feeder. Since this feeder is relatively short and uses a relatively thick cable, we encounter no voltage problems, but encounter a current overload at 33 PV installations leading to a maximum PV penetration rate of 58%. Note that these simulations are carried out with only the basic household load and PV installations, meaning that EV chargers are not considered here.

5.2.5 Summary

For the sub-urban scenario, problems with EV penetration rates may start to appear from 45-50% onward. Since we have a large set of these type of feeders together, we can expect a high number of blackouts in the Netherlands. With the annual energy consumption based on the demographic inputs, we were able to simulate suitably sized PV installations. According to the results, it may be possible to equip up to 58% of the households with PV installations on this specific feeder before problems start to appear. The sub-urban feeder type is relatively short, so problems with overloading the cables is always prior to critical voltage drops. Since there may be an overlap (in time) between EV charging power demand and PV power

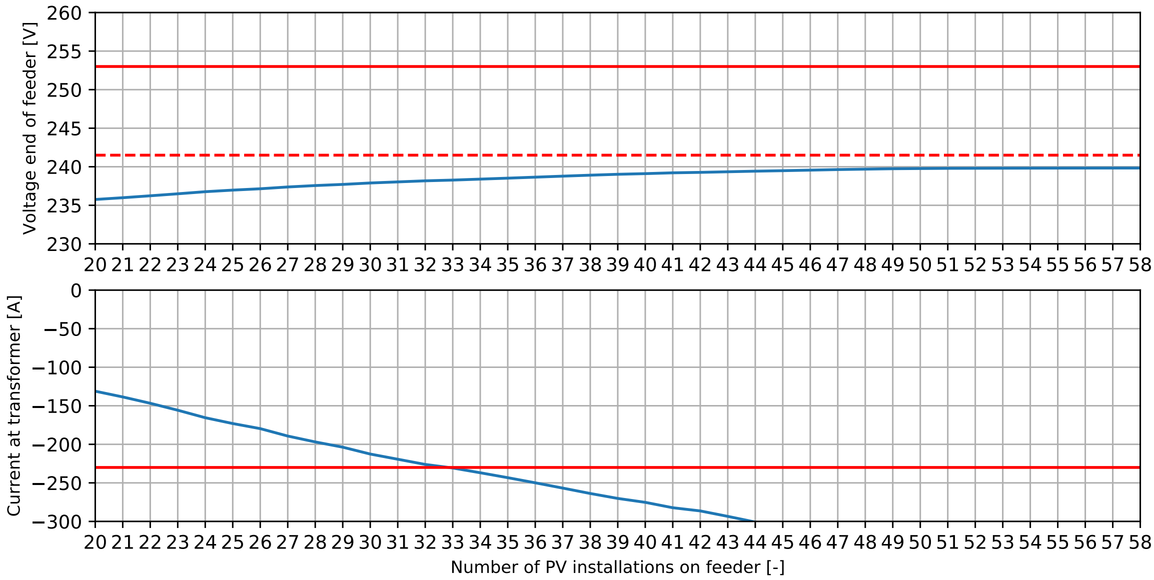

Figure 5.5: Simulation results of adding PV installations starting from the end of the sub-urban feeder.

generation surplus, this might influence the results. If surplus PV power can directly be supplied to an EV, the overloading of the transformer due to PV generation might be (partly) mitigated and the number of simultaneously charging EVs at that moment might be higher. However, increasing electrification with e.g. heatpumps and induction cooking might again lower the possible EV penetration rate.

5.3 Rural feeder scenario

A rural feeder is typically characterized by its relatively large length and few connections, which is a direct consequence of how the houses in such areas are located: with relatively large distances in between. For the analysis, we consider a feeder with 18 connections and a length of 1084 meter. We simplify the analysis by choosing in this subsection one type of cable for the full length (70 Cu).

5.3.1 Demographic inputs

Since this is a rural area, all the houses are considered to be relatively large detached houses with energy loads as the *FamilyDualWorker* type described in Section 3.3.1. This choice represents the higher energy consumption and PV installation sizes in these relatively large detached houses. In detail, this implies that each household on the feeder consumes 5260 $\pm$ 1800 kWh annually. Note that this does not cover operating farms, which probably consume a lot more energy. Their effect on EV penetration rates remains a topic of further research.

5.3.2 Feeder limits

Installing three 11 kW chargers at the last positions of the feeder (as seen from the transformer) already causes a severe voltage drop. In Figure 5.6 a part of the simulation for this scenario in which two 11 kW chargers on the last positions of the feeder start charging at 17:00 is given.

Due to the relatively long length, the maximum EV penetration rate is location sensitive. Placing EV chargers in the end of the feeder, more than one kilometer away from the transformer, becomes problematic very quickly, as shown in Figure 5.7. In Figure 5.8, where we place EV chargers on the first positions (as

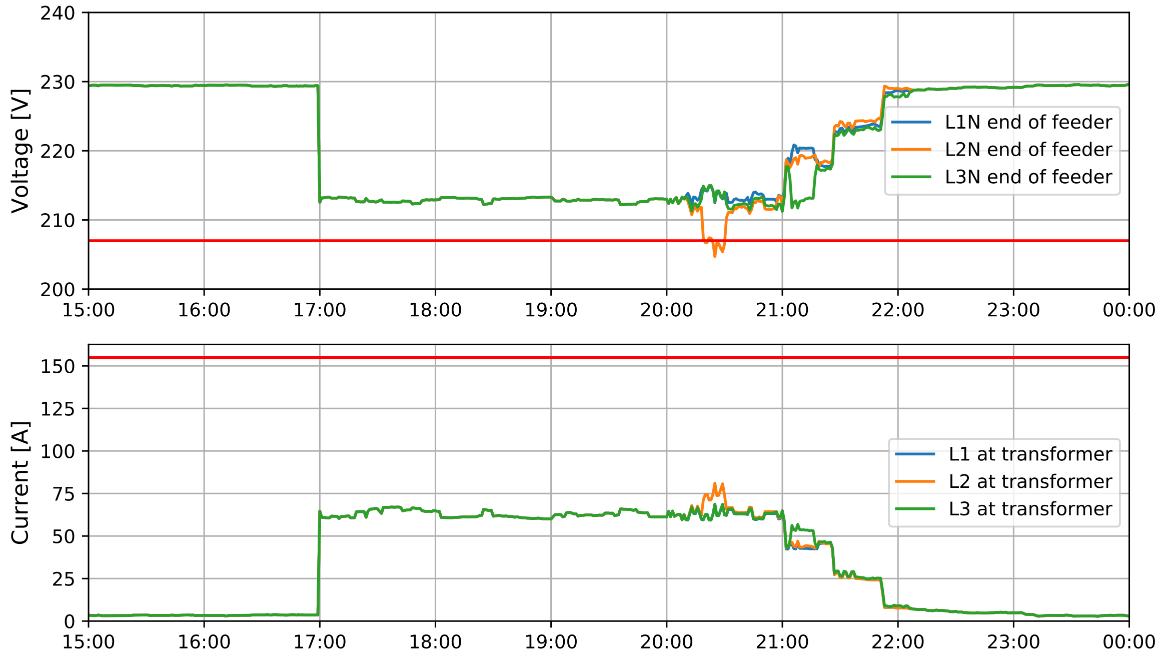

Figure 5.6: Simulation result of installing three 11 kW EV chargers at the last positions of the rural feeder.

seen from the transformer) towards the end, the current limit is reached even prior to a critical voltage drop.

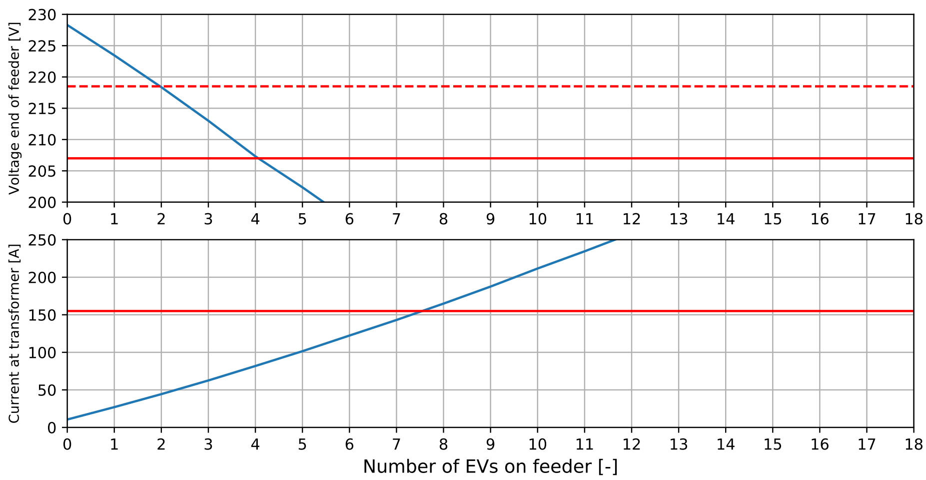

Figure 5.7: Simulation result of installing 11 kW EV chargers at the last positions of the rural feeder.

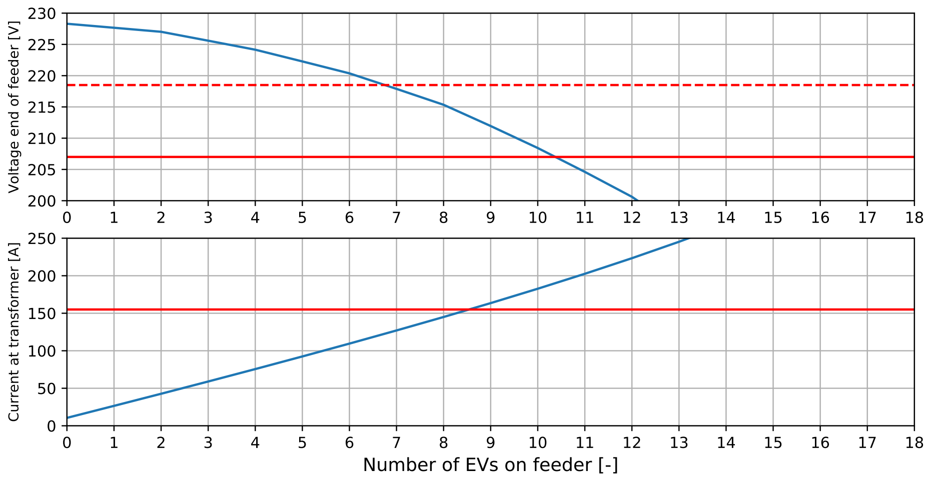

Figure 5.8: Simulation result of installing 11 kW EV chargers at the first positions of the rural feeder.

Thus, by charging EVs near the end of the feeder, on positions the furthest away from the transformer, we can only host three 11 kW EV chargers, while when we install the EV chargers by starting from the transformer, we can host seven 11 kW chargers. For 3.7 kW charging, the situation is different. With only 18 households, every household can charge an EV with 3.7 kW simultaneously and this is even regardless of the location according to Figure 5.9 and Figure 5.10. In the next section we analyze the impact of these different limiting factors.

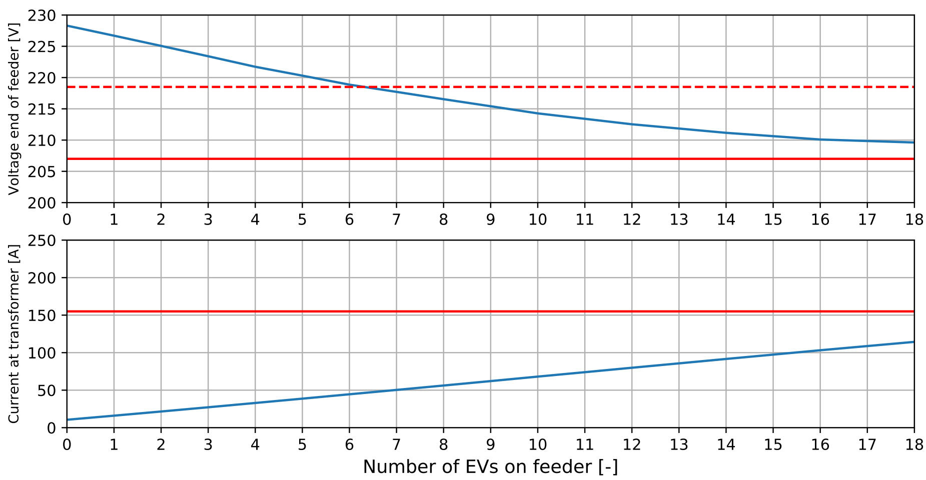

Figure 5.9: Simulation result of adding 3.7 kW EV chargers from the last position of the rural feeder.

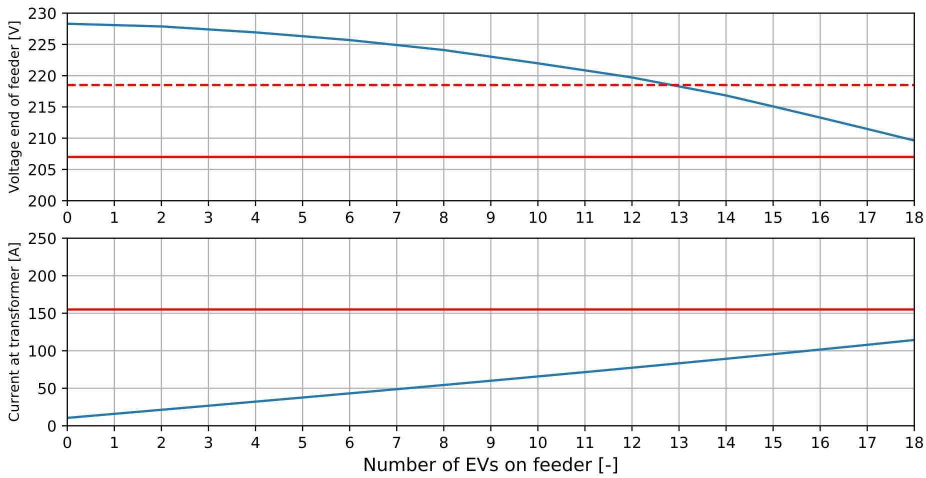

Figure 5.10: Simulation result of adding 3.7 kW EV chargers from the first position of the rural feeder.

5.3.3 EV penetration

The previous section shows that the rural feeder in this example can host an EV charging load of 18×3.7 kW $= 66.6$ kW if we distribute the load uniformly along the feeder by charging with 3.7 kW at every household. However, if we increase the charging power and redistribute the load towards the very end of the feeder, we can only host $3\times$ 11 kW$= 33$ kW. As an alternative, we simulate a 50/50 ratio between both power levels, where every household receives either a 3.7 kW or an 11 kW EV charger, alternately starting with a 3.7 kW charger at the end of the feeder. The results are shown in Figure 5.11 and Figure 5.12. For this scenario, the maximal number of EV chargers is seven if we install EV chargers on the last positions on the feeder. Installing chargers at the first positions allows to charge about twelve EVs.

We analyze the impact of the positioning of the EV chargers by comparing the effect on estimated blackouts in both situations. The corresponding results using the *55/15/10/10/10* charging regime distribution are given in Figure 5.13. Notice that the probability of a blackout becomes very small in the case of charging EVs in the first positions, when we can host a maximum of twelve EVs. Charging EVs on the last positions of the feeder, with a maximum of seven EVs, becomes problematic, since there is a higher probability of a blackout in the form of a critical voltage drop.

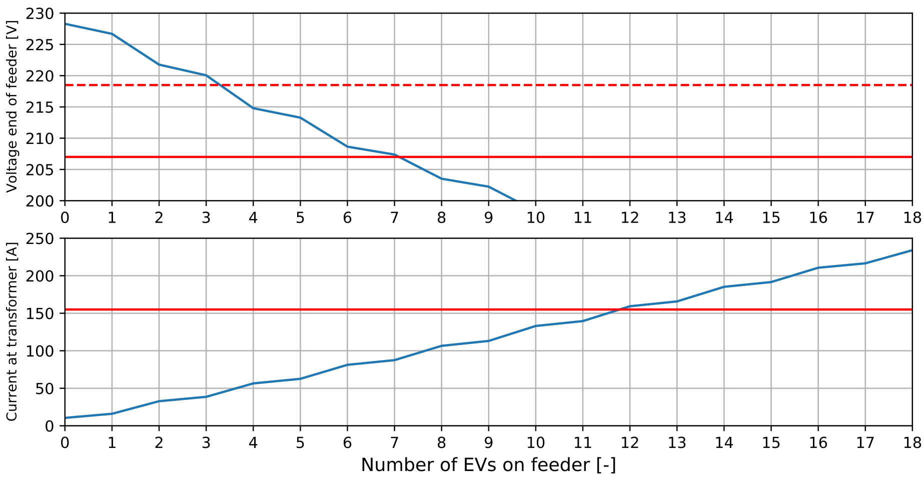

Figure 5.11: Simulation result from adding a 50/50 mixture of both power levels EV chargers on the last positions of the rural feeder.

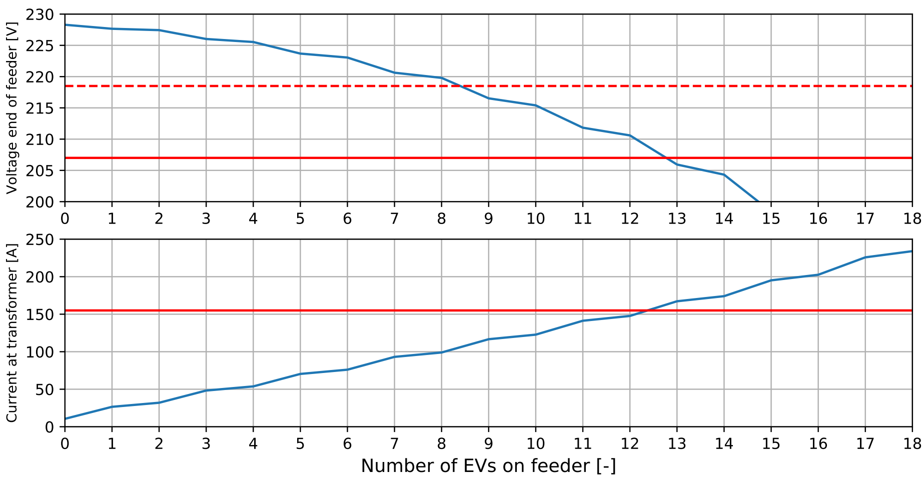

Figure 5.12: Simulation result of adding a 50/50 mixture of both power levels EV chargers on the first positions of the rural feeder.

5.3.4 PV penetration

In contrast to the short sub-urban feeder of Section 5.2, where voltage problems did not play a role, rural type feeders are more likely to experience voltage problems due to their length. This is shown in Figure 5.14, where only six PV installations are installed on the last positions of the feeder. This situation results already in a violation of the voltage limits on days with the highest solar irradiance. The PV installations are designed with the Dutch net-metering regulations in mind, thus accordingly to the approach described in Section 3.5.

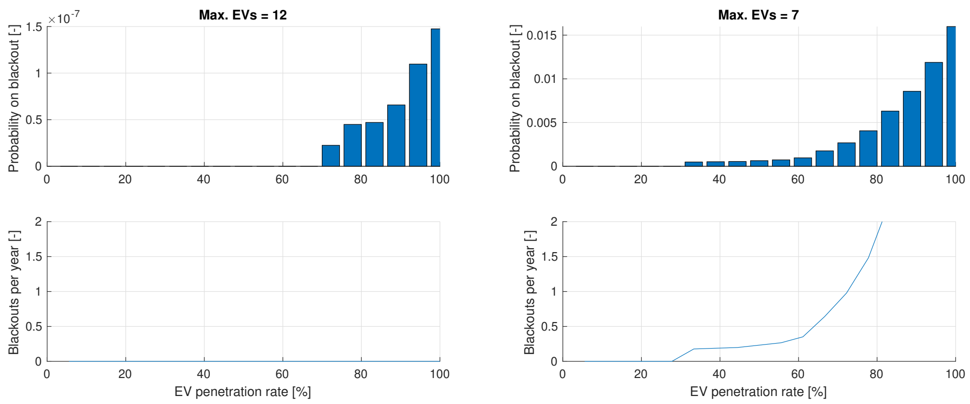

Figure 5.13: Comparison of the effect on blackout probability and blackouts per year, using the *55/15/10/10/10* charging regime distribution with a maximum of twelve vs. seven simultaneously charging EVs.

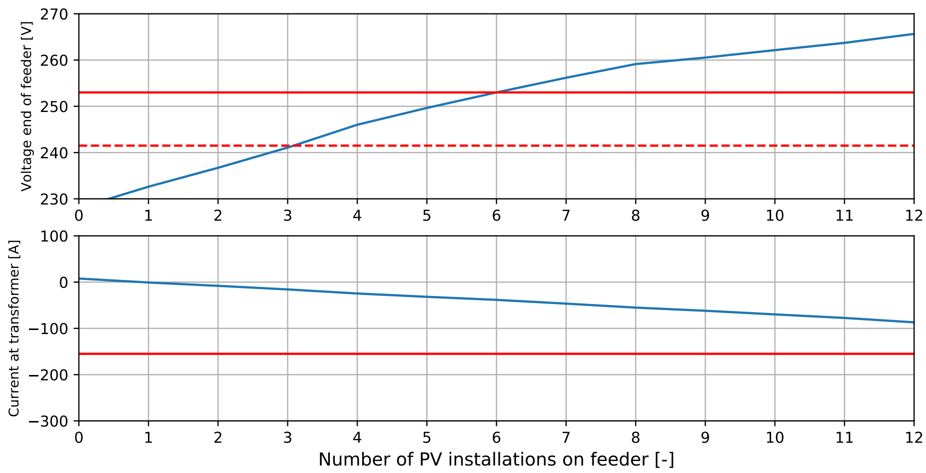

Figure 5.14: Simulation results of placing PV installations on the last positions (as seen from the transformer) on the rural feeder.

5.3.5 Summary

The rural feeder illustrates the problem that most feeders of this type experience: voltage drops below the limits occur before violating the current capacity of the feeder, due to the relatively large length of the cable. Simulations show that charging even two or three EVs with 11 kW chargers on the last positions of the feeder is already problematic, while charging seven or even eight 11 kW chargers in the first positions, close to the transformer, might not be as problematic. This severely influences the blackout probability, since already a small number of simultaneously charging EVs can create a blackout. This makes analysis not as straightforward compared to feeders in which we experience current capacity problems prior to a critical voltage drop. The same holds for power generation: when six out of the eighteen households near the end of the feeder in this example install a PV installation, voltage limits are already exceeded on days with a lot of solar irradiance, while the current capacity is still far away from its limit.

5.4 Lochem

In this section, a scenario is considered which is based on an existing LV grid network located in the neighborhood Zuiderenk in the town of Lochem. This scenario is interesting since it contains an actual existing LV grid network instead of the two synthetic ones from the previous sections. Also, the topology of this network and the correct cable properties are known and a field test was carried out in which this particular feeder was overloaded by mainly due to a larger number of EV chargers being used simultaneously [10]. The transformer where this feeder originates is named based on its location: 'Mauritsweg'. Figure 5.15 shows a Google Maps satellite image of the situation, with a line drawn on top to indicate the feeder location. The feeder is mainly located on the Graanweg, Haverkamp and Koedijk and consists of 80 connections, 21 of them being apartments in the same building. The model topology is shown in Figure 5.16. We distinguish two split points of the feeder which result in three branches. The longest section of the feeder, from from node 00 to 124, is about 800 meter and is referred to as Branch 1. The second longest section is from node 00 to 101, which is about 580 meter and is referred to as Branch 2. The section from node 00 to node 87 is about 480 meter and is referred to as Branch 3. Node 00 to 74 is the common part of all three branches and node 88 to 94 is the common part of Branch 1 and Branch 2. We choose to indicate the branches by their full length from the last position to the first position node 00 to clarify the placements of loads later on in the simulation results.

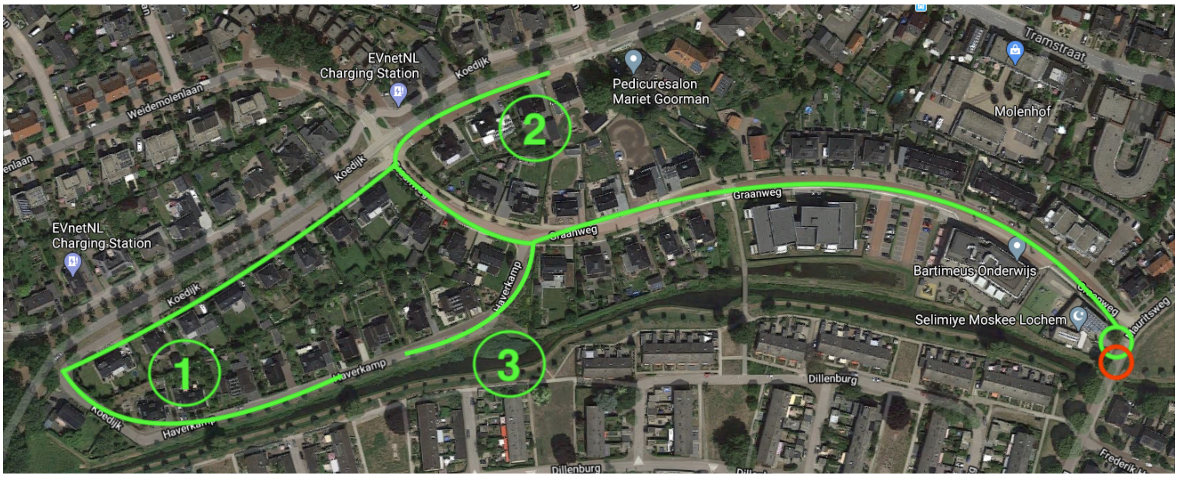

Figure 5.15: Google Maps satellite image of the feeder on the transformer at the Mauritsweg, located in the neighborhood Zuiderenk, municipality of Lochem.

5.4.1 Demographic inputs

The demographic household distribution for the Zuiderenk is shown in Figure 5.17, indicating a relativity large share of single-person households and households without children.

5.4.2 Feeder limits

To analyze the Lochem feeder, we simulate a number of different situations to analyze the effect of the branches. We start by adding EV chargers on the first positions of the feeder. Note, that the first positions from node 00 to node 74 are part of all the three branches. This part can host 34 households, thus potentially 34 EVs. Since we start on the first positions of the feeder, we experience a current capacity overload prior to a critical voltage drop. Starting from nine 11 kW EV chargers plugged in simultaneously,

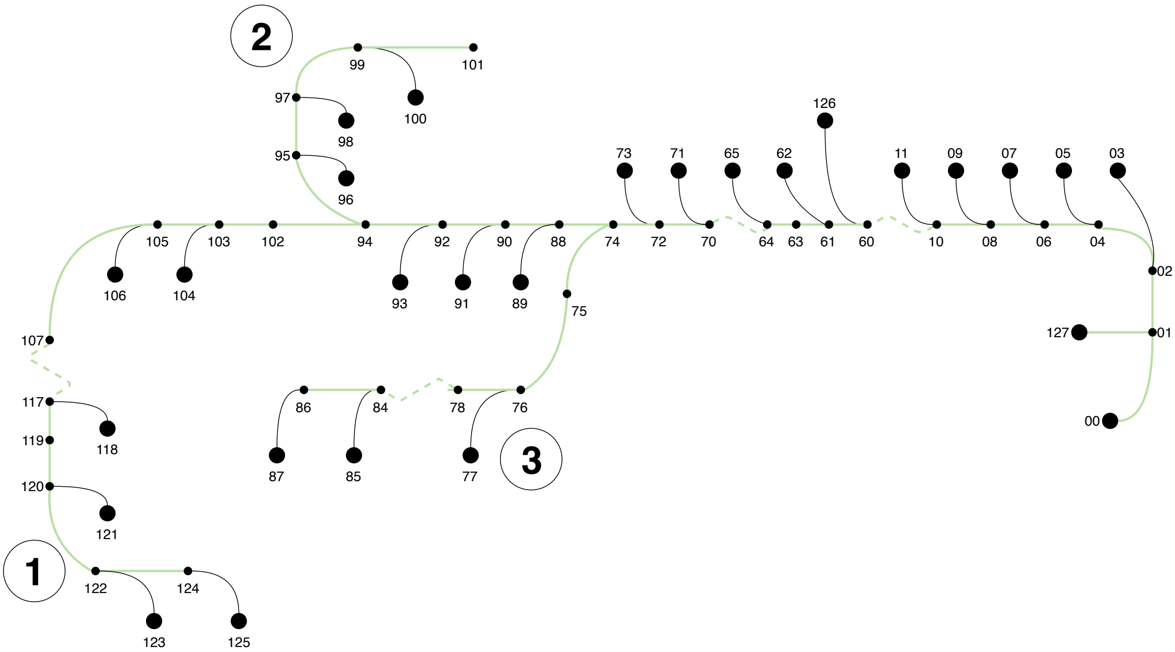

Figure 5.16: Model topology of the feeder for the Lochem case. The dashed lines are used to fit the figure for this thesis, but represent a continuation of the applied numbering scheme for use in the model.

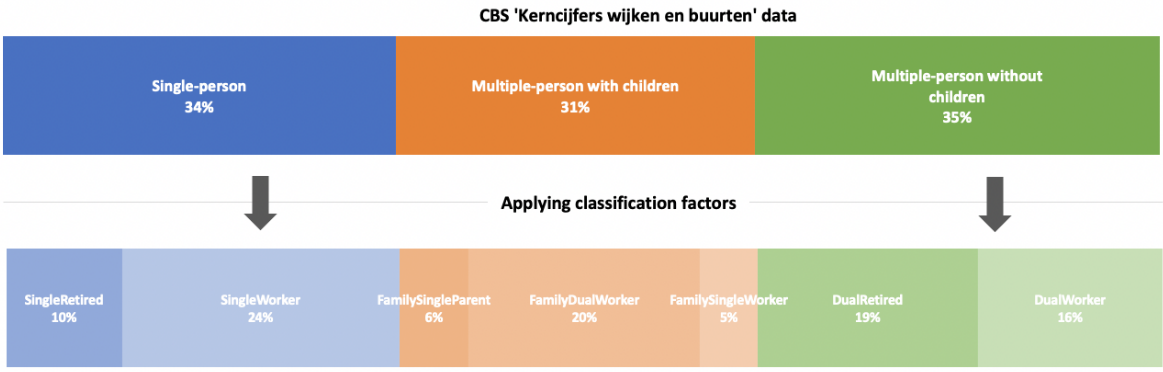

Figure 5.17: The demographic household distribution for the neighborhood Zuiderenk, Lochem.

the feeder current capacity is exceeded. When applying 3.7 kW chargers, the limit is 28 simultaneously charging EVs. However, since we are also interested in the effect of the unequal length of the three branches, it is most interesting to add EVs from the ends of all three branches towards the transformer. For 11 kW charging, we only find voltage related problems in Branch 1. In Branch 2 and 3, the voltage dropped significantly, but it did not fall below the 207 V limit. In those cases, again the current capacity limit of the cable is reached before a critical voltage drop appears. For 3.7 kW charging, current capacity problems occurred at 28 chargers, always prior to a critical voltage drop. The results are summarized in Table 5.1. The findings are considered in line with the field test carried out on the same network (see [10]), where similar power loads caused a short service interruption by heavily overloading a fuse for a substantial amount of time. The maximum peak power overhead for this feeder is thus determined as somewhere around 100 kW (9×11 kW $= 99$ kW and 28×3.7 kW $= 103.6$ kW). However, in contrast to the situation of the field test, we use an equal distribution of the EVs over the phases and a nominal voltage of 230 V, whereas one of the main problem in the field test was a severe unbalance on the phases and the nominal phase voltage before the start of the stress test was a few volts higher.

Simulation	**Maximum 11 kW chargers**	**Maximum 3.7 kW chargers**
Total feeder - begin to end	9 (P)	28 (P)
Branch 1 - end to begin	7 (V)	28 (P)
Branch 2 - end to begin	9 (P)	28 (P)
Branch 3 - end to begin	9 (P)	28 (P)

Table 5.1: Simulation results for the feeder in Lochem.

5.4.3 EV penetration

Based on the results of the previous subsection we identified the peak power that is available on this feeder: around 100 kW. In this subsection we use this to determine the possible EV penetration rate. For this, we again use the proposed *55/15/10/10/10* charging regime distribution and the 50/50 ratio for the two charging power levels. The maximum number of EVs we can simultaneously charge is chosen to be 14, since 7×3.7 kW $= 25.9$ kW and 7×11 kW $= 77$ kW which is together a total load of 102.9 kW. Figure 5.18 shows that the probability of a blackout for such a situation is relatively low. Even at 50% EV penetration rate, so 40 EVs on this feeder, the probability of a blackout on this single feeder looks almost negligible. Again, for this particular single feeder, problems may seem small, but since we have thousands of similar feeders in the Netherlands, expected blackouts for the total LV grid in the Netherlands rise, shown in Figure 5.19 for 10,000 of these type of feeders together.

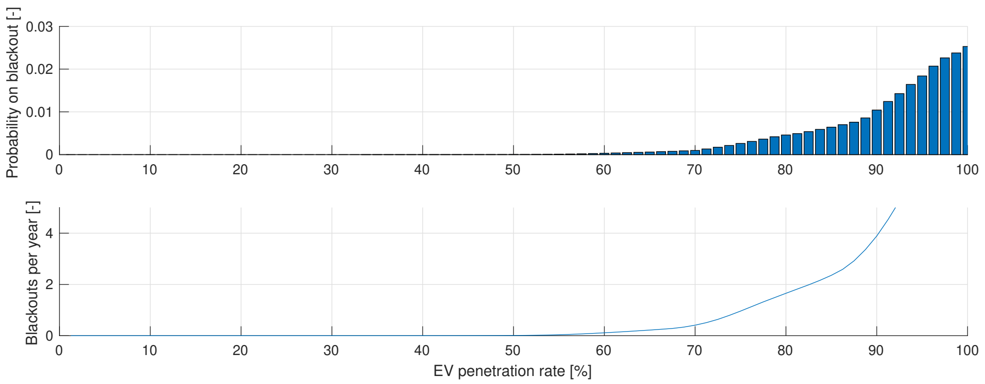

Figure 5.18: Expected blackout probability and total expected blackouts per year at increasing EV penetration rates for the feeder in Lochem.

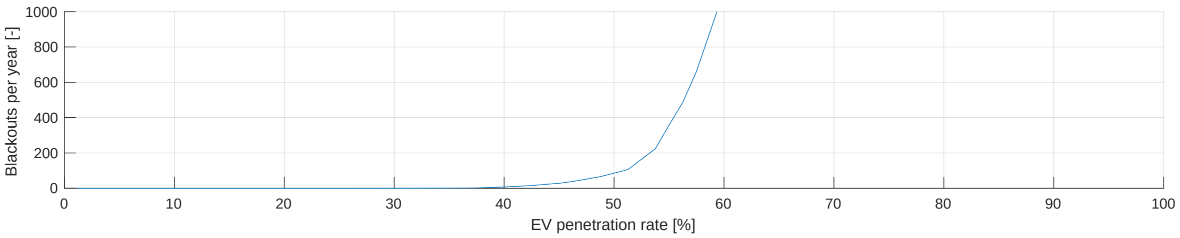

Figure 5.19: Expected number of blackouts per year for all possible EV penetration rates in 10,000 of the Lochem scenario single feeders together, using the *55/15/10/10/10* charging regime distribution and the 50/50 ratio between 3.7 and 11 kW charging power.

5.4.4 Summary

The simulations for the Lochem scenario show that the branching of the feeder has little effect on the maximum EV penetration rate, since the branches 2 and 3 did not show any divergent outcomes. Branch 1 did show a problem with high power 11 kW chargers near the end, but this is mainly caused by the length of this branch itself and the voltage drop that occurs because of that, not because of two other branches being present. Problematic EV penetration rates for this individual feeder are only visible from 60-70% onward. However, similar to the sub-urban scenario, with thousands of such feeders together we may expect a steep increase in blackouts all across the Netherlands from 50% EV penetration rates onward.

5.5 Summary

This section presents three small case-studies that show the coupling between the demographic model and the grid model. Section 5.2 shows an analysis of a typical sub-urban area. We found the probability of a blackout for this type of feeder with the mentioned charging regimes. We also showed the impact of such a single type of feeder when considering more similar feeders to the LV grid: a low blackout probability on a single type of feeder might become problematic if we consider thousands of them in the same electricity grid. From 40-50% EV penetration rate the number of expected blackouts for these type of feeders increases significantly. Since we encounter current capacity problems prior to critical voltage drops, the location of the EV chargers along this feeder type does not influence the results. This makes the analysis easier when comparing this to the rural-type feeder of Section 5.3, where location of the EV charger plays a role. The simulations show that, if all 18 households on the feeder would only charge with 3.7 kW, no problems would occur here. Using the 50/50 mix of the two power levels, the maximum number of simultaneously charging EVs was found to be seven or twelve, depending on the location. However, when the last two or three households in the end of the feeder both have an 11 kW charger for their EV, the situation changes again and even less than seven charging EVs might become problematic. The scenario based on an existing LV grid in Section 5.4 uses a verified grid model and contains some branches, whereas the two synthetic examples do not have any branches and consist out of one type of cable for the whole feeder. Analysis showed that these branches did not severely influence the EV charging capacity.

The demographic model is used only to specify the demographic composition and corresponding energy consumption in the neighborhood. In future work, we propose to extend this with demographic information to model the features of the type of EVs that are present and the energy demand of EVs in these areas. Furthermore, next to EV and PV installations, additional electrification in the form of induction cooking and using heat pumps instead of gas heating is gaining popularity. This means that the possible number of simultaneously charging EVs decreases, since induction cooking and heatpumps may draw a significant amount of power from the LV grid when owners want to charge their EV. However, an increasing EV penetration rate in a neighborhood also offers opportunities, since the surplus of PV generation can be stored in these EV batteries. Using the available information on plug-in times, we may be able to predict the effect of this. Simultaneously generating PV power and charging EVs might also mitigate a part of the voltage problems, because their seems to be at least some overlap in time between those two in most cases.

By analyzing the three scenarios, it becomes clear that local differences may play a large role for the possibilities of EV charging in residential areas. The result of the general analysis on the whole of the Dutch LV grid of Section 4.7 is indeed a very general analysis. Especially the models of rural areas might need additional attention to cover the specific features of these type of feeders. Their relatively large length ensures that the placement of the different loads significantly influences the results.

Chapter 6

Conclusions and recommendations

6.1 Conclusions

This section provides answers to the research questions stated in Chapter 1, by using the findings from the literature, the investigated data and the simulation results. The first main research question focuses on the effects of a significant increase of EV penetration in the current LV grid:

"What penetration rate of electric vehicles will cause problems for the Dutch electricity grid in its current form, if no preventive measures are taken? "

To answer this first main question, three sub-questions are answered:

"I. How to characterize the current Dutch LV grid in a systematic way that makes it possible to identify different frequently occurring situations? Hereby it is important to leave out enough detail to avoid the need for a case-by-case approach."

The answer to this question is presented in Chapter 3, specifically in Section 3.2. Hereby, the basis of the used grid and load flow models was already present in DEMkit [26]. By using the outcomes of the data clustering approach found in [28], we were able to describe a large part of the LV grid by exploiting the common characteristics of LV feeders. This gives the opportunity to study the characteristics of the entire LV grid with a relatively small set of generic feeders and thus to avoid the need for a case-by-case approach. The clustering method reduces a set of approximately 300,000 feeders to a set of 94 generic types. With the 26 most common types, we are able to reconstruct the main characteristics like length, number of connections and an approximation of cable type for 71.3% of the Dutch LV grid.

"II. How to characterize the future loads in Dutch LV grids with regard to the integration of EV charging?

Section 2.3 introduces the main features and considerations for the uptake and integration of EV in the Netherlands. It describes the required power levels and gives an indication of the energy demand. Section 3.4 dives deeper into the usage of EV and describes the actual modeling method. To characterize future loads with regard to the integration of EV charging, data of real charging sessions is used. The probability that a single EV charges on a given feeder is used to characterize the behavior of a set of EVs on a single feeder. With this information, we can approximate the probability that certain combinations of EVs charge simultaneously and thus might cause a blackout on an LV feeder. The multiple charging regime modeling method introduced in Section 4.6 combines a plug-in time distribution, discretized energy demands and two charging power levels in a single model to calculate not only the blackout probability, but also the timeslot with the highest blackout probability. The used inputs can easily be altered by using different plug-in time distributions or energy demands, which makes this model a proper basis for further research on EV charging.

"III. How to model the expected future loads with corresponding LV grid structures to identify potential problematic combinations of loads and grid structures?"

The household load model introduced in Section 3.3 uses the ALPG [27] as basis, creating typical household energy load profiles. These typical household configurations are coupled to demographic data from the CBS [31], such that the energy load of every neighborhood in the Netherlands can be estimated. Using these energy load profiles on typical LV feeder configurations allows flexible configuration of different scenarios. Examples of this can be found in Chapter 5, where two archetypes of feeder configurations and one existing feeder used in a field test are simulated and analyzed. Using this approach, with a separation of the grid model and the household load model, gives us the flexibility to quickly adapt the model for different scenarios and allows us to distribute EVs, PV installations and other equipment and user behavior on a very detailed level among the households.

The answer to the main research question is given in Chapter 4, specifically in Section 4.7. Using the proposed scenario in which every EV travels 38 kilometer per day, we estimate the maximum EV penetration to be around 10% if all these EVs would use 11 kW charging only. For only 3.7 kW charging, the risk of overloading the grid is much lower, with EV penetration rates possible in the range of 50 to 60%. In reality, there exists a mix between different charging powers, with main power levels at 3.7 and 11 kW charging. The proposed method shows an increase in expected blackouts starting at EV penetration rates in the range of 20 to 30%. Considering the EV fleet size estimations for 2030 given in Section 2.3.1 with optimistic scenarios of 27.6% and 33.6% penetration rate and considering a 50/50 mix of 3.7 and 11 kW charging, one may expect an increase in black-out events already by 2030, if no adequate measures are taken. Important here is the observation that if the EV penetration rate on a feeder passes a certain point, a sort of turning point, where the total expected number of blackouts for the whole of the Netherlands starts to rise steeply.

Looking in more detail to the different scenarios of Chapter 5, we have to conclude that local situations can vary significantly. For sub-urban areas, the expected possible penetration rate is higher compared to rural areas. This is mainly due to the typical characteristics of rural feeders. Because of their relatively large length, critical voltage drops occur often prior to a current capacity violation.

Based on the estimated maximum EV penetration rate for the Netherlands, we may have to look for opportunities to extend this penetration rate. If suitable preventive measures in any form are taken, it should be possible to increase the maximum penetration rate of EVs without creating additional blackouts. This rises the second main research question:

"What are possible solutions for scenarios with problematically high EV penetration rates in local grids and how do these solutions increase the allowed penetration rate?"

The first observation is that, to extend the maximum EV penetration rate, it is essential to reduce the peak loads on the LV grid, either by lowering power demand or by shifting energy demand in time. The simulations and calculations in this thesis show that it is always preferable to charge with 3.7 kW compared to 11 kW, because the advantage of a factor 3 shorter duration of charging sessions does not make up for the spreading of charging power demand. Lowering power demand for all EVs from 11 kW to only 3.7 kW could improve the maximum EV penetration rate from about 10% to somewhere in the range of 50 to 60%, as was explained before. Furthermore, we observed that charging an EV only once a week with a longer charging session time imposes the least stress on the LV grid compared to charging more often with smaller energy demands. However, this holds if and only if these charging sessions are spread evenly over the weekdays. But, according to the available data, this is true for the current situation in the Netherlands. It may be possible to motivate EV owners to charge only on certain days, but we can not force them, so we do not consider this as a viable solution. This research shows that, if we allow uncontrolled EV charging in residential areas, Smart Charging initiatives that implement features like peak shaving by controlling the charging power of (a part of) the EVs in a neighborhood is necessary to prevent LV feeders from blackouts.

From the perspective of the LV feeder cables, we found that typically a given set of five clusters are the main cause of problems (i.e. at the low EV penetration rates), as explained in Section 4.7.3. These clusters are typically characterized by their relatively large number of household connections and relatively large length. Together, these five clusters represent about 15% of the Dutch LV grid. Replacing these type of feeders by more suitable designs may decrease the expected blackouts at EV penetration rates of up to 50% significantly. The other 85% of the feeders are only problematic starting from an EV penetration rate of around 55%, according to the findings using the *55/15/10/10/10* charging regime and the 50/50 charging power ratio for the whole of the Netherlands. However, 15% of 300,000 feeders means that 45,000 LV network cables need to be replaced. If we aim to replace these before 2030, this is equal to replacing more than 17 complete LV feeders *per working day* until 2030. This is a very difficult (if not practically impossible) and costly operation, which again stresses the need for a functional smart charging solution as e.g. the so-called 'Profile Steering' approach proposed in [38].

6.2 Recommendations

To further increase the usefulness of the proposed models, it is essential to use more detailed information on the LV feeder network in the Netherlands. The used clustering approach is a good starting point, but it lacks detailed information on the exact composition of LV cables. Furthermore, the assumed maximal current capacity of the feeders is probably overestimated, since each feeder is secured by a fuse that is rated with a lower current value than the actual cable current capacity, for safety reasons. Also, the decision to only simulate the clusters that represent 71.3% of all the feeders in the Netherlands and from there extrapolate this to 100% is a simplification that needs additional research, since the remaining 28.7% of the grid could show deviating behavior due to their different features.

Evidence was found that feeders with a relatively high number of households and a relatively long cable length are causing the first problems with increasing EV penetration rates. To prevent problems, the best approach would be to start with solutions especially for this type of feeders. An estimated 15% of the total 300,000 feeders are problematic at significantly lower EV penetration rates compared to the other 85% in which problems are expected, but only at relatively higher EV penetration rates. Further research could focus on exactly these type of feeders and investigate their impact in more detail. For DSOs this information might be useful to identify the problematic areas that cause problems first.

This research focused on individual LV feeders. It does not take into account overloading at the transformer that can occur prior to overloading a single feeder due to the stacking effect of multiple feeders connected to one transformer: the maximal capacity of all the given feeders connected to one transformer together is almost always higher than the transformer capacity itself. Probably, this stacking effect further reduces the possible maximum EV penetration rate, but this needs additional research. The model presented in this thesis can be fairly easily extended to account for this.

By choosing the scenario in which every EV drives 38 kilometer per day we ignore variations in the driving distance. Furthermore, by assuming that all EVs charge all that required energy in a residential area, we ignore all energy that is charged at e.g. work or other destinations such as shopping malls. Further research has to be done to identify what the effect of this destination charging is for the EV energy demand in residential areas.

There seems to be a reasonable overlap in time between surplus PV generation and expected EV charging energy demand and it is worthwhile to further investigate this synergy. From a feeder capacity perspective, this overlap might increase the maximum EV penetration rate since PV production might decrease the current level at the transformer and decrease the voltage drops along the feeder.

The proposed multiple charging regime model to estimate the probability of blackouts can be further extended by using not only probability distributions over time for the plug-in time, but also for the energy demand and traveled kilometers (instead of using five discretized regimes). Also, by choosing the 50/50 power level, we ignored all the cases in which this ratio is different. Probably, there are situations in which this ratio for the connected EVs on a feeder deviates and the model should be extended to account for this. With these improvements, the model is also applicable to other situations. E.g. for parking lots or large parking spaces on company premises, we only need to adjust the parameters for plug-in time, charging power and energy demand.

Bibliography

[1] Volkspartij voor Vrijheid en Democratie (VVD), Christen-Democratisch Appèl (CDA), Democraten '66 (D66) en ChristenUnie (CU), "2017–2021 Coalition Agreement," Available at https://www.government.nl/documents/publications/2017/10/10/coalition-agreement-confidence-in-the-future (Accessed 17-02-2020).

[2] Rijksdienst voor Ondernemend Nederland (RVO), "Cijfers Elektrisch Vervoer," Available at https://www.rvo.nl/onderwerpen/duurzaam-ondernemen/energie-en-milieu-innovaties/elektrisch-rijden/stand-van-zaken/cijfers (Accessed 17-02-2020).

[3] Tesla, "EU Models," Available at https://www.tesla.com/en_eu/models (Accessed 07-07-2020).

[4] CBS, "OViN," Available at https://www.cbs.nl/nl-nl/onze-diensten/methoden/onderzoeksomschrijvingen/korte-onderzoeksbeschrijvingen/onderzoek-verplaatsingen-in-nederland--ovin-- (Accessed 22-06-2020).

[5] 'CBS', "Energieverbruik van particuliere huishoudens," Available at https://www.cbs.nl/nl-nl/achtergrond/2018/14/energieverbruik-van-particuliere-huishoudens (Accessed 10-07-2020).

[6] R. van den Hoed, S. Maase, J. Helmus, R. Wolbertus, Y. Bouhassani, J. Dam, M. Tamis, and B. Jablonska, *E-mobility: getting smart with data*. Amsterdam: Amsterdam University of Applied Sciences, July 2019.

[7] J. van der Burgt, S. P. Vera, B. Wille-Haussmann, A. N. Andersen, and L. H. Tambjerg, "Grid impact of charging electric vehicles; study cases in Denmark, Germany and the Netherlands," in *2015 IEEE Eindhoven PowerTech*, June 2015, 6 pages.

[8] C. H. Tie, C. K. Gan, and K. A. Ibrahim, "The impact of electric vehicle charging on a residential low voltage distribution network in Malaysia," in *2014 IEEE Innovative Smart Grid Technologies - Asia (ISGT ASIA)*, May 2014, pp. 272–277.

[9] A. Dubey and S. Santoso, "Electric vehicle charging on residential distribution systems: Impacts and mitigations," *IEEE Access (vol. 3)*, vol. 3, pp. 1871–1893, 2015.

[10] G. Hoogsteen, A. Molderink, G. Smit, J. Hurink, B. Kootstra, and F. Schuring, "Charging electric vehicles, baking pizzas, and melting a fuse in lochem," *CIRED: Open Access Proceedings Journal*, vol. 2017, no. 1, pp. 1629–1633, October 2017.

[11] P. van Oirsouw, *Netten voor distributie van elektriciteit*. Phase to Phase, (ISBN = 9789081798303), 2011.

[12] www.cleanpng.com, "'CleanPNG'," Available at https://www.cleanpng.com/png-product-design-brand-engineering-line-pattern-powe-5948043/preview.html (Accessed 11-08-2020.

[13] Nederlandse Overheid - Autoriteit Consument en Markt, "Netcode elektriciteit," Available at https://wetten.overheid.nl/BWBR0037940/2020-01-01 (Accessed 19-02-2020).

[14] S. Nykamp, M. Andor, and J. L. Hurink, "'Standard' incentive regulation hinders the integration of renewable energy generation," *Energy Policy*, vol. 47, pp. 222 – 237, 2012.

[15] A. Hoekstra and N. Refa, "Characteristics of Dutch EV drivers," *EVS30 Symposium, Stuttgart, Germany*, October 9-11, 2017.

[16] J. Hagman, S. Ritzén, J. J. Stier, and Y. Susilo, "Total cost of ownership and its potential implications for battery electric vehicle diffusion," *Research in Transportation Business Management*, vol. 18, pp. 11 – 17, 2016, innovations in Technologies for Sustainable Transport. [Online]. Available: https://doi.org/10.1016/j.rtbm.2016.01.003

[17] P. Slowik and N. Lutsey, "Evolution of incentives to sustain the transition to a global electric vehicle fleet, International Council on Clean Transportation - white paper, page 3," November 2016.

[18] R. Gijlswijk, E. Eijk, E. van Kempen, N. Ligterink, and E. Cox, "Inputs and considerations for estimating large scale uptake of electric vehicles in the dutch passenger car fleet up to 2030," *TNO report, The Hague, the Netherlands*, August 2018.

[19] ElaadNL, "Smart Charging Guide," Available at https://www.elaad.nl/news/nieuw-smart-charging-guide/ (Accessed 26-02-2020).

[20] CBS, "StatLine," Available at https://opendata.cbs.nl/statline/#/CBS/nl/ (Accessed 02-06-2020).

[21] ElaadNL, "Open database," Available at https://platform.elaad.io/analyses/ElaadNL_opendata.php (Accessed 22-06-2020).

[22] RN7, "Wijchen wil geen kabels elektrische laadpalen over trottoir," Available at https://rn7.nl/nieuws/wijchen-wil-geen-kabels-elektrische-laadpalen-over-trottoir (Accessed 18-02-2020).

[23] E. Delmonte, N. Kinnear, B. Jenkins, and S. Skippon, "What do consumers think of smart charging? Perceptions among actual and potential plug-in electric vehicle adopters in the United Kingdom," *Energy Research and Social Science*, vol. 60, 2020. [Online]. Available: https://doi.org/10.1016/j.erss.2019.101318

[24] AutoWeek, "Zoveel duurder is een Tesla Model 3 in 2020," Available at https://www.autoweek.nl/autonieuws/artikel/zoveel-duurder-is-een-tesla-model-3-in-2020/ (Accessed 18-02-2020).

[25] EV Database, "All electric vehicles," Available at https://www.ev-database.org/ (Accessed 17-02-2020).

[26] G. Hoogsteen, "A cyber-physical systems perspective on decentralized energy management," Ph.D. dissertation, University of Twente, ISBN = 978-90-365-4432-0, December 2017.

[27] G. Hoogsteen, A. Molderink, J. L. Hurink, and G. J. M. Smit, "Generation of flexible domestic load profiles to evaluate demand side management approaches," *2016 IEEE International Energy Conference (ENERGYCON), Leuven*, 2016, 6 pages.

[28] M. Nijhuis, M. Gibescu, and J. Cobben, "Clustering of low voltage feeders from a network planning perspective," in *Proceedings of the 23rd International Conference on Electricity Distribution (CIRED), 15-18 June 2015, Lyon, France*, 2015.

[29] M. Nijhuis, "Long-term planning of low voltage networks," Ph.D. dissertation, Technische Universiteit Eindhoven, ISBN = 978-90-386-4351-9, October 2017.

[30] Liander, "Website for Liander customers on type of grid connection," Available at https://www.liander.nl/consument/aansluitingen/soorten-aansluitingen (Accessed 26-02-2020).

[31] Centraal Bureau voor de Statistiek (CBS), "Kerncijfers Wijken en Buurten 2017," Available at https://www.cbs.nl/nl-nl/dossier/nederland-regionaal/wijk-en-buurtstatistieken/kerncijfers-wijken-en-buurten-2004-2019 (Accessed 18-02-2020).

[32] CBS, "WoonOnderzoek Nederland 2015," Available at https://www.cbs.nl/nl-nl/onze-diensten/methoden/onderzoeksomschrijvingen/korte-onderzoeksbeschrijvingen/woononderzoek-nederland--woon-- (Accessed 02-03-2020).

[33] J. Quirós-Tortós, L. F. Ochoa, and B. Lees, "A statistical analysis of EV charging behavior in the UK," in *2015 IEEE PES Innovative Smart Grid Technologies Latin America (ISGT LATAM)*, October 2015, pp. 445–449.

[34] J. Cross and R. Hartshorn, "My electric avenue: Integrating electric vehicles into the electrical networks," in *6th Hybrid and Electric Vehicles Conference (HEVC 2016), London, United Kingdom*, 2016.

[35] C. Develder, N. Sadeghianpourhamami, M. Strobbe, and N. Refa, "Quantifying flexibility in EV charging as DR potential: Analysis of two real-world data sets," in *2016 IEEE International Conference on Smart Grid Communications (SmartGridComm)*, November 2016, pp. 600–605.

[36] Netbeheer Nederland, "Betrouwbaarheid," Available at https://www.netbeheernederland.nl/dossiers/betrouwbaarheid-23 (Accessed 03-07-2020).

[37] M. Nijhuis, M. Gibescu, and J. Cobben, "Incorporation of on-load tap changer transformers in low-voltage network planning," in *2016 IEEE PES Innovative Smart Grid Technologies Conference Europe (ISGT-Europe), 9-12 October 2016, Ljubljana, Slovenia*, Feb. 2017, 6 pages.

[38] M. E. T. Gerards, H. A. Toersche, G. Hoogsteen, T. van der Klauw, J. L. Hurink, and G. J. M. Smit, "Demand side management using profile steering," in *2015 IEEE Eindhoven PowerTech*, June 2015, 6 pages.